# ESKIMO II. MAGAZINE SEPARATION TEST

Frederick H. Weals

Naval Weapons Center
China Lake, California

September 1974

# Naval Weapons Center

AN ACTIVITY OF THE NAVAL MATERIAL COMMAND

R. G. Freeman, III, RAdm., USN ..... Commander

G. L. Hollingsworth ..... Technical Director


## FOREWORD

This report describes a full-scale magazine separation test conducted at the Naval Weapons Center in May 1973. The test work was conducted for the Department of Defense Explosives Safety Board (DDESB) using funds provided by that organization. The work was identified by Army Program Element Number 6.57.02.A and Project and Task Area Number 4A765702M857.

Based on data derived from the test, DDESB has made significant gains in information relating to hazards criteria.

Appendix A of the report, which was prepared by Mr. Ralph Reisler and Mr. Warren Baity of the Ballistic Research Laboratories, discusses loading predictions. Appendix B, covering vehicle and traffic route investigations and window glass hazard studies, was prepared by Dr. Donald R. Richmond and Dr. Royce B. Fletcher of the Lovelace Foundation for Medical Education and Research.

This report has been reviewed for technical accuracy by DDESB staff members Mr. Russell G. Perkins and Dr. Thomas A. Zaker. Mr. Perkins and Dr. Zaker also played major roles in the design of the test.

Captain Peter F. Klein, USN, Chairman of DDESB, provided technical, administrative, and policy guidance during the preparation, execution, and reporting of the test.

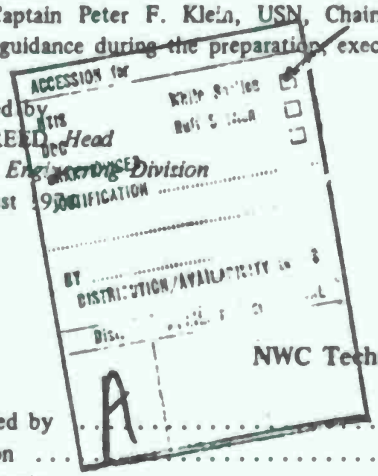


Released by
J. L. REED, *Head*
*Project Engineering Division*
1 August 1973

Under authority of
W. R. HATTABAUGH, *Head*
*Test and Evaluation Department*


NWC Technical Publication 5557

Published by ..... Technical Information Department

Collation ..... Cover, 46 leaves

First printing ..... 110 unnumbered copies

UNCLASSIFIED

SECURITY CLASSIFICATION OF THIS PAGE (When Data Entered)

AD/A-0000 89

## REPORT DOCUMENTATION PAGE

READ INSTRUCTIONS BEFORE COMPLETING FORM

| | |
|---|---|
| 1. REPORT NUMBER: NWC TP 5557 | 2. GOVT ACCESSION NO. |
| 3. RECIPIENT'S CATALOG NUMBER | |
| 4. TITLE (and Subtitle): ESKIMO II MAGAZINE SEPARATION TEST | 5. TYPE OF REPORT & PERIOD COVERED: A test report |
| 6. PERFORMING ORG. REPORT NUMBER | |
| 7. AUTHOR(s): Frederick H. Weals | 8. CONTRACT OR GRANT NUMBER(s) |
| 9. PERFORMING ORGANIZATION NAME AND ADDRESS: Naval Weapons Center, China Lake, CA 93555 | 10. PROGRAM ELEMENT, PROJECT, TASK AREA & WORK UNIT NUMBERS |
| 11. CONTROLLING OFFICE NAME AND ADDRESS: Department of Defense Explosives Safety Board, Washington, DC 20314 | 12. REPORT DATE: September 1974 |
| | 13. NUMBER OF PAGES: 90 |
| 14. MONITORING AGENCY NAME & ADDRESS (if different from Controlling Office) | 15. SECURITY CLASS. (of this report): UNCLASSIFIED |
| | 15a. DECLASSIFICATION/DOWNGRADING SCHEDULE |

16. DISTRIBUTION STATEMENT (of this Report)

Approved for public release, distribution unlimited.

17. DISTRIBUTION STATEMENT (of the abstract entered in Block 20, if different from Report)

18. SUPPLEMENTARY NOTES

19. KEY WORDS (Continue on reverse side if necessary and identify by block number)

Detonation Tests, Eskimo II
Eskimo II
Explosives Hazards Test
Igloo Structures, Test of Instrumentation
Magazine Separation Test

20. ABSTRACT (Continue on reverse side if necessary and identify by block number)

See back of form



DD FORM 1 JAN 73 1473 EDITION OF 1 NOV 65 IS OBSOLETE
S/N 0102-014-6601

UNCLASSIFIED

SECURITY CLASSIFICATION OF THIS PAGE (When Data Entered)

(U) *ESKIMO II Magazine Separation Test*, by Frederick H. Weals. China Lake, Calif., Naval Weapons Center, September 1974. 90 pp. (NWC TP 5557, publication UNCLASSIFIED.)

(U) In an instrumented test in May 1973 at the Naval Weapons Center, 27,800 pounds of Tritonal explosive contained in 72 M117 bombs were detonated simultaneously within an open top earth revetment enclosure surrounded by five earth-covered igloos placed with face-on exposures and at essentially equal distances from the donor blast. The principal objective was to evaluate the protection afforded by several different types of igloo headwall and door constructions against communication of explosion. The test results, showing a wide range of door and headwall responses, indicated that no change in the separation standards established by the Department of Defense Explosives Safety Board is required at this time. Additionally, the results have provided guidance for the selection of promising types of walls and doors to be tested more extensively. The test also included investigation of the response of a new noncircular steel-arch magazine structure, of safety distances specified for public traffic routes, and of the hazards associated with window glass used in commercial and institutional buildings. The report also contains data on fragment sizes and distributions, igloo damage and structural motion, air blast pressures at the site, and vehicle and window damage.

## CONTENTS

## INTRODUCTION

At the request of the Department of Defense Explosives Safety Board (DDESB), the Naval Weapons Center (NWC) on 22 May 1973 conducted at the Randsburg Wash Test Range a large-scale explosives hazards test known as ESKIMO II. (ESKIMO is an acronym for Explosive Safety Knowledge IMprovement Operation.) This was the second in a series of full-scale tests of earth-covered magazines sponsored by the DDESB. The main purpose of this test was to evaluate the protection afforded by five igloo magazines against communication of explosion when the headwall of one magazine faces the earth-covered side or rear wall of another.

ESKIMO I, the first test, was conducted in December 1971 to determine a safe, practicable minimum separation distance for face-on exposures of U.S. Army standard steel-arch magazines (Reference 1). Explosion communication occurred to an acceptor igloo of this design at a distance in feet equal to $1.25 \times W^{1/3}$, in which W is the weight in pounds of the high explosive in storage, but failed to occur at a distance of $2.0 \times W^{1/3}$ to the rear of the donor. Further, the test revealed that safety and economy might be increased through improved design for closer balance in strength between the doors and headwall of the magazine.

ESKIMO II, a full-scale proof test of other existing and modified door and headwall designs, utilized structures and facilities remaining from ESKIMO I, rebuilt as necessary to meet the aims of the test. ESKIMO II extended investigation conducted in ESKIMO I, making use of information derived from that test. In ESKIMO I the separation distances and orientation of the acceptor magazines relative to a donor magazine were varied for the primary objective of selecting appropriate separation distances. In ESKIMO II the separation distances from a donor stack of bombs were approximately the same for all five acceptor magazines, and all magazines faced the stack.

## TEST OBJECTIVES

The primary test objective was to evaluate the protection afforded by magazine structures against communication of explosion with the headwall of one magazine facing the earth-covered side or rear wall of another. Other objectives were

1. Evaluation of the resistance of several types of igloo doors and headwalls and of proposed modifications to existing designs in a blast environment simulating that from a magazine explosion.
2. Evaluation of a proposed noncircular steel-arch igloo design.

3. Investigation of hazards associated with window glass and window frames placed at several distances from the explosion, with emphasis on window types used in commercial and institutional buildings.

4. Evaluation of blast damage to foreign automobiles and to several types of domestic vehicles placed at distances from magazine structures specified by various authorities for public traffic routes.

5. Acquisition of data regarding fragment hazards from a specific bomb.

## NEAR FIELD TEST LAYOUT

### IGLOOS

Five magazines were exposed face-on at approximately the same distance from the explosion source, as shown in Figure 1. The magazine structures were earth-covered semicircular corrugated steel

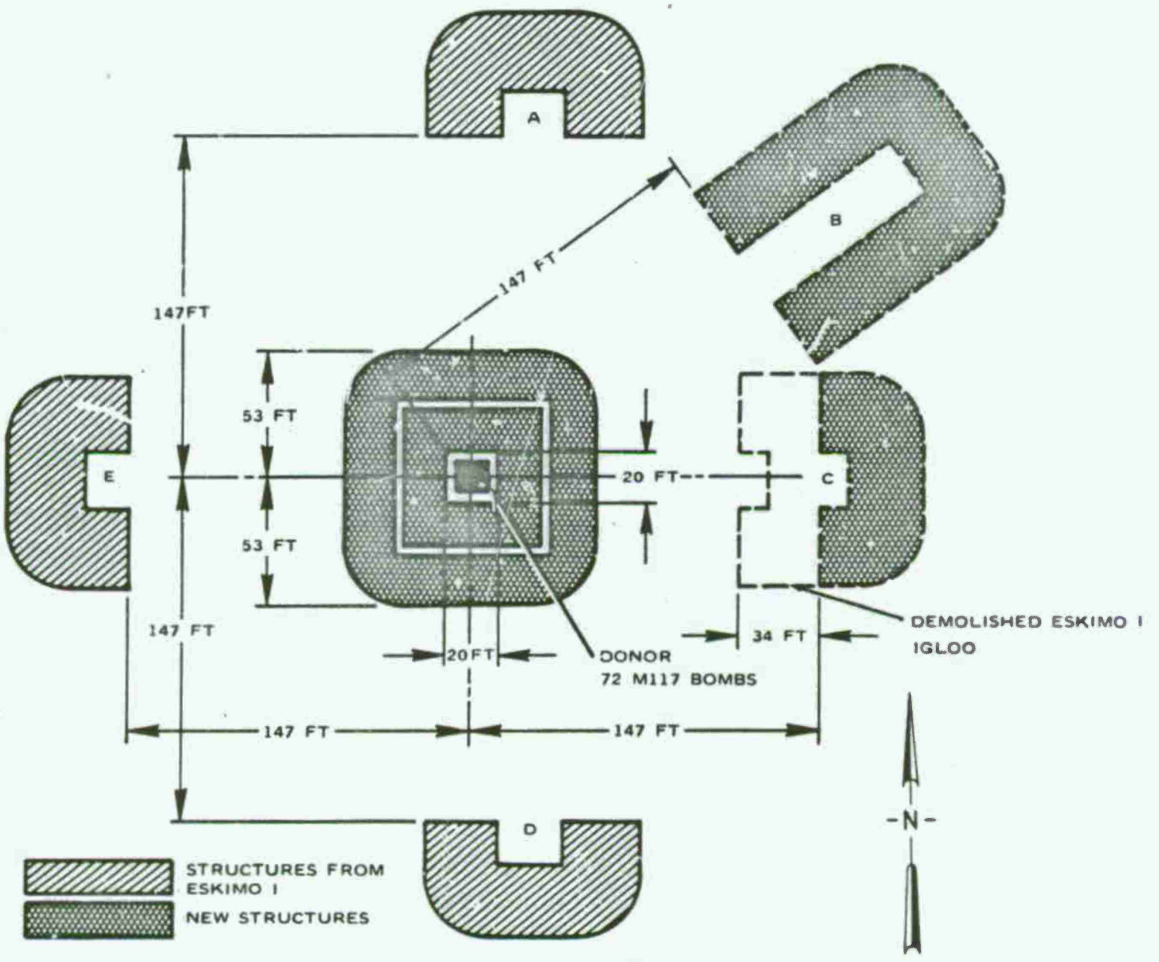


Figure 1. Layout of Test Structures for ESKIMO II Magazine Separation Test. A, B, C, D, and E indicate igloo designations.

arches, except for a new type of noncircular steel-arch magazine (Igloo B), built to a length of 80 feet in the northeast sector of the array. The construction of the various acceptor igloos is described in Table 1, and steel-arch construction is illustrated in Figure 2. Door construction for each igloo is described in Table 2, and door types are illustrated in Figure 3. Door details of Igloos A, C, D, and E are shown in Figures 4 through 7.

TABLE 1. Igloo Construction.

| Igloo | Position relative to donor | Length, ft | Steel arch, floor, rear wall, wing walls, and earth cover | Headwall type | Headwall drawing |
|---|---|---|---|---|---|
| A | North | 20 | Remaining from ESKIMO I | Navy Type II | NAVFAC dwg. 649-602 |
| B | Northeast | 80 | All new; steel arch design approximates size and shape of Stradley igloo | Stradley | OCE std. dwg. 33-15-61 |
| C | East | 10 | All new construction; design same as ESKIMO I | Same as ESKIMO I | OCE std. dwg. 33-15-64 |
| D | South | 20 | Remaining from ESKIMO I | Same as ESKIMO I except for door modifications | OCE std. dwg. 33-15-64 |
| E | West | 20 | Remaining from FSKIMO I | Same as ESKIMO I except for door modifications | OCE std. dwg. 33-15-64 |

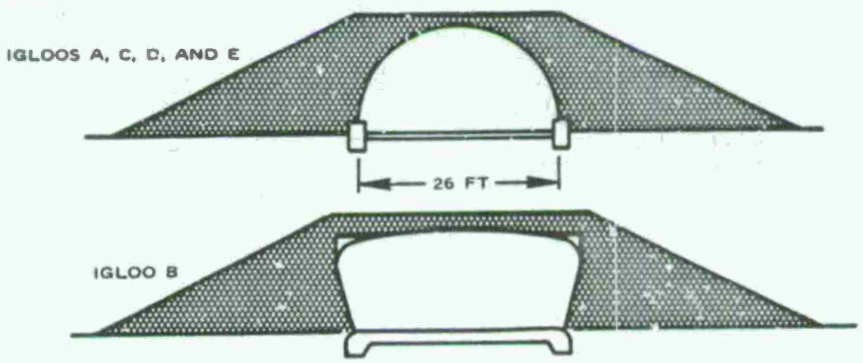


Figure 2. Cross Sections of Steel-Arch Construction for the Igloos of ESKIMO II.

TABLE 2. Door Construction.

| Igloo | Nominal door size, ft | | Door type | Door drawing |
|---|---|---|---|---|
| | Height | Width | | |
| A | 10 | 8 | Double leaf, hinged | NAVFAC 649-604 |
| B | 10 | 10 | Biparting, sliding | OCE std. dwg. 33-15-61 |
| C | 10 | 10 | Double leaf, hinged | OCE std. dwg. 33-15-64 |
| D | 10 | 10 | Single leaf, sliding | Black & Veatch unnumbered dwg., 25 Oct 1972 |
| E | 10 | 10 | Double leaf, hinged; with removable steel beam reinforcing | OCE std. dwg. 33-15-64, modified by Black & Veatch dwg. |

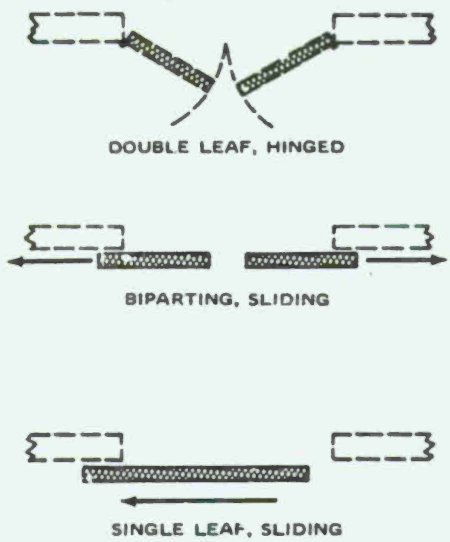


Figure 3. Types of Doors Used on ESKIMO II Igloos.

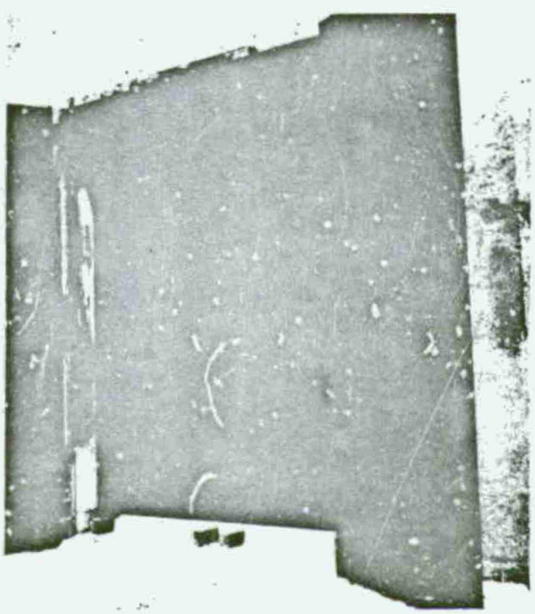

Figure 4. Doorway of Igloo A. Note door construction and door arrestors at top and bottom.

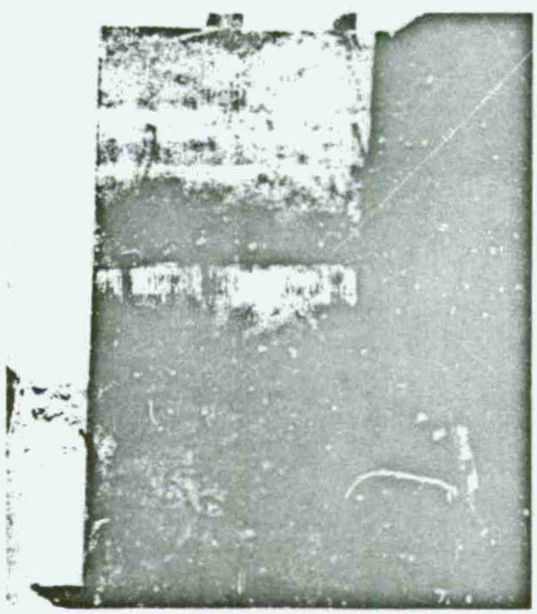

Figure 5. Interior Surface of Door on Igloo C.

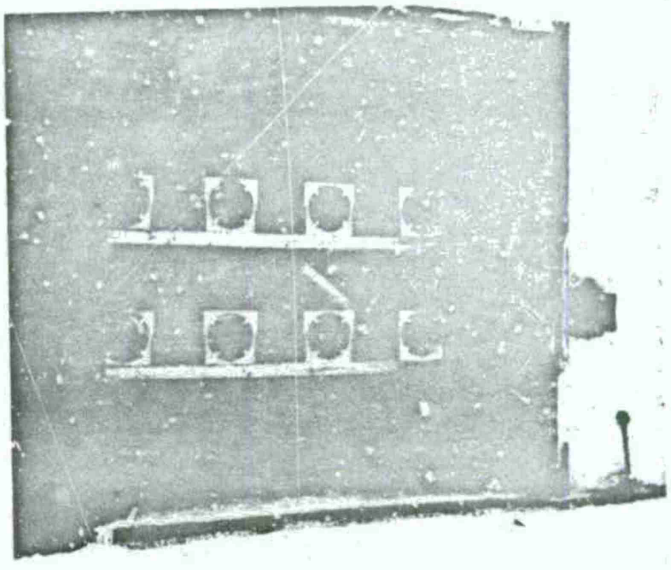

Figure 6. Door and Door Opening of Igloo D. Rack of acceptor land mines (two mines are hidden by the door on the left) in place prior to test; acceptor arrangement is typical for Igloos A, D, and E.

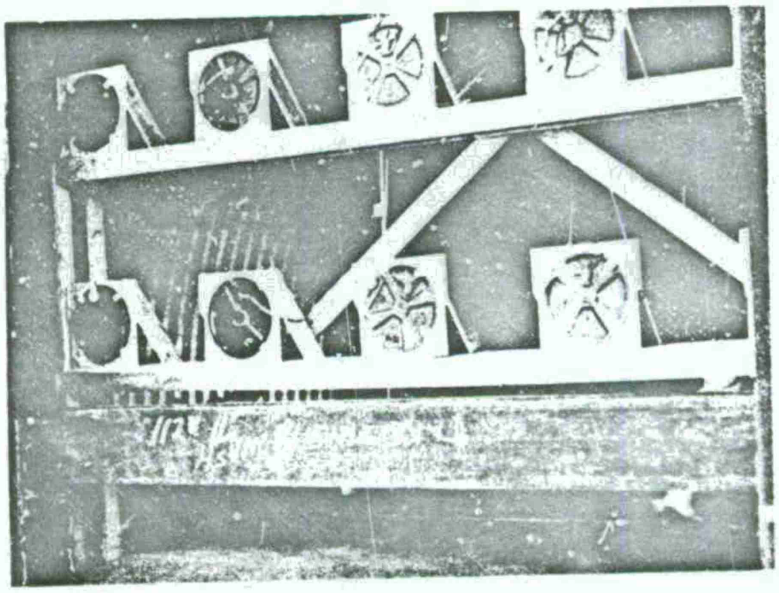

Figure 7. Door Opening of Igloo E Showing Steel I-Beam. Acceptor charges in place.

## DONOR CHARGE

The ESKIMO II explosion source was designed to approximate the blast loading expected from an earth-covered magazine containing 500,000 pounds of explosives, the maximum permitted in a single magazine by Department of Defense explosives safety standards.

In late 1971 and in 1972, explosion tests were conducted in the United Kingdom on model igloos (representing their prototypes nominally at one-tenth scale) geometrically similar in external features to U.S. magazines.

Because bulk explosives (W = 141 pounds) were used in the UK model tests, rather than explosives cast into heavy-walled projectiles, the design of the ESKIMO II explosion source was based primarily on the loadings measured on the front wall of a target magazine 10.4 feet ($2.0 \times W^{1/3}$) to the rear of the donor in the model tests. As the principal criterion for the ESKIMO II explosion source design, the observed total impulse of the positive phase of loading was selected, on the assumption that this parameter is the primary determinant of the velocity with which door and headwall material will move into the magazine and act as the agent of explosion communication upon impact with the contents of the acceptor magazine. This assumption is strictly true only if the major portion of the load is applied within a time that is short compared with that required for door and headwall material to traverse the distance to acceptor explosive charges.

Loading unpulse and the corresponding positive-phase duration values at model scale were increased by the applicable scale factor to obtain the design loading for the ESKIMO II explosion source.

The positive-phase impulse load of 72 psi-msec representative of observations in the UK model tests was multiplied by the scale factor $(500{,}000/141)^{1/3} = 15.3$ to obtain the corresponding value applicable to a full-scale magazine containing 500,000 pounds of explosives. This gives 1,100 psi-msec, the value utilized as the principal criterion in determining the explosion source size required for ESKIMO II.

The final explosion source design consisted of 72 M117 bombs, each weighing 750 pounds and filled with Tritonal. The donor charge, containing 27,800 pounds of explosives, had an expected TNT equivalent weight of approximately 24,000 pounds, based on effective TNT weight values for Tritonal-filled M117 bombs as shown in Table 3 of Reference 2. The bombs were tightly stacked on their sides in two triangular stacks of 36 each, with each succeeding layer stacked in the spaces between the bombs in the layer below. The bombs were stacked on a steel plate 1 inch thick by 98 inches wide by approximately 156 inches long. The two stacks were arranged so that the bombs in one stack were in base-to-base contact with the bombs of the other stack. Figure 8 shows the arrangement of the completed donor charge.

The nose fuze well of each bomb was primed with C-4 explosive imbedded with a Primacord lead. Two groups of 36 cords (each group serving one side of the stack) were formed, and all 72 Primacord leads were of the same length. Electrical initiation of each Primacord group was accomplished by two Engineer Specials blasting caps.

This source shape was selected in an attempt to reduce directional effects and to approximate a hemispherical aboveground source. After adjustment for explosive composition and bomb case effects, loading calculations performed by Ballistic Research Laboratories (Appendix A) for this explosion source yielded the predicted values of 38 psi, 45.5 msec, and 1,100 psi-msec for the incident overpressure, positive-phase duration, and headwall impulse loading, respectively, at a distance of 147 feet, the test area radius in ESKIMO II. The impulse load of 1,100 psi-msec was the value expected from explosion of a full-size earth-covered magazine filled to capacity at the reduced rear-to-front

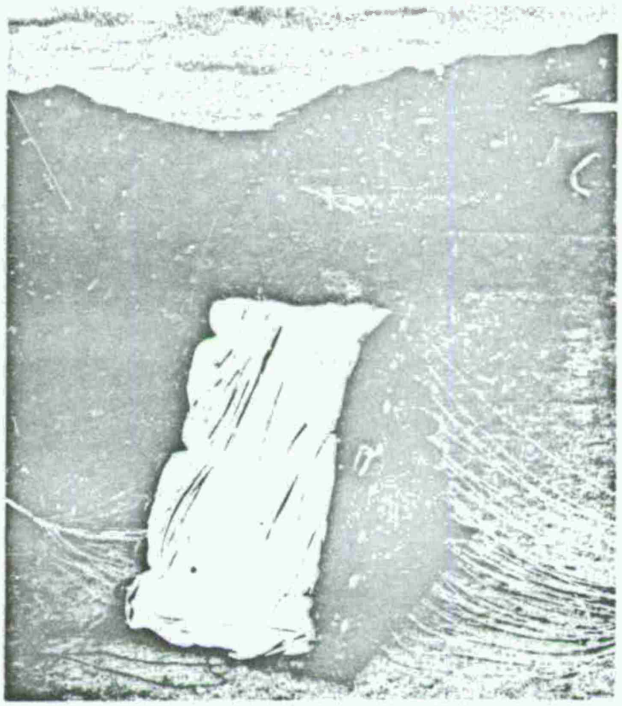

Figure 8. Completed Donor Charge Consisting of 72 M117 Bombs.

separation distance of 2.0 × $W^{1/3}$ determined in ESKIMO I.

In order to intercept low-angle primary fragments from the bombs, an earth revetment 10 feet high was placed around the stack of bombs, with the inner toe delineating all four sides of a 20- by 20-foot interior leveled area. The crest of the mound was 3 feet wide. Figure 9 shows the arrangement.

See Appendix A for additional comments concerning design of the donor charge.

## ACCEPTOR CHARGES

High-explosive acceptor charges were omitted from Igloo C (the control igloo) and Igloo B. Twelve M15 land mines were used as acceptor charges in each of the other three acceptor igloos. These land mines were positioned in two rows of six, one approximately 3 feet from the floor and one approximately 6 feet from the floor in Igloos A, D, and E (designated the north, south, and west igloos in ESKIMO I). The land mines were secured on the edges of trays so that the bottom surface (whole diameter) was vertical and susceptible to possible headwall and door fragment attack. In each row, there was one mine on either end that was opposite the concrete headwall of the magazine. The trays were so positioned that the acceptor explosives were approximately 3 feet from the plane of the inside surface of the headwall. This arrangement of acceptor charges in the igloos is shown in Figures 6 and 7.

Figure 9. Aerial View of the Test Site Prior to the Detonation Showing the Stack of M117 Bombs Used as a Donor Charge. Also visible are the five acceptor magazines.

## FAR FIELD TEST LAYOUT

One objective of the test was to acquire additional data relating to selection of appropriate separation distances between inhabited buildings and public highways and sites for handling and storage of explosives. To obtain these data, window test structures and common types of vehicles were placed in the blast and fragment field in accordance with plans outlined in Figure 1 of Appendix B.

### WINDOW TEST STRUCTURES

Ten wood frame cubes, approximately 9 feet on a side, were constructed in the shops of the Public Works Department. The cubes served as structures for the mounting of selected typical window frames and window glass. After completion of shop fabrication, the cubes were transported to the ESKIMO II site and installed at 1,210, 1,700 (Figures 10 and 11), and 3,400 feet from the

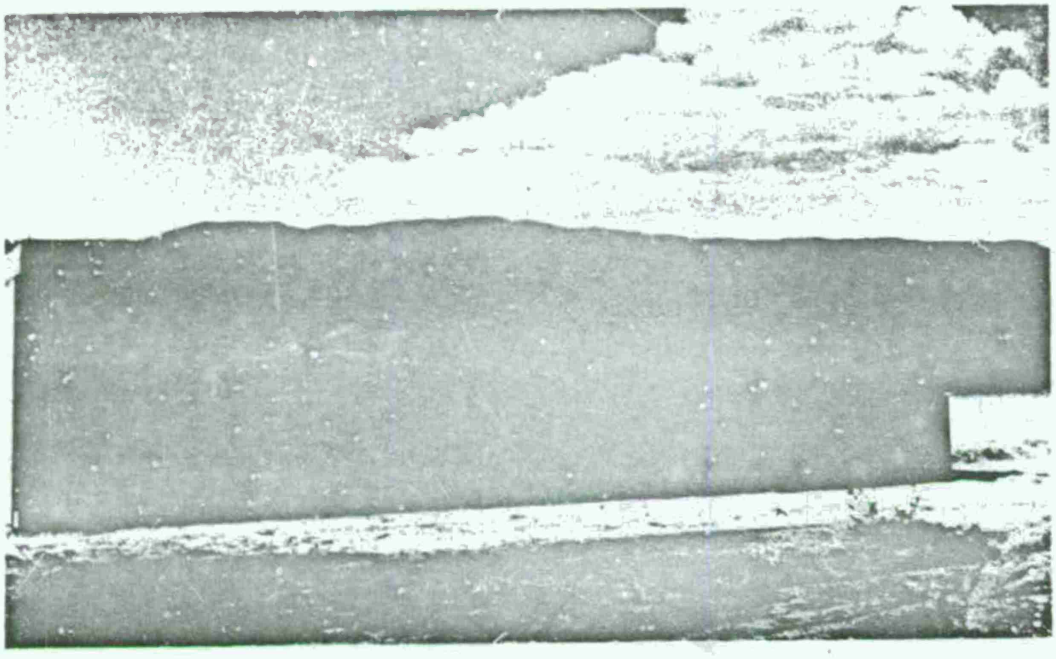

Figure 10. Window Cubes at 1,210 Feet, Prior to Detonation.

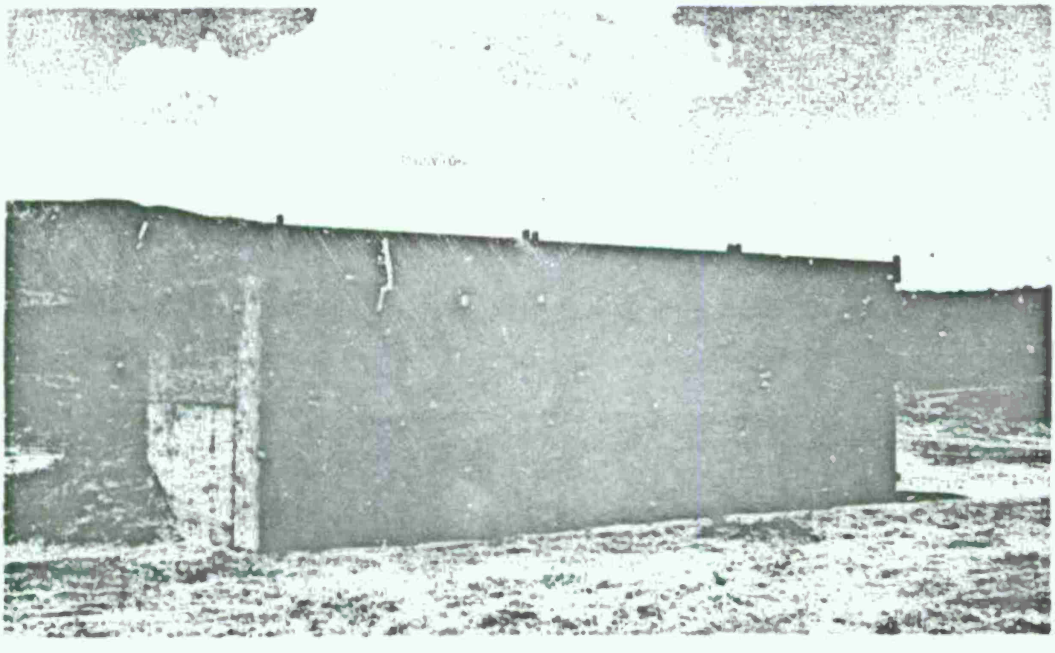

Figure 11. Window Cubes at 1,700 Feet, Prior to Detonation.

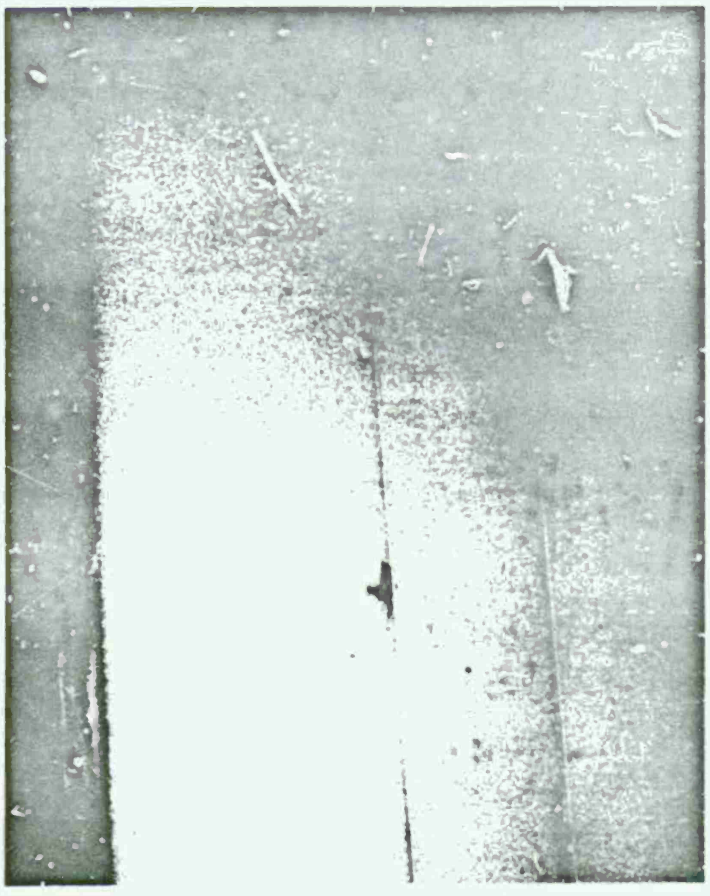

Figure 12. Glass Fragment Traps in Place on Back Wall of Window Boxes at 1,700 Feet.

donor charge center. During installation the cubes were bolted together in groups of three or four and secured against overturning by bracing and earth fill on the rear. Seven of the 10 cubes were equipped with Styrofoam witness panels (glass fragment traps as in Figure 12), provided by the Lovelace Foundation for Medical Education and Research, under NWC contract. One of the cubes, positioned at 1,210 feet from the donor, contained an anthropomorphic dummy provided by the Lovelace Foundation. The responses of the dummy and of the window in front of the dummy were recorded by an NWC 16-mm camera operating at approximately 400 frames per second. Window test cubes were constructed, sited, installed, and fitted with accessories in accordance with NWC Dwg. IR No. 7-4777/A-1 A-2, Shop Control WO 57-282.

For information on test results for these structures, see Appendix B.

## VEHICLES

Five vehicles were placed side-on to the blast at 730 feet from the donor on the northwest radial line:

1. Volkswagen sedan ("bug")
2. Dodge station wagon
3. Peugeot sedan
4. Chevrolet sedan
5. Defueler tank truck

While an average distance of 730 feet from the donor was maintained for all five vehicles, the positions of individual vehicles were staggered so that the cameras situated atop the instrument barricade would have a clear view of each vehicle. These cameras recorded vehicle response.

The Dodge station wagon contained an anthropomorphic dummy provided by the Lovelace Foundation. Responses of the dummy located in the driver's seat and of the side windows adjacent to the driver were recorded by a 16-mm camera operating at 400 frames per second.

Two vehicles, a Lincoln sport sedan and a Volkswagen microbus, were oriented side-on to the blast at a distance of 1,130 feet on the northwest radial; and one vehicle, an Oldsmobile sport sedan, was also oriented side-on at a distance of 1,700 feet on the same radial. Cameras were not used to cover the responses of these three vehicles.

Two vehicles, a Pontiac sport sedan and a Renault sedan, were oriented head-on at a distance of 730 feet from the donor on the southwest radial. Vehicle response was covered from a camera atop the instrument barricade. Spacing of these vehicles was staggered to facilitate camera coverage.

Appendix B discusses the responses of all vehicles to the test.

## AIRCRAFT

The B-29 aircraft, previously located at 1,300 feet and 330 degrees azimuth from the former ESKIMO I donor, was moved to a position near the northwest radial and at a distance of 1,210 feet from the center of the ESKIMO II donor. Holes in the aircraft were covered, and the damaged tail was partially repaired.

# INSTRUMENTATION

## PRESSURE GAUGES AT OR NEAR IGLOO HEADWALLS

Table 3 describes gauges placed to record side-on pressure 2 feet forward of igloo headwalls and 2 feet off igloo centerlines at ground level. The table also describes gauges used to measure reflected pressure in wingwalls or headwalls approximately 4 feet above the ground surface.

TABLE 3. Placement of Gauges at or Near Headwalls.

| Igloo | Gauges | | | | |
|---|---|---|---|---|---|
| | Postion | Number | Type | Rating, psi | Max. calibration step, psi |
| A | Wingwall | 2 | Kistler [a] | 5 to 500 | 150 |
| A | Ground | 1 | Kistler | 0 to 100 | 100 |
| B | Headwall | 2 | Kistler | 0 to 500 | 150 |
| B | Ground | 1 | Kistler | 0 to 100 | 100 |
| C | Headwall | 1 | Kistler | 0 to 500 | 150 |
| C | Headwall | 1 | Kistler | 0 to 5,000 | 150 |
| C | Ground | 1 | Kistler | 0 to 100 | 100 |
| D | Headwall | 1 | Kistler | 0 to 500 | 150 |
| D | Headwall | 1 | Kistler | 0 to 5,000 | 150 |
| D | Ground | 1 | Kistler | 0 to 100 | 100 |
| E | Headwall | 2 | Kistler | 10 to 3,000 | 150 |
| E | Ground | 1 | Kistler | 0 to 100 | 100 |
| E | Ground | 1 | Bytrex [b] | 0 to 150 | 100 |

[a] All Kistler gauges are piezoelectric.
[b] Strain gauge type.

## FAR FIELD PRESSURE GAUGES

Ballistic Research Laboratories (BRL) self-recording mechanical gauges were placed in pairs at 730, 1,130, 1,210, 1,700, and 3,400 feet on the northwest radial and at 730 feet on the southwest radial. These are positions also designated for vehicles or window test cubes or both; care was exercised to assure that structures or vehicles did not shield the gauges. Gauges were not closer than 20 feet to any vehicle or structure measured perpendicularly to the radial from the donor center. The selection of gauge capsules was based on the following schedule:

| *Distance from donor* | *Expected peak overpressure, psi* | *Capsule rating, psi* |
|---|---|---|
| 730 | 2.4 | 5.0 |
| 1,130 | 1.75 | 5.0 |
| 1,210 | 1.2 | 5.0 and 1.0 |
| 1,700 | 0.75 | 1.0 |
| 3,400 | 0.29 | 0.5 |

## ACCELEROMETERS

Accelerometers were placed at mid-height near the free edge of each leaf of each hinged door and at a similar position (near mating edges) of biparting sliding doors. For the single sliding door (Igloo D) two accelerometers were symmetrically placed approximately 12 inches apart near the centroid of the frontal area.

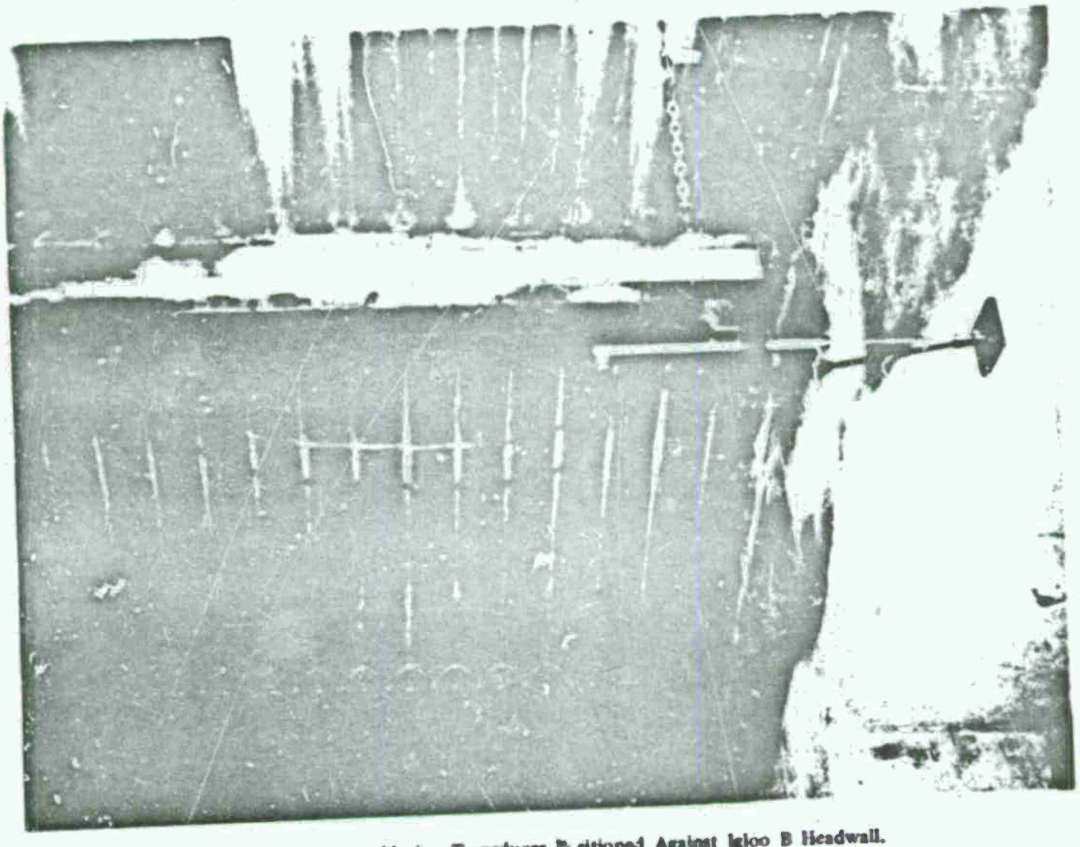

Figure 13. Linear Motion Transducer Positioned Against Igloo B Headwall.

## LINEAR MOTION TRANSDUCERS

Motion transducers were placed approximately 10 inches above the top of the doorway and on or near the igloo centerline (Figure 13) to measure the movement of the concrete headwall. The female part of the transducer was attached to a universal joint mounted on a rail section suspended from the corrugated metal roof of the igloo by chains. The male or rod portion was supported by universal joints, as in ESKIMO I, with one universal joint securely attached to the headwall at the desired point of measurement.

## ZERO TIME INDICATOR

Zero time or detonation time for the M117 bombs was determined by:

1. An ionization probe or switch buried in the bomb stack between bomb butt ends
2. A light sensing device mounted atop Igloo D, directed toward the bomb stack and shielded from light not originating from the bomb stack

## PHOTO-OPTICAL COVERAGE

Photographic records of the test were obtained by 6 high-speed (up to 5,000 frames per second) 16- and 35-mm ground-based cameras and by other cameras operating from 24 to 1,000 frames per second. Most cameras were located 1,500 feet to the west and south of the test site; 16-mm cameras, operating at 400 frames per second, were used to cover the response of the dummies in one vehicle and one window cube. In addition, response of the vehicles was obtained by 35-mm cameras operating at 500 to 600 frames per second.

Airborne motion-picture or sequencing type cameras were also used. Black-and-white and color pictures of pretest and post-test conditions were taken by still cameras as necessary for documentation.

Oblique views of the headwalls of the donor and the five acceptor igloos were obtained, as well as overall views of the entire site. Photography of the interior of the igloos showed the inward collapse of the doors.

## TIMING

A timing correlation at 1,000 cps was recorded on all tape records of Kistler and Bytrex gauges, accelerometers, and motion transducers, and on motion-picture film records of cameras operating at 400 frames per second or higher.

# ESKIMO II DETONATION

At 1100 on 22 May 1973, the donor charge was detonated. The explosion source in ESKIMO II was designed to produce an impulse load of 1,100 psi-msec on each of the acceptor igloo fronts, with an initial peak reflected pressure of 130 psi. Measurements of blast loading made during the test show, however, that the actual loadings were significantly higher than the design level, and exhibited strong directional effects. The measured impulse loads ranged from 1,300 psi-msec with an initial reflected peak of about 200 psi on Igloo E (west), to 2,200 psi-msec with an initial peak of 270 psi on Igloo D (south). The reasons for the strength and directionality of the near field blast loading are not clearly understood. However, similar effects have been observed in prior tests using donors of cubical and other plane-faced configurations.

The high blast loads observed in this event demonstrate the difficulty in designing an explosion source from available surplus ammunition to produce, accurately and repeatably, a specified level of loading for test purposes.

# TEST RESULTS

Based on fragment size and presently available data from gauge records, it is believed that

Figure 14. Test Site After Detonation. Note that earth revetment around donor remains essentially intact. D Magazine is in the background.

complete, or essentially complete, detonation was achieved. The crater produced was basically a deepening of the 20- by 20-foot area within the four-sided earth embankment surrounding the donor charge. The interior sides of the embankment were eroded only slightly and the top of the embankment was not breached by the explosion (Figure 14). Varying amounts of structural damage were incurred by the test magazines. Details on this damage are presented with illustrations in the following sections.

## OBSERVED STRUCTURAL RESPONSE

### Igloo A (North)

On Igloo A, the standard U.S. Navy headwall and door combination was tested at a blast impulse loading about 60% greater than the test design level. Despite this, none of the 12 acceptor charges received sufficient damage to induce burning or explosion; however, some of the charges were

severely damaged and broken open to release fragmented explosive. Igloo structural response was as follows:

1. The doors were forced inward, bending to pass the door stops, and were separated from their hinges, coming to rest in the corresponding forward corners of the igloo.

2. The concrete headwall was severely cracked. Fragments spalled completely from portions of the wall, leaving only the reinforcing mesh in place (Figures 15-17).

3. Steel door stops at the top and bottom of the door opening remained intact. The door jambs were separated from the concrete headwall except at the extreme top of the door opening.

## Igloo B (Northeast)

Igloo B, also subjected to blast impulse loading 60% greater than the design level, did not contain explosive acceptors. Damage was as follows:

1. The relatively light gauge steel sheets that had been plug-welded to the inside faces of the door leaves were stripped off (Figure 18). (In most storage situations, initiation of explosives by impact of these sheets would be unlikely.) The inboard support trolleys were also detached, allowing the inner door edges to swing into the door opening. The outboard trolleys also detached from the support rail, but, despite severe deformation, the doors remained upright (Figures 19 and 20).

2. Modest damage to the headwall was sustained (Figures 21 and 22). Cracking of the headwall was most pronounced at the top corners of the door opening, especially at the right side (from a position facing the igloo). Some spalling occurred on the inside.

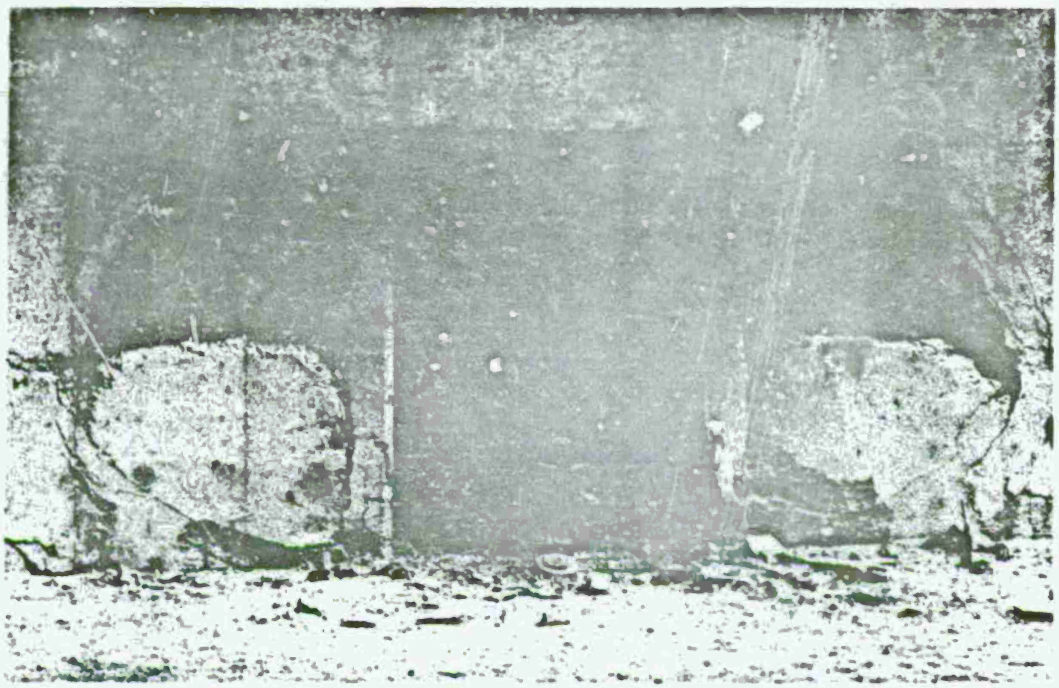

Figure 15. Door Opening of Igloo A Showing Two Land Mines (Acceptors) Where They Came to Rest.

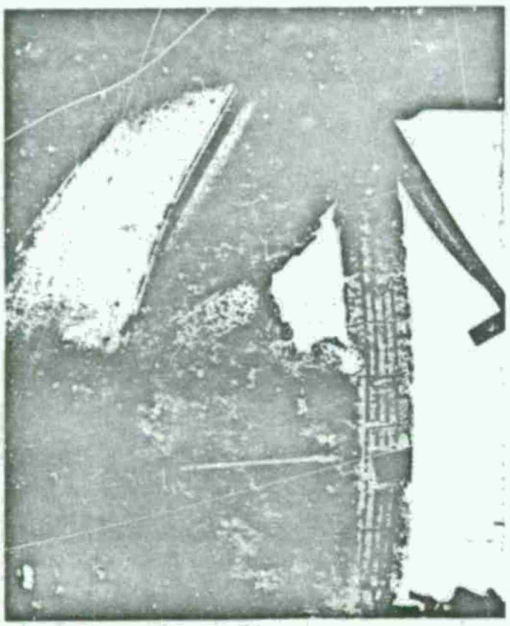

Figure 16. Damaged Headwall Inside Igloo A, East of Door Opening.

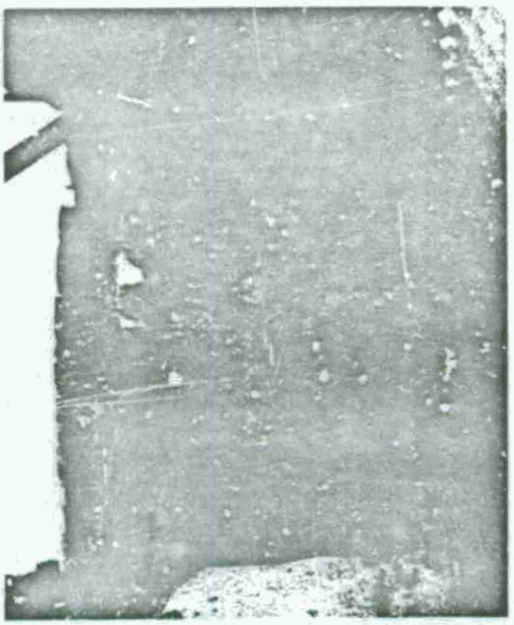

Figure 17. Damaged Headwall Inside Igloo A, West of Door Opening.

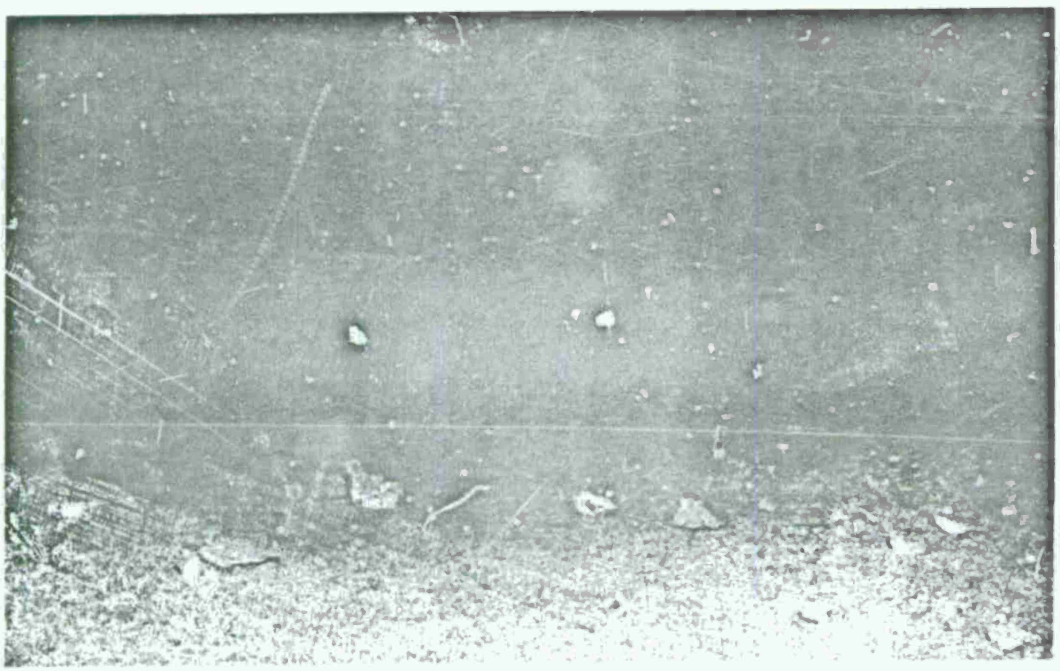

Figure 18. Steel Sheet From Inside Face of Igloo B Door.

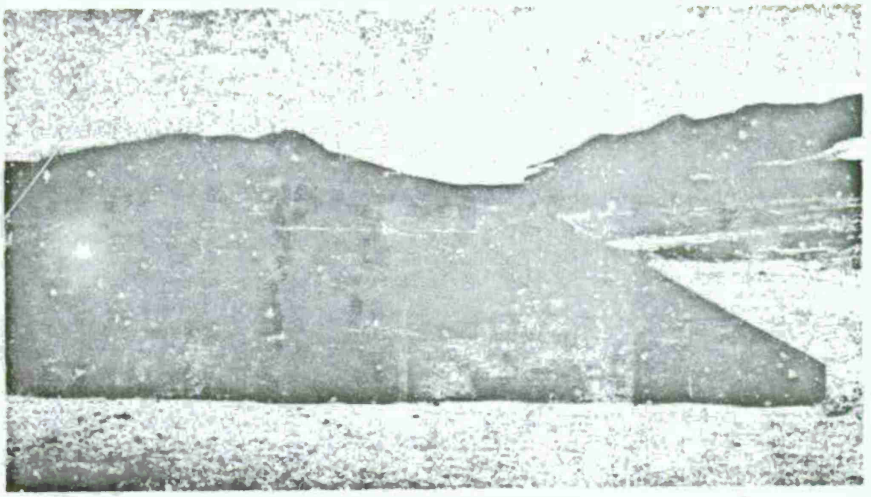

Figure 19. Front of Igloo B Showing Damage to Doors and Headwall.

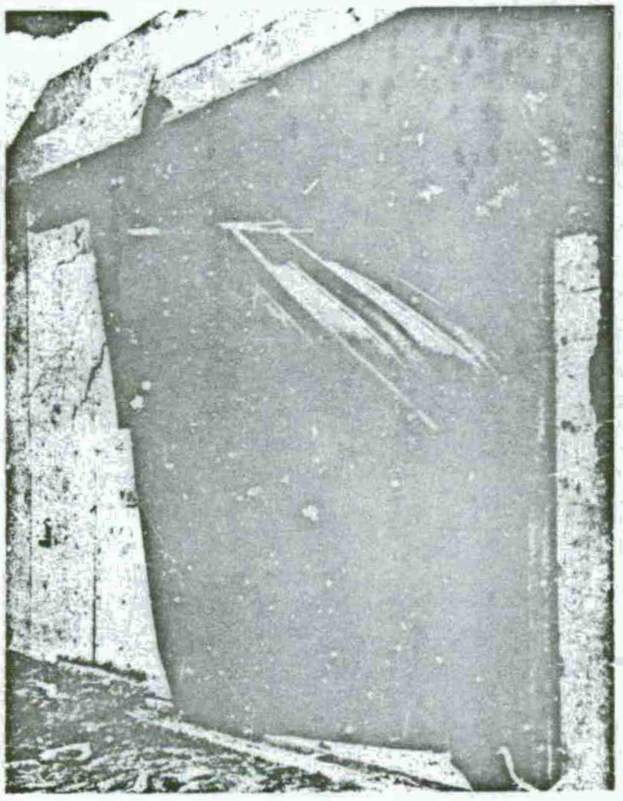

Figure 20. Damaged Doors and Headwall of Igloo B.

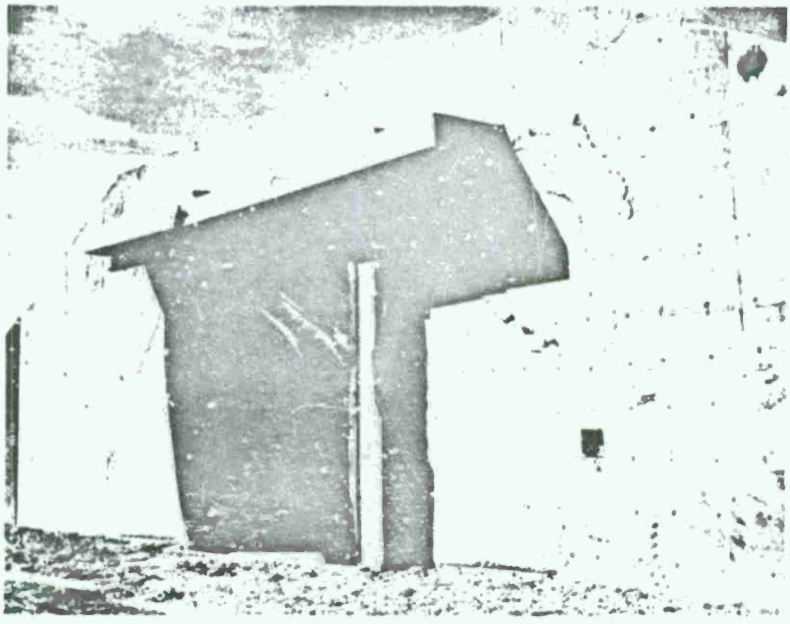

Figure 21. Doorway of Igloo B Showing Damaged Headwall and Doors.

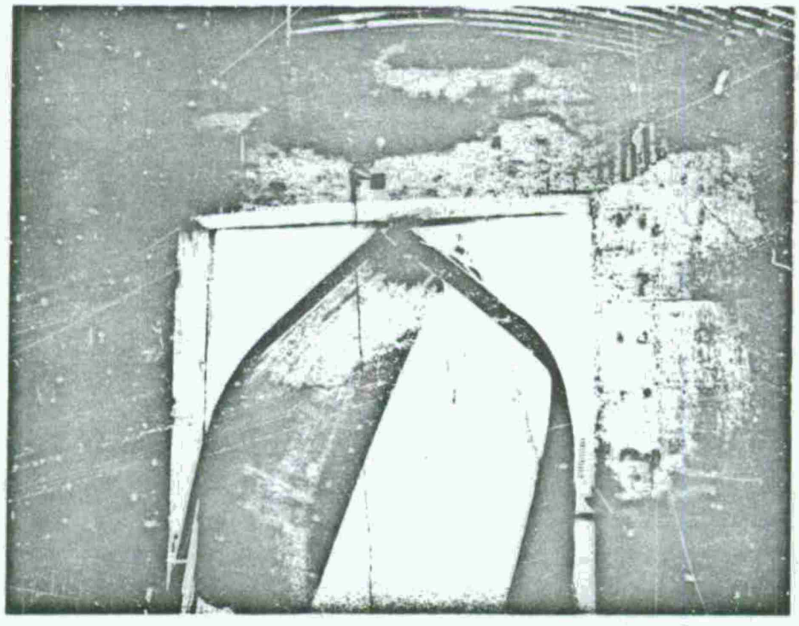

Figure 22. Inside Surface of Headwall in Igloo B. Also shown is the linear motion gauge still in place above the doorway.

## Igloo C (East)

Igloo C was built with the headwall and door combination (Figure 5) for the current standard steel-arch magazine. The igloo was identical to the structures tested in ESKIMO I. It was included in ESKIMO II for test control and comparison purposes.

Igloo C did not contain explosive acceptor charges. Structural damage was as follows:

1. The doors were thrown inward by the blast and, after experiencing considerable bending and distortion, they came to rest in the interior of the igloo (Figures 23-25).

2. The headwall cracking pattern resembled that of the igloos of ESKIMO I (Figures 26 and 27). The permanent deformation incurred was greater than that experienced by either the south igloo or the right side of the west igloo of ESKIMO I.

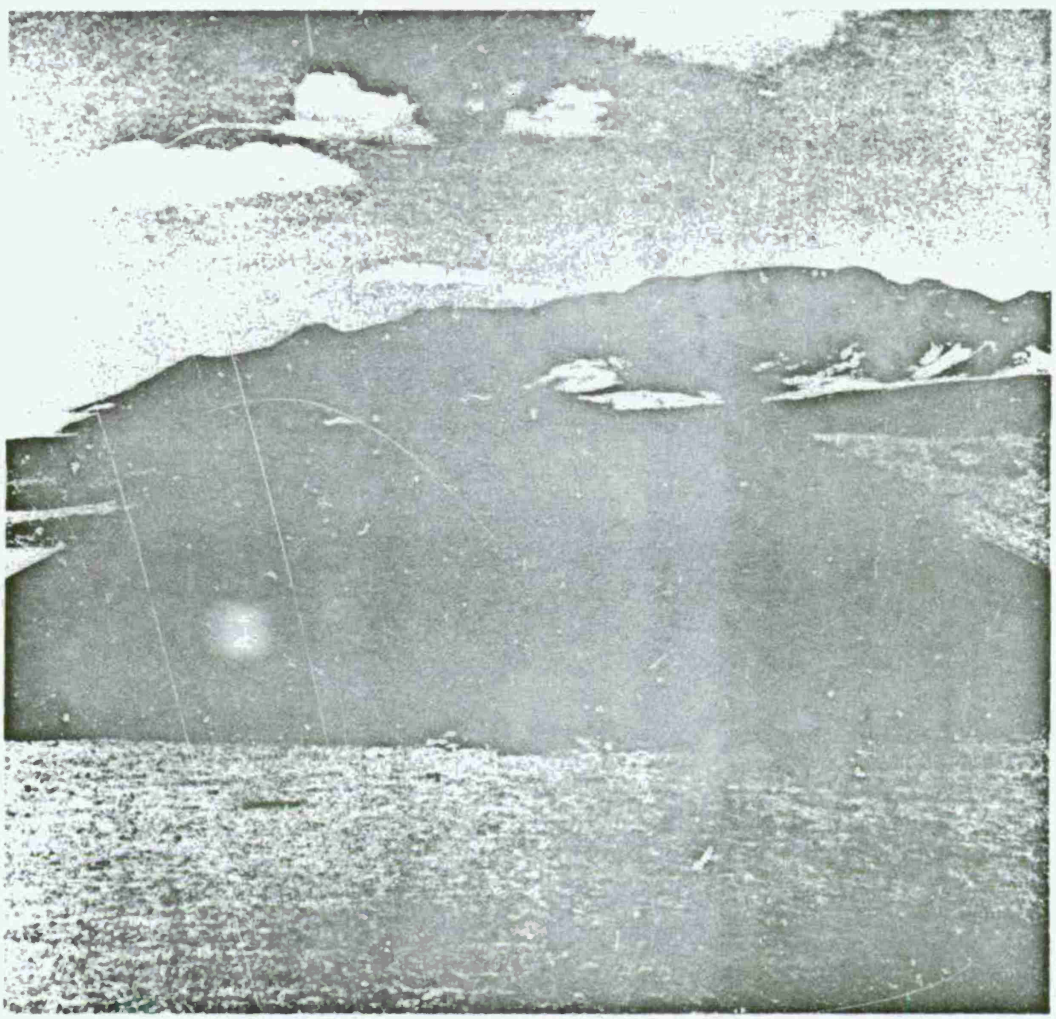

Figure 23. Overall Post-Test View of Control Igloo C.

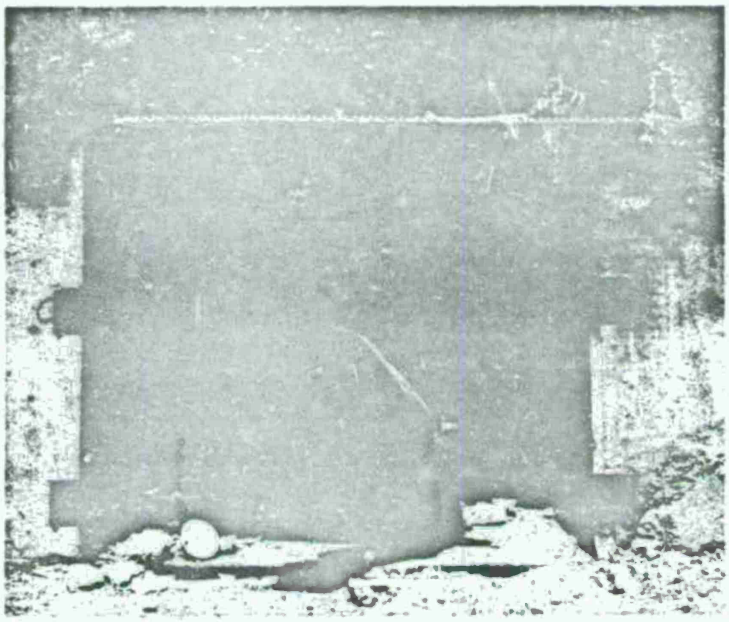

Figure 24. Crumpled Door and Damaged Headwall of Control Igloo C.

Figure 25. Hinge Plate and Bottom of Door Jamb on Igloo C Showing Method of Failure.

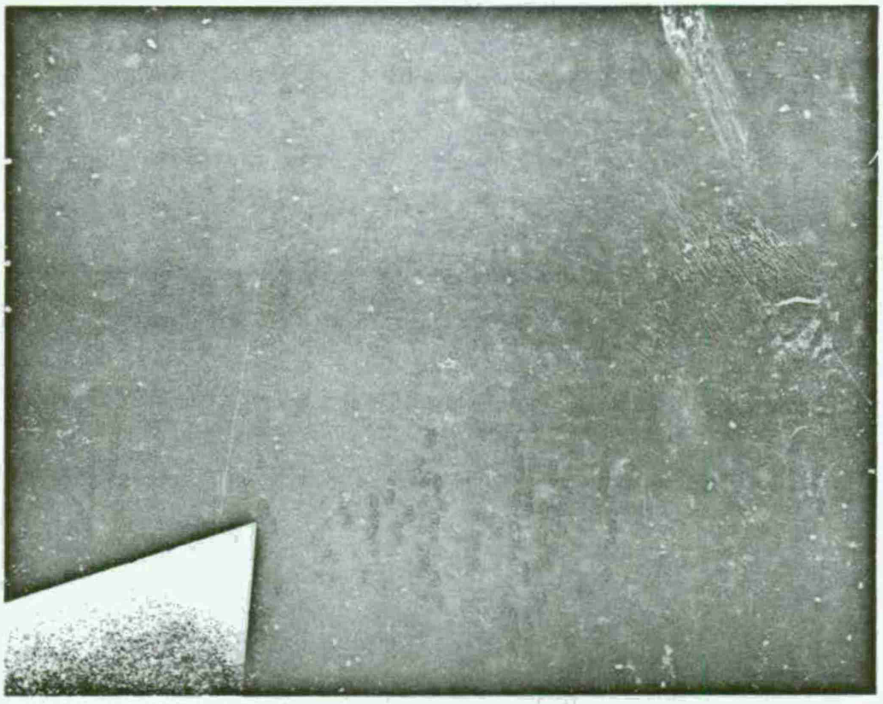

Figure 26. Inside Doorway of Control Igloo C Showing Damage to Inside of Headwall.

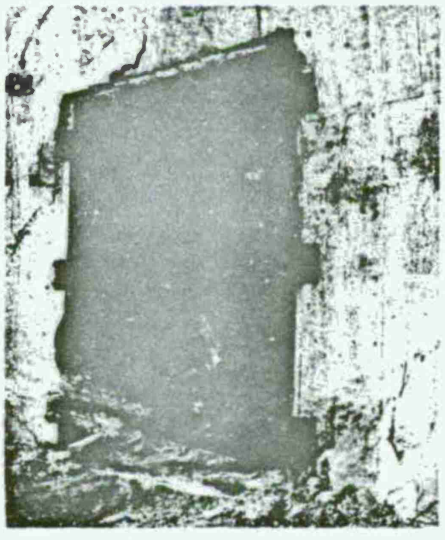

Figure 27. Damaged Headwall of Control Igloo C. Crumpled door and plates are visible.

## Igloo D (South)

The acceptor land mines in Igloo D were somewhat damaged, but to a lesser degree than those in A and E (Figures 28 and 29). No burning occurred. Structural damage was as follows:

1. The one-piece, trolley-suspended, steel door was designed to span the door opening horizontally under blast loading, thus making the sides of the door opening the reaction lines for the loading. The basic portion of this newly designed door maintained its integrity, with rather minor distortion. The bow in the door was approximately 9 3/4 inches at the bottom edge. Figures 30 and 31 show damage to locking mechanism and trolleys.

2. Essentially all of the portion of the headwall that adjoined the interior magazine space (the space under the arch) was destroyed (Figures 32-34). It is believed that the headwall carried all the blast load impinging on the headwall and door and did not benefit by the load relief afforded at the other magazines by door failure or rotation. The upper corners of the headwall moved forward about 3 inches.

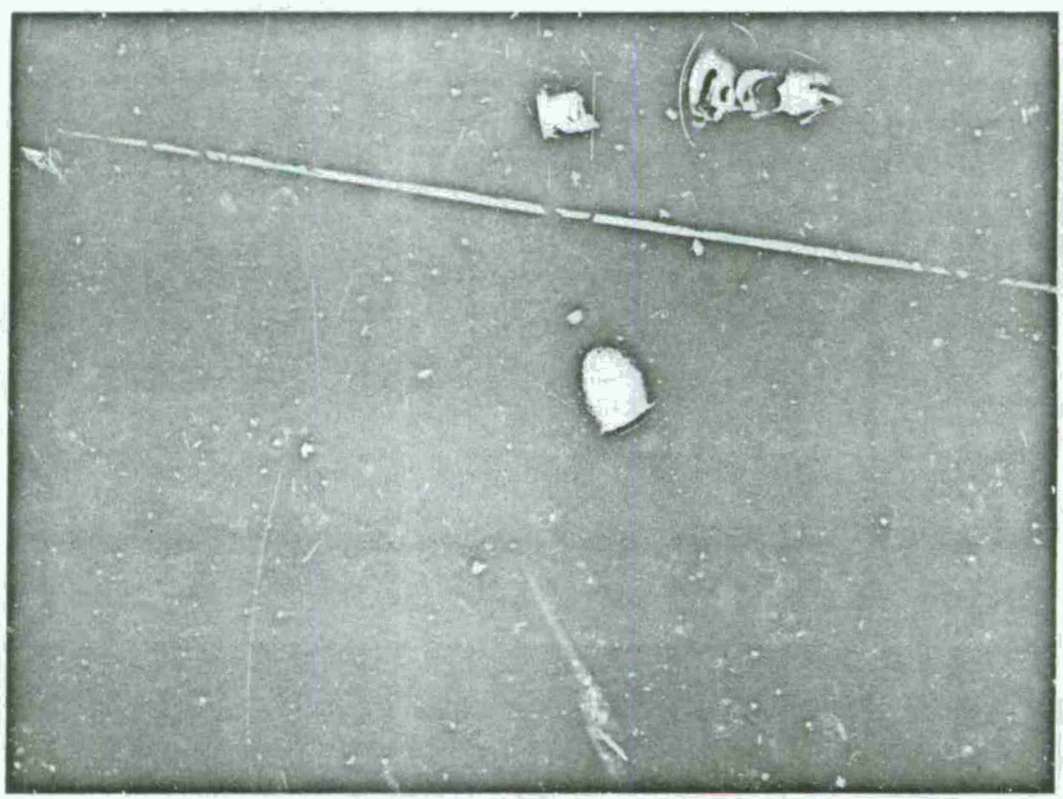

Figure 28. Inside Igloo D Showing Acceptor Land Mine Partially Under the Door. Blast blew door inward.

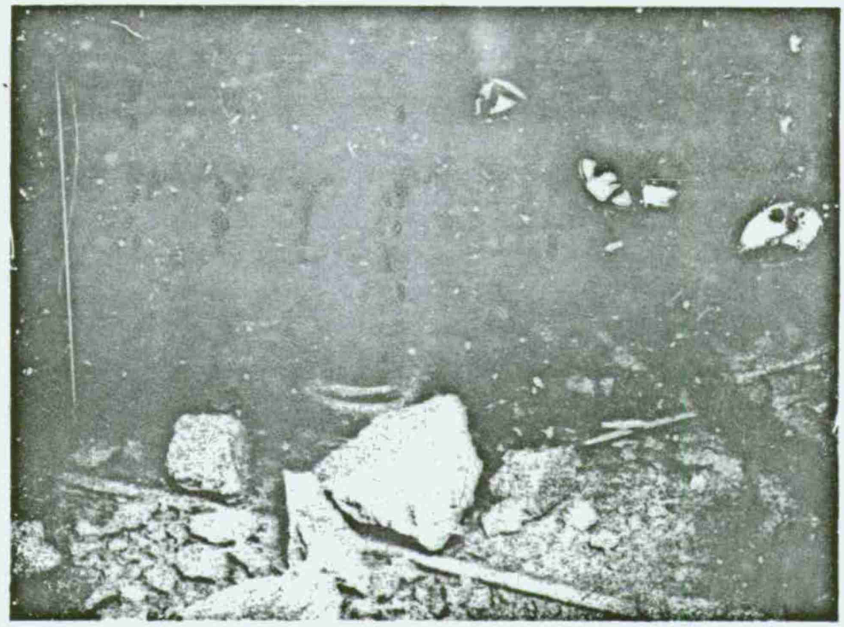

Figure 29. Debris on Floor Inside Igloo D. None of the mines burned or exploded.

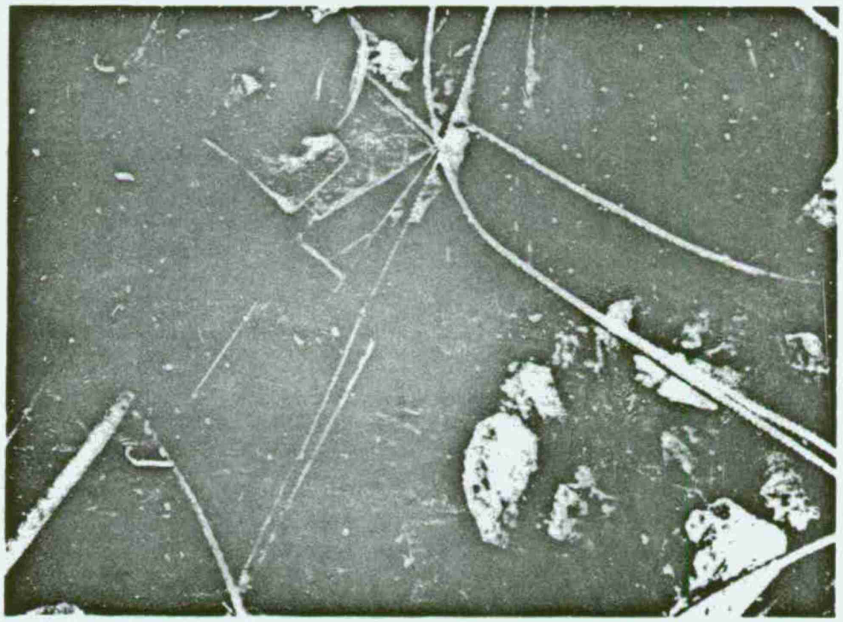

Figure 30. Door Locking Mechanism for Igloo D Showing Method of Failure. As door buckled inward, the piece of locking mechanism under head of pin was torn off.

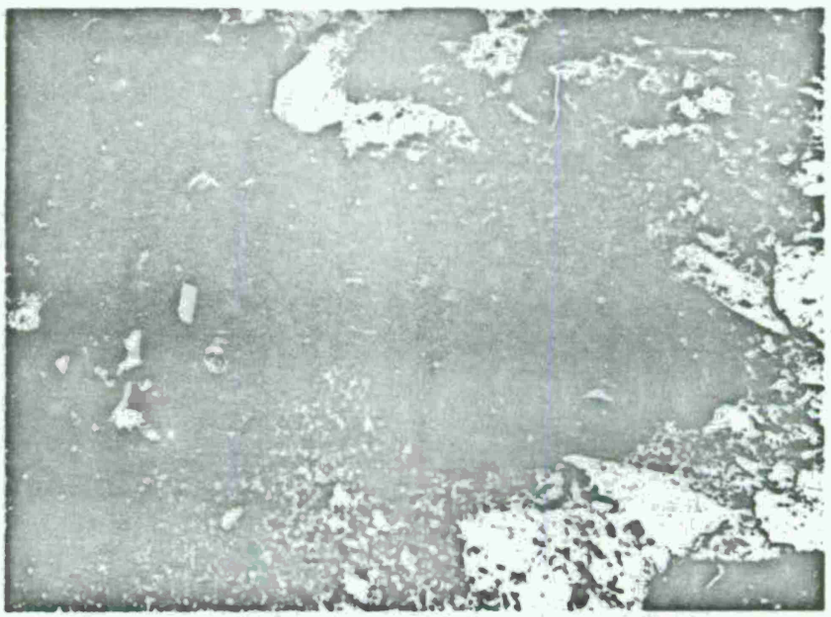

Figure 31. Overhead Door Trolleys From Igloo D. Both hangar bolts failed in tension.

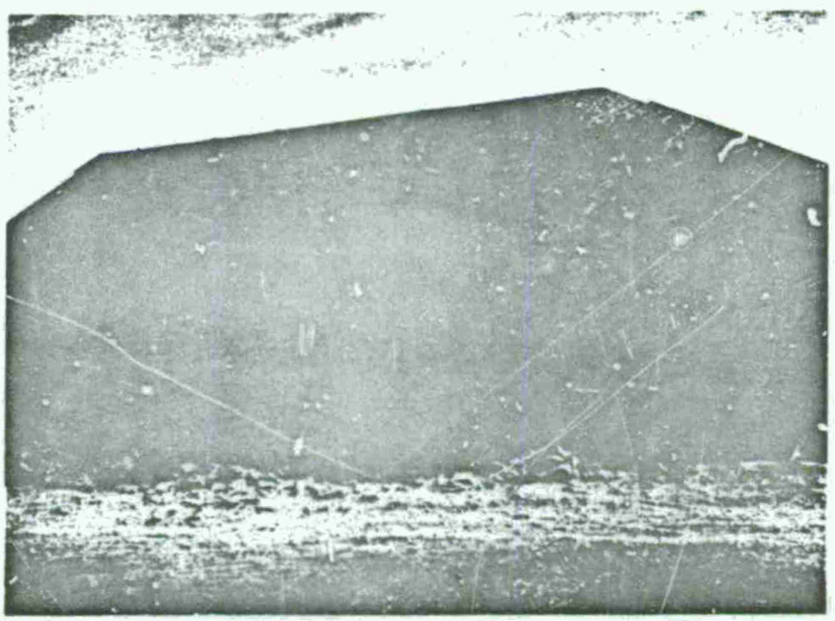

Figure 32. Igloo D After Blast Showing Damage to Concrete Headwall and to Door Frame.

Figure 33. Looking Into Igloo D From Doorway Showing Shattered Headwall and Warped Door. None of the 12 mines in this magazine exploded or burned; one was badly shattered.

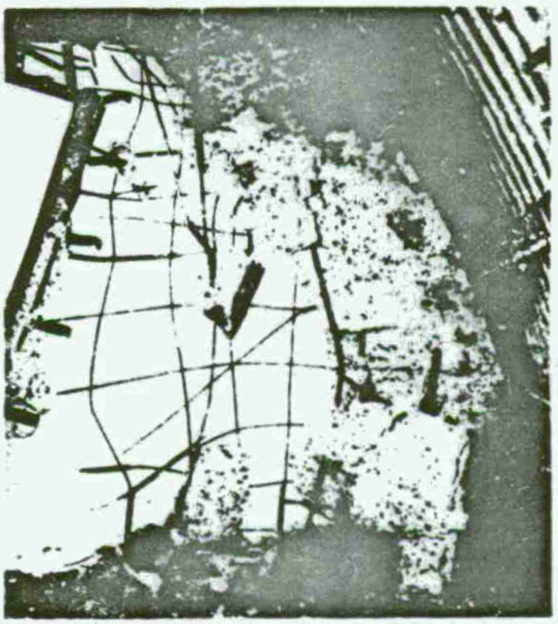

Figure 34. Shattered Headwall East of Door Inside Igloo D.

## Igloo E (West)

Igloo E was of the same construction as the igloos of ESKIMO I, but the doors were strengthened by the addition of a movable structural beam that spanned the opening behind the door. The igloo was subjected to an impulse load only slightly greater than the test design level, yet the headwall sustained significantly greater damage than the headwall of Igloo C.

Eight of the 12 land mine acceptors burned; however, there was no way to determine how many of these were burned as a result of fragment attack and how many were burned as a result of heat generated by burning explosive (Figures 35 and 36). Structural damage was as follows:

1. The large steel beam that spanned the door opening horizontally and that was planned to support the door under blast loading failed at points of attachment to the headwall (Figures 37 and 38). (There was an apparent tension failure in the two 3/4-inch bolts attached at the side of the headwall.)

2. The doors were supported against blast loading at the hinges and at the top and bottom. Further door support was provided by bearings on stops welded to the head of the door and by a round steel rod projecting inward and bearing on the steel beam. During the test the doors were dislodged and thrown to the back of the magazine. Door deformation was of moderate degree and was consistent with the location of the support points (Figure 39).

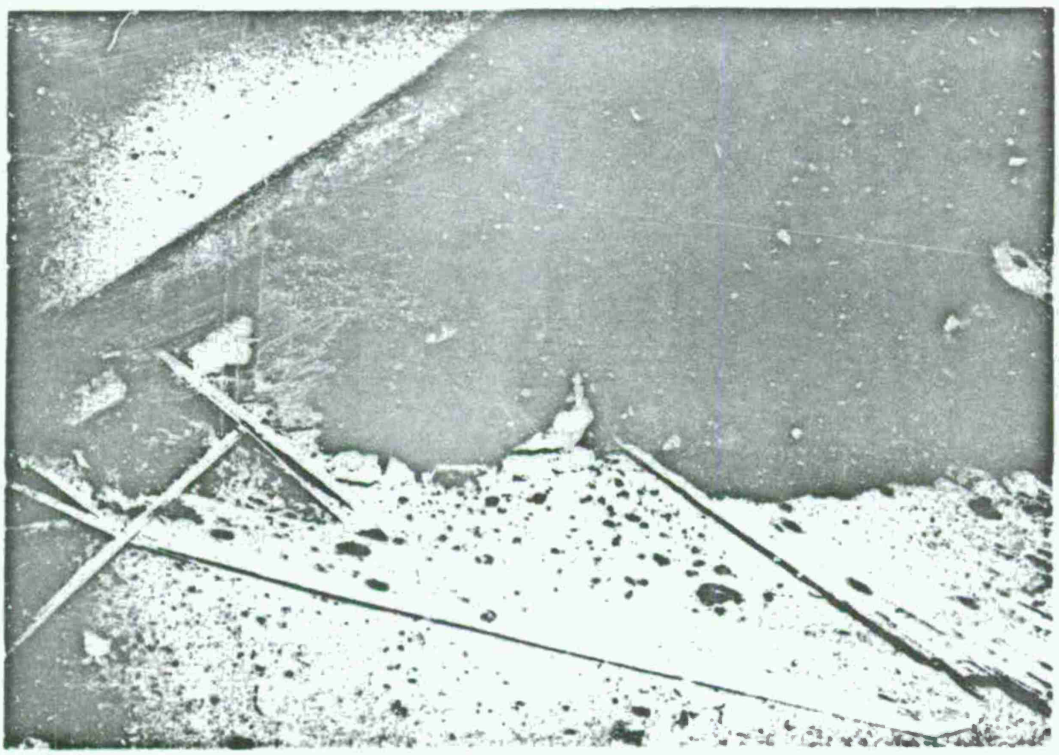

Figure 35. Burned-out Mine Case in Igloo E. Also shown are one damaged door and the large beam used as door restraint.

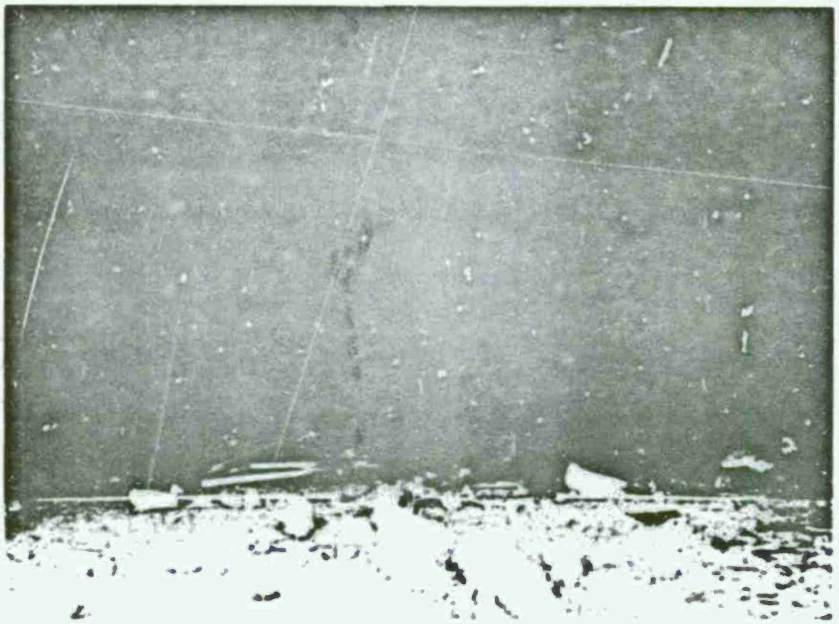

Figure 36. View of Interior of Igloo E Showing Debris at Rear Wall. Eight of the acceptor land mines burned along this rear wall. Railroad rail hanging down in foreground supported the linear motion gauge.

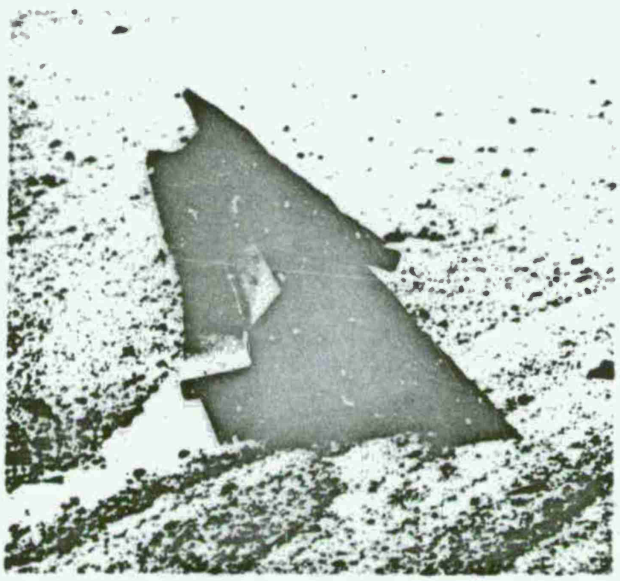

Figure 37. Twisted I-Beam Recovered From Igloo E. This beam was bolted to door frame to provide additional restraint to door.

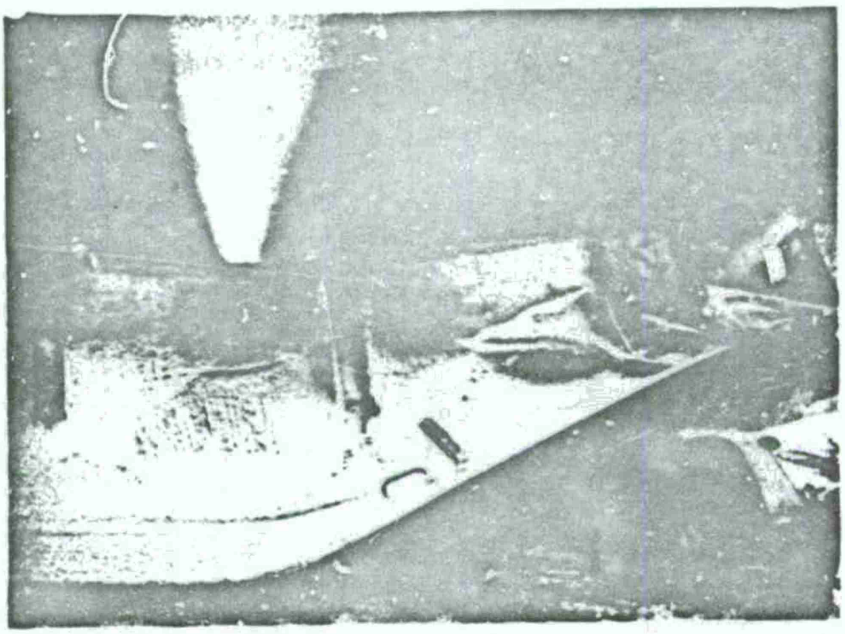

Figure 38. Piled Against Rear Wall Are Remains of One Door and Large Steel Beam Used to Restrain Doors on Igloo E. Note also discoloration of wall where mines burned on floor.

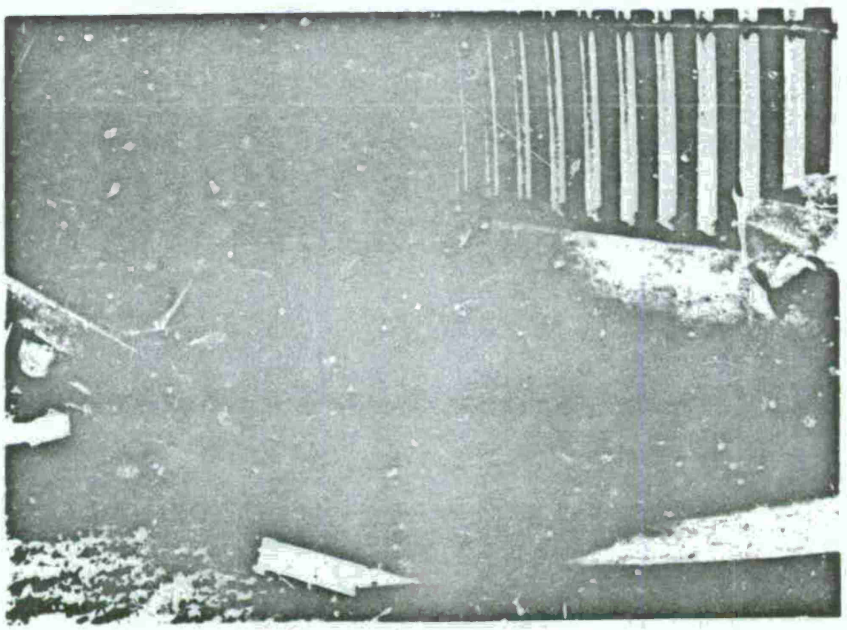

Figure 39. Remains of Left Door Along South Wall Inside Igloo E.

3. The headwall damage was less than that of Igloos A and D, but somewhat more than that of Igloo C (Figure 40). The portion of headwall above the door opening experienced a large deformation because of the reaction of the door against the door stops. Although they were bent backward, the door stops remained attached (Figure 41).

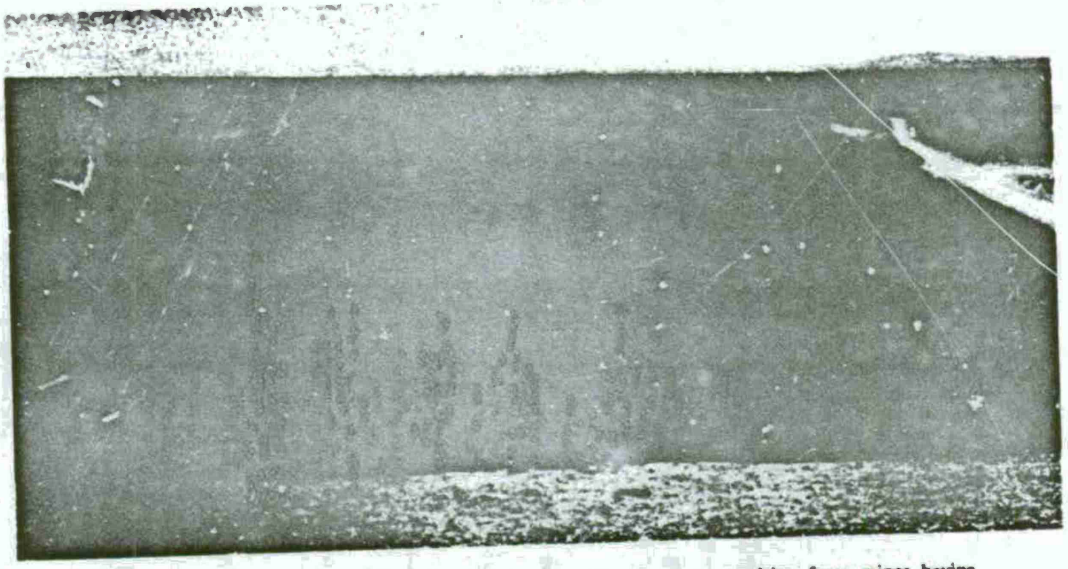

Figure 40. Overall View of Igloo E. Note smudge over the door resulting from mines having burned inside.

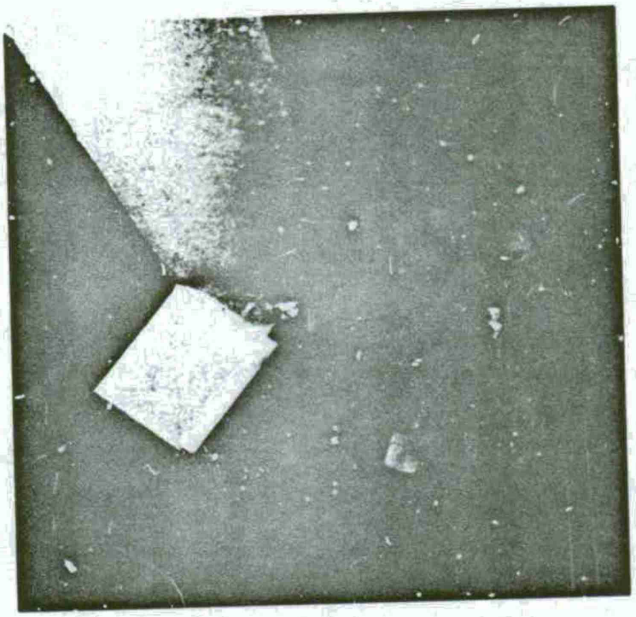

Figure 41. Door Stops Bent Backward Over Doorway of Igloo E.

## STATIC MEASUREMENTS OF STRUCTURAL RESPONSES

### Arch Motion in Igloo B

Three simple scratch gauges were installed in an attempt to secure an approximation of the movement of points on the noncircular arch at the igloo mid-position, that is, halfway between forward and rear walls. One gauge rod extended vertically from the center of the floor to a point at the crown of the arch. Two others were inclined at an angle of approximately 30 degrees from the vertical, one on each side of vertical. Total dynamic movements in feet relative to the floor attachment during the blast were as follows:

| *North* | *Vertical* | *South* |
|---|---|---|
| 0.076 | 0.15 | 0.05 |

The vertical height at the center was restored to a permanent deformation of 0.11 foot.

### Permanent Deformation of All Headwalls and Arch Deformation in Igloo B

The permanent deformation of headwalls (Figures 42-44 and Tables 4 and 5) and of the steel arch in Igloo B (Figure 45 and Table 6) was determined by "before" and "after" measurements of selected positions. Headwalls were measured from a vertical plane approximately 3 feet away from the wall surface established by monuments outside the immediate blast area. Figure 44 graphically

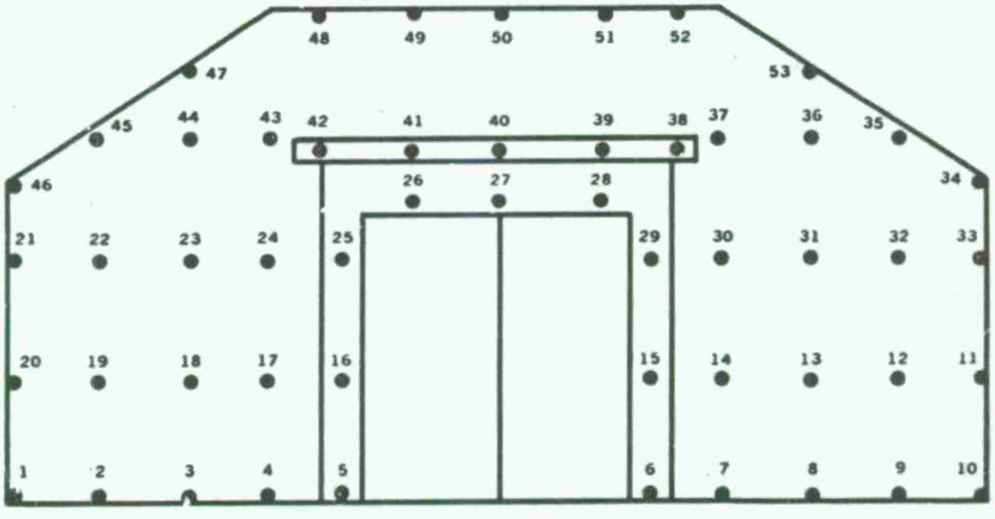


Figure 42. Position Key for Deformation Measurements, Igloo B Headwall.

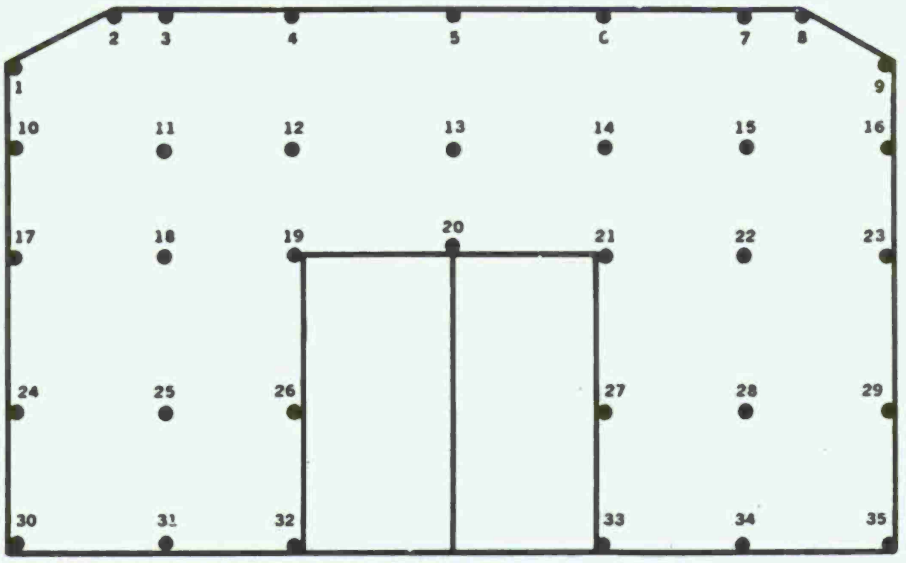


Figure 43. Position Key for Deformation Measurements, Headwalls of Igloos A, C, D, and E.

compares deformations of headwalls of the south igloo of ESKIMO I and Igloo C of ESKIMO II. Differences between average blast load parameters for these two igloos are recapitulated below:

| *Igloos* | *Peak overpressure, psi* | | *Impulse, psi-msec* |
|---|---|---|---|
| | *Incident* | *Reflected* | |
| South igloo, ESKIMO I | 33 | 61 | 619 |
| Control Igloo C, ESKIMO II | 60 | 245 | 1,480 |

The arch measurements were made from a steel ball (trailer hitch) screwed into a female attachment fixed to the floor of Igloo B, so that the measurements shown reflect relative movement between the floor and arch.

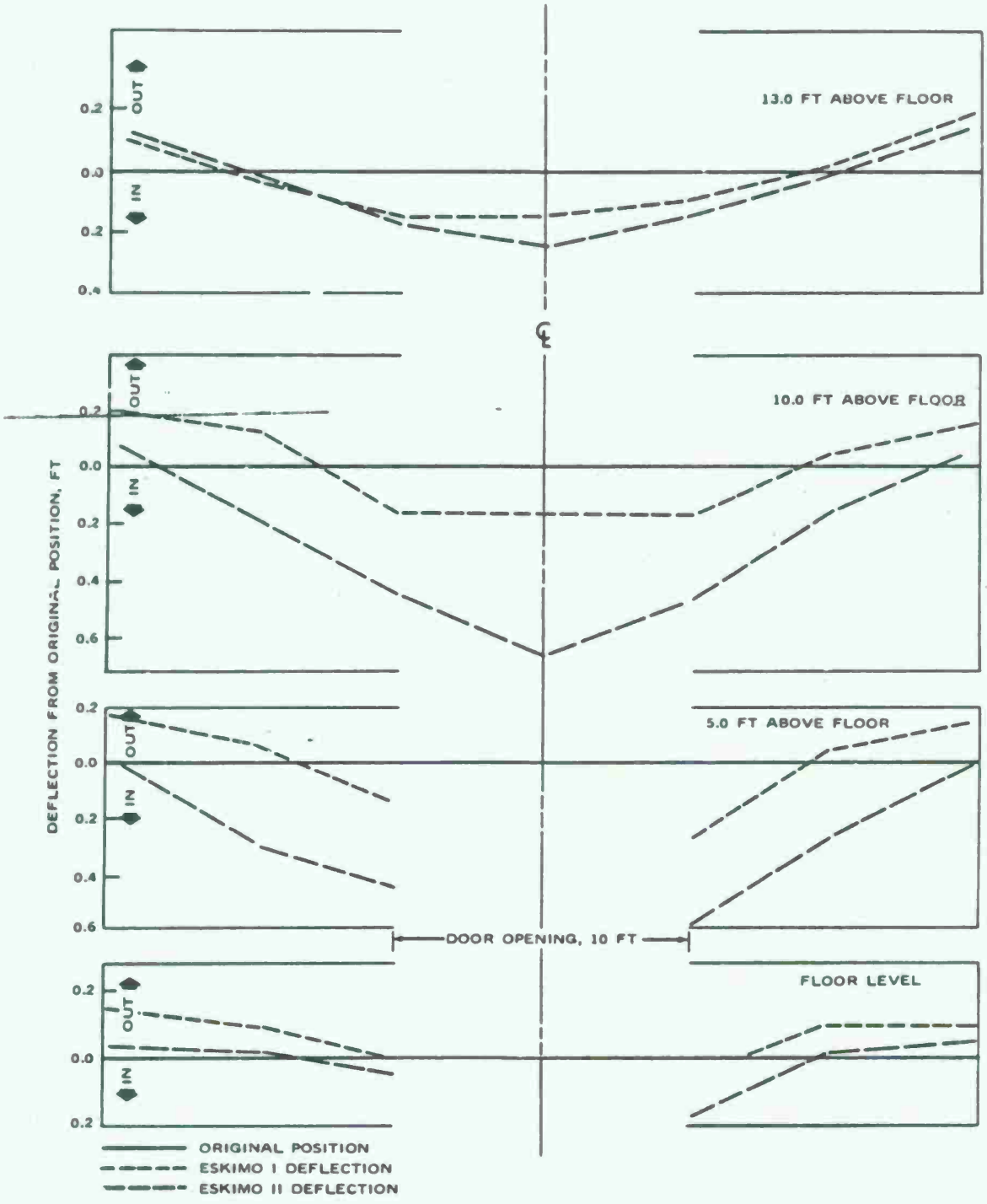


Figure 44. Comparison of Headwall Deformations, South Igloo of ESKIMO I and Control Igloo C of ESKIMO II.

TABLE 4. Summary of Headwall Permanent Movement in Feet for Igloos A, C, D, and E.

Negative values indicate outward deformation; positive values, inward. For locations of positions measured, see Figure 43.

| Position identification | Igloo A | Igloo C | Igloo D | Igloo E |
|---|---|---|---|---|
| 1 | −0.20 | −0.16 | −0.26 | −0.19 |
| 2 | − .20 | − .12 | − .25 | − .16 |
| 3 | − .11 | − .10 | − .14 | − .12 |
| 4 | − .01 | − .05 | − .07 | − .06 |
| 5 | .01 | − .03 | − .07 | − .07 |
| 6 | .00 | − .07 | − .06 | − .08 |
| 7 | − .10 | − .11 | − .15 | − .16 |
| 8 | − .21 | − .22 | − .23 | − .22 |
| 9 | − .20 | − .23 | − .26 | − .23 |
| 10 | − .11 | − .11 | − .16 | − .08 |
| 11 | .01 | .05 | .02 | .03 |
| 12 | .09 | .20 | .10 | .14 |
| 13 | .11 | .27 | .15 | .28 |
| 14 | .07 | .17 | .12 | .17 |
| 15 | .03 | .03 | .04 | .01 |
| 16 | − .09 | − .12 | − .14 | − .10 |
| 17 | − .01 | − .03 | .02 | .00 |
| 18 | .14 | .20 | .29 | .13 |
| 19 | .16 | .44 | .53 | .50 |
| 20 | .17 | .64 | 1.24 | 1.19 |
| 21 | .17 | .46 | missing | .58 |
| 22 | .22 | .16 | .27 | .15 |
| 23 | .02 | − .02 | .04 | .00 |
| 24 | .19 | .02 | .11 | .06 |
| 25 | .72 | .29 | 1.05 | .30 |
| 26 | .84 | .42 | missing | .79 |
| 27 | .75 | .55 | missing | .74 |
| 28 | .65 | .27 | 2.83 | .34 |
| 29 | .10 | .03 | .18 | .08 |
| 30 | .03 | − .03 | .03 | − .06 |
| 31 | .01 | − .03 | .01 | − .12 |
| 32 | .06 | .05 | missing | .28 |
| 33 | .05 | .22 | missing | .15 |
| 34 | .03 | − .02 | .76 | − .25 |
| 35 | 0.01 | −0.03 | 0.01 | −0.03 |

TABLE 5. Igloo B Headwall Permanent Movement in Feet.

Negative values indicate outward deformation; positive values, inward. For locations of positions measured, see Figure 42.

| Position identification | Deformation | Position identification | Deformation |
|---|---|---|---|
| 1 | −0.03 | 28 | 0.17 |
| 2 | .01 | 29 | .22 |
| 3 | .00 | 30 | .01 |
| 4 | − .05 | 31 | .02 |
| 5 | .00 | 32 | .02 |
| 6 | .00 | 33 | .02 |
| 7 | .00 | 34 | .03 |
| 8 | .01 | 35 | .04 |
| 9 | .02 | 36 | .04 |
| 10 | .00 | 37 | .08 |
| 11 | .02 | 38 | .09 |
| 12 | .03 | 39 | 12 |
| 13 | .05 | 40 | .14 |
| 14 | .11 | 41 | .10 |
| 15 | .15 | 42 | .01 |
| 16 | .14 | 43 | .03 |
| 17 | .08 | 44 | .01 |
| 18 | .04 | 45 | −.02 |
| 19 | − .03 | 46 | .03 |
| 20 | − .03 | 47 | .03 |
| 21 | − .03 | 48 | .08 |
| 22 | .02 | 49 | .06 |
| 23 | .01 | 50 | .05 |
| 24 | .02 | 51 | .10 |
| 25 | .21 | 52 | .10 |
| 26 | .16 | 53 | 0.07 |
| 27 | 0.19 | | |

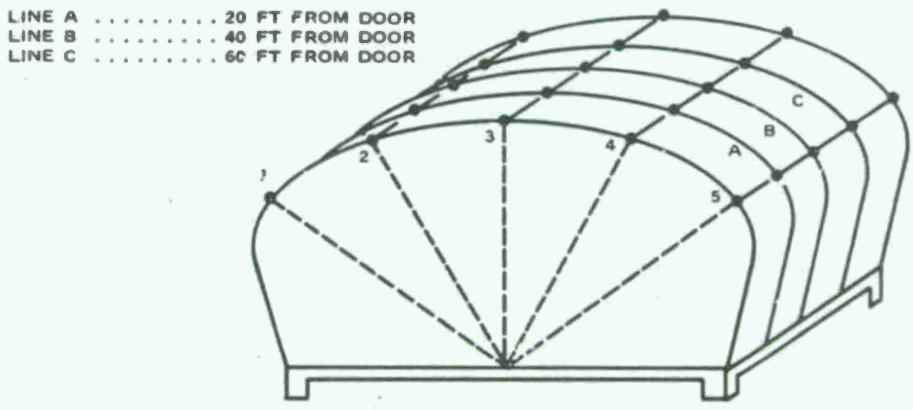


Figure 45. Position Key for Measurement of Arch Deformations on Igloo B.

TABLE 6. Permanent Arch Deformations of Igloo B in Feet.

Figure 45 illustrates locations where deformations were measured.

| Line | Arch positions | | | | |
|---|---|---|---|---|---|
| | 1 | 2 | 3 | 4 | 5 |
| A | 0.01 | 0.07 | 0.12 | 0.05 | −0.01[a] |
| B | .00 | .03 | .11 | .05 | .00 |
| C | 0.01 | 0.03 | 0.06 | 0.02 | 0.00 |

[a] Negative value indicates outward deformation.

## FRAGMENT COLLECTION AND ANALYSIS

### Fragment Collection

In the ESKIMO I test, three 5-degree sectors (shown in Figure 13 of Reference 1) were cleared of vegetation and debris for fragment collection by a magnet truck driven over the sectors. Additionally, a number of 50- by 50-foot and 100- by 100-foot areas were laid out, and fragments were collected in these areas by foot search and hand pickup. The manual method of collection was considered to be more thorough than magnet collection in areas where the smallest fragments weighed approximately 0.05 pound.

For ESKIMO II, collection by magnet truck was not attempted. Instead, many of the hand pickup areas searched in ESKIMO I were searched again for fragments after ESKIMO II. Additionally, new hand pickup areas were laid out and searched in the 5-degree magnet pickup sectors. Some new search areas were laid out and examined in areas previously unused in ESKIMO I. Table 7 identifies

TABLE 7. Areas Used in Fragment Collection.

| Size of collection area, ft | Distance from donor center to center of collection area, ft | | | | |
|---|---|---|---|---|---|
| | North, 356 deg | Southeast, 135 deg | South, 174 deg | West, 266 deg | Northwest, 330 deg |
| 50 x 50 | ... | 1,225 | 775 | 1,025 | ... |
| | ... | 1,425 | 1,175 | 1,525 | ... |
| | ... | 1,625 | 1,375 | ... | ... |
| | ... | ... | 1,575 | ... | ... |
| | ... | ... | 1,775 | ... | ... |
| 50 x 100 | 1,025 | ... | 1,000 | ... | ... |
| | 1,555 | ... | ... | ... | ... |
| 100 x 100 | ... | 1,850 | 2,050 | 1,750 | 1,950 |
| | ... | 1,950 | 2,150 | 1,850 | 2,050 |
| | ... | 2,050 | 2,250 | 2,050 | 2,150 |
| | ... | 2,150 | 2,350 | 2,150 | 2,250 |
| | ... | 2,250 | 2,450 | 2,250 | 2,350 |
| | ... | 2,350 | ... | 2,450 | 2,450 |
| 100 x 230 | ... | ... | 2,950 | ... | ... |

the areas searched in ESKIMO II. In all cases it was important to distinguish between ESKIMO I and ESKIMO II fragments, particularly so in those areas in which fragments had not been picked up after ESKIMO I. It should be noted that the ESKIMO I search techniques were imperfect and that fragments from that test were found despite prior attempts to pick the areas clean. This was particularly true in the magnet pickup sectors.

The foot searches and manual pickups in ESKIMO I and ESKIMO II were conducted by two men moving in mutually perpendicular paths. In areas of soft, loose earth, all fresh craters, even small ones, were probed for fragments. The craters often yielded metal fragments not visible without probing.

## Fragment Analysis

In fragment analysis, the principal emphasis was placed on producing data that would identify fragment hazards in various directions from the donor stack by comparison with existing standards. An additional objective was the presentation of data in a manner that would facilitate additional analysis in the event it was desired to vary either the fragment density criterion or energy level criterion in the standards.

The graphs shown in Figures 46 through 48 were derived to show the increase in the cumulative number of fragments per 10,000 $ft^2$ with decreasing fragment weight for various collection distances. Because the donor stack was symmetrical north-south and east-west, the data from the north and south collections were combined; similarly, the northwest and southeast data were combined. In neither case were the collection areas directly opposite; however, the angular deviation from direct opposition was not considered significant.

Figures 49 through 51 show variations in the number of fragments, equal to or above specific weight levels, per 10,000 $ft^2$ for various distances away from the donor stack. These figures are plotted for fragment weight levels of 0.08 and 0.28 pound.

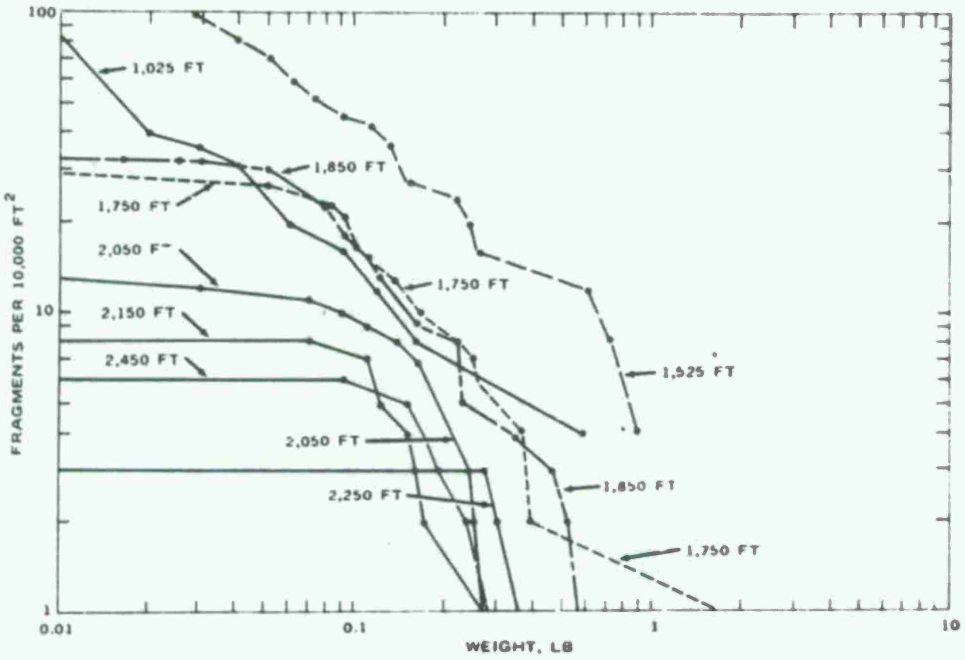


Figure 46. Cumulative Number of Fragments per 10,000 $ft^2$ Versus Weight in Pounds for Various Westerly Distances From the Donor.

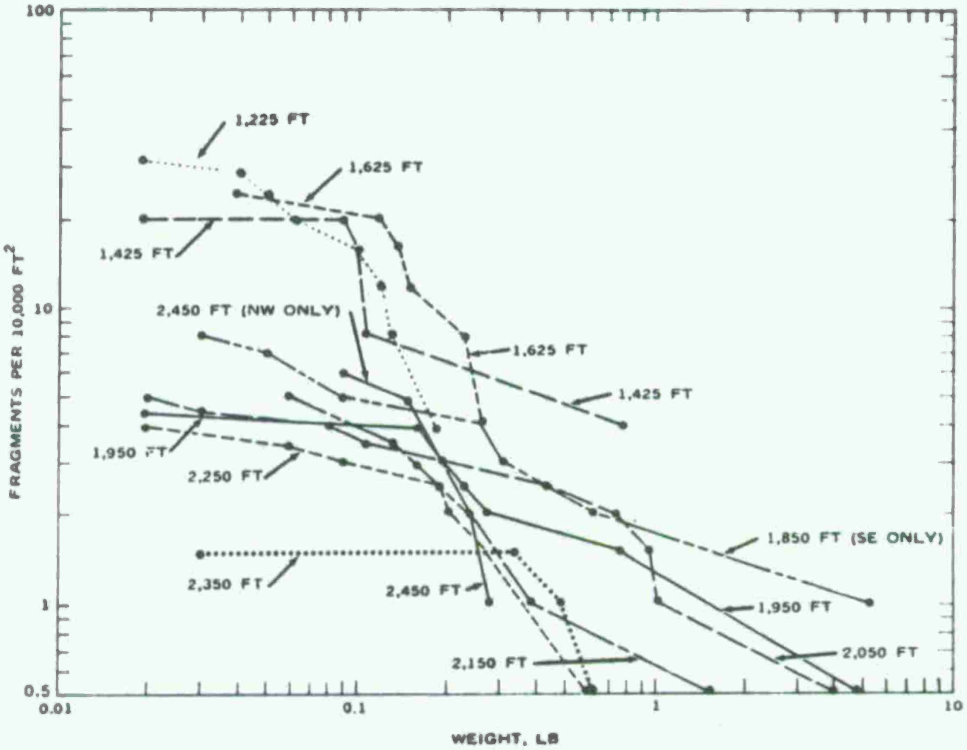


Figure 47. Cumulative Number of Fragments per 10,000 $ft^2$ Versus Weight in Pounds for Various Southeasterly and Northwesterly Distances From the Donor.

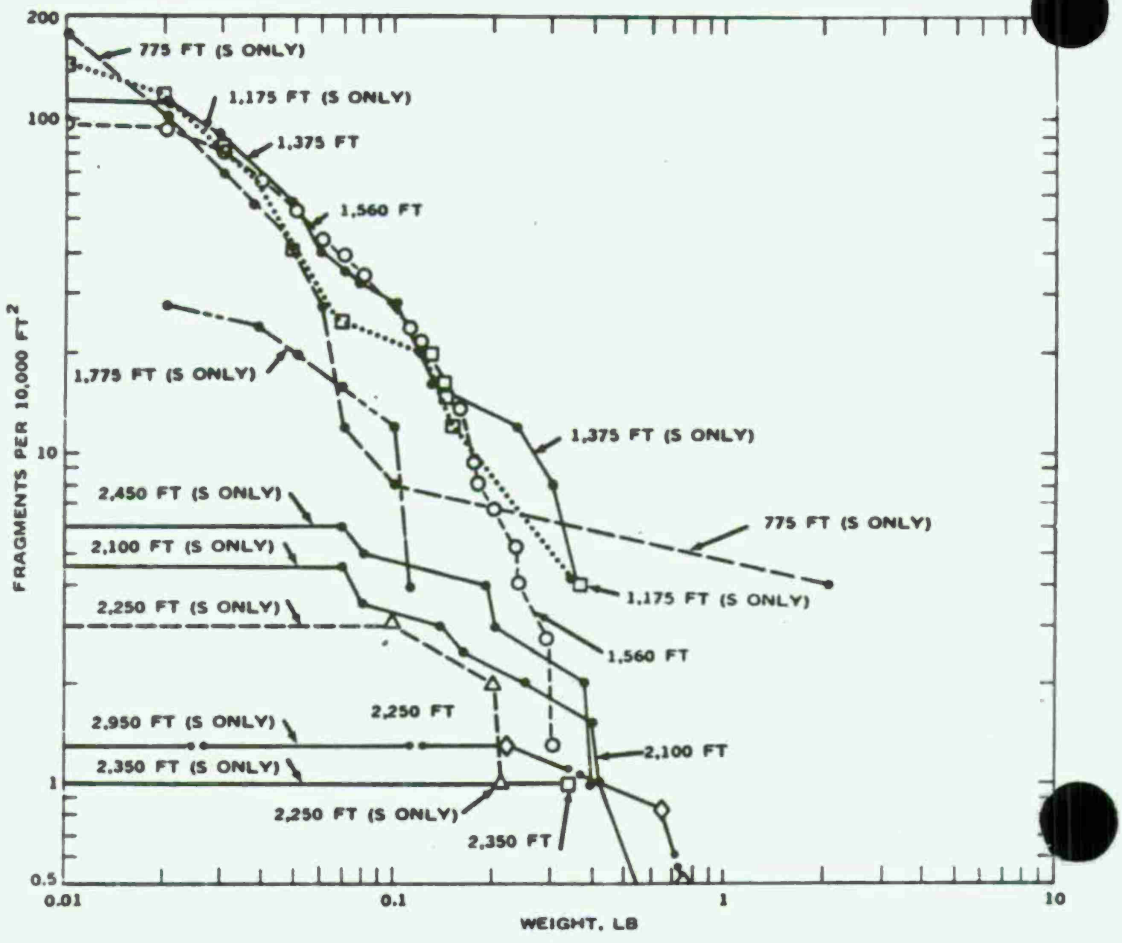


Figure 48. Cumulative Numbers of Fragments per 10,000 $ft^2$ Versus Weight in Pounds for Various Southerly and Northerly Distances From the Donor.

The selection of the 0.28-pound level was based on the following rationale:

1. The present DDESB criterion for exposure of unprotected personnel to hazardous fragments stipulates an acceptable density of not more than one per 600 $ft^2$, a hazardous fragment being defined as one having a kinetic energy of 58 ft-lb or greater. By analysis of ballistic trajectories, it can be shown that fragments reaching large distances from an explosion strike the ground surface at approximately their terminal velocity in free fall.

2. The distribution of fragments in this test made it of interest to investigate the safe fragment distance based on the above criterion. From Figure 3 of Reference 3, the value of 0.28 pound was derived as the weight of a 58-ft-lb fragment moving at terminal velocity. Figure 66 of Reference 1 shows the limits of fragment hazard for the ESKIMO I test, based on the above standards.

The choice of the 0.08-pound level was also derived from Figure 3 of Reference 3 for a fragment with 11 ft-lb of kinetic energy (an energy criterion recommended by some investigators) moving at terminal velocity.

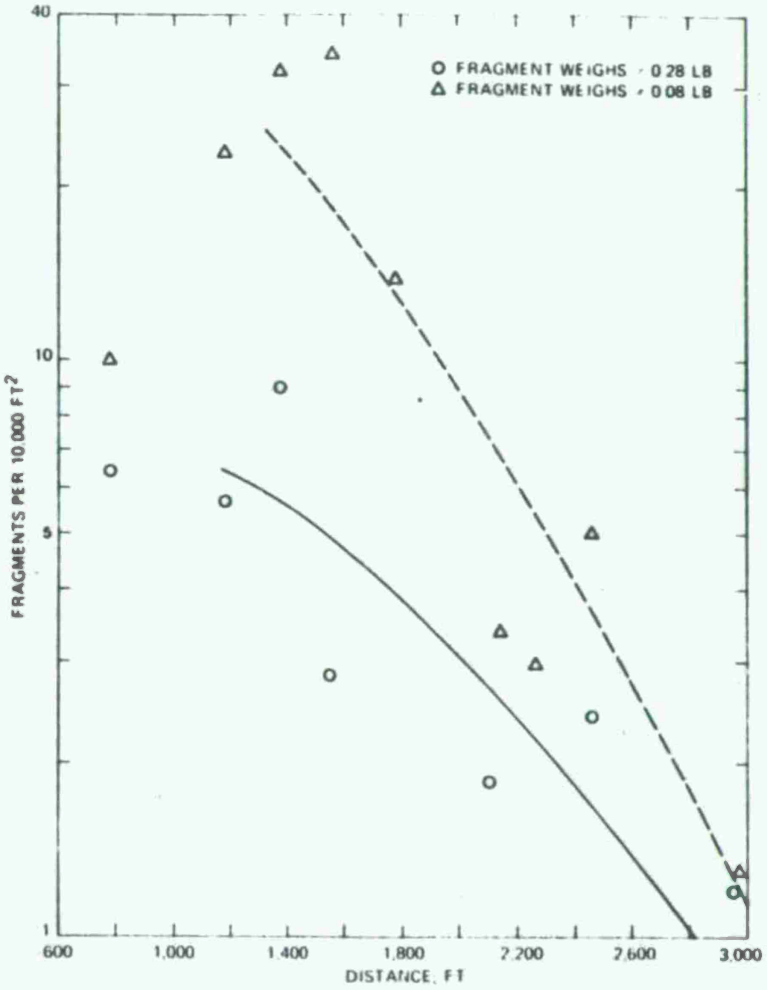


Figure 49. Number of Fragments per 10,000 $ft^2$ Versus Distances North and South of Donor.

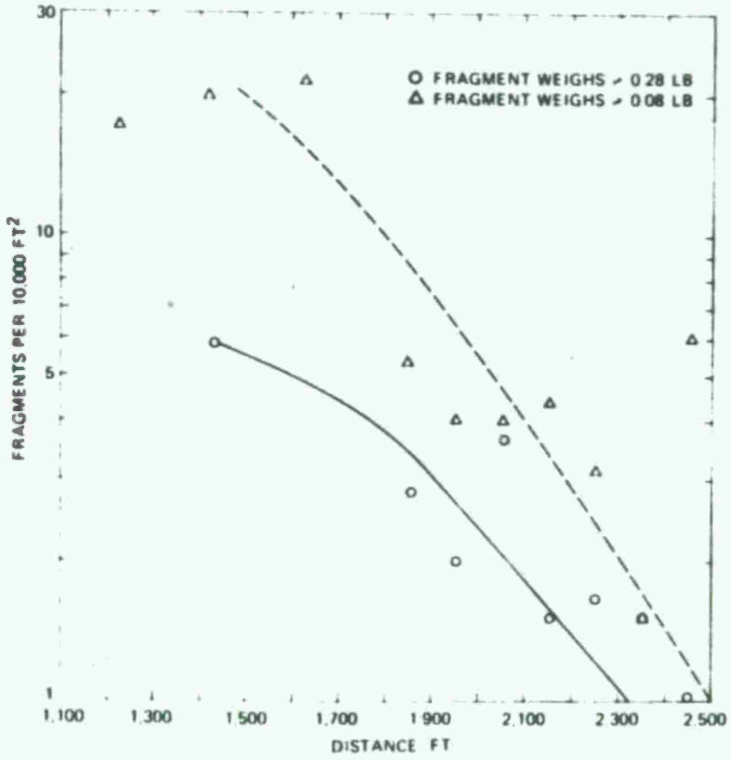


Figure 50. Number of Fragments per 10,000 $ft^2$ Versus Distances Northwest and Southeast of Donor.

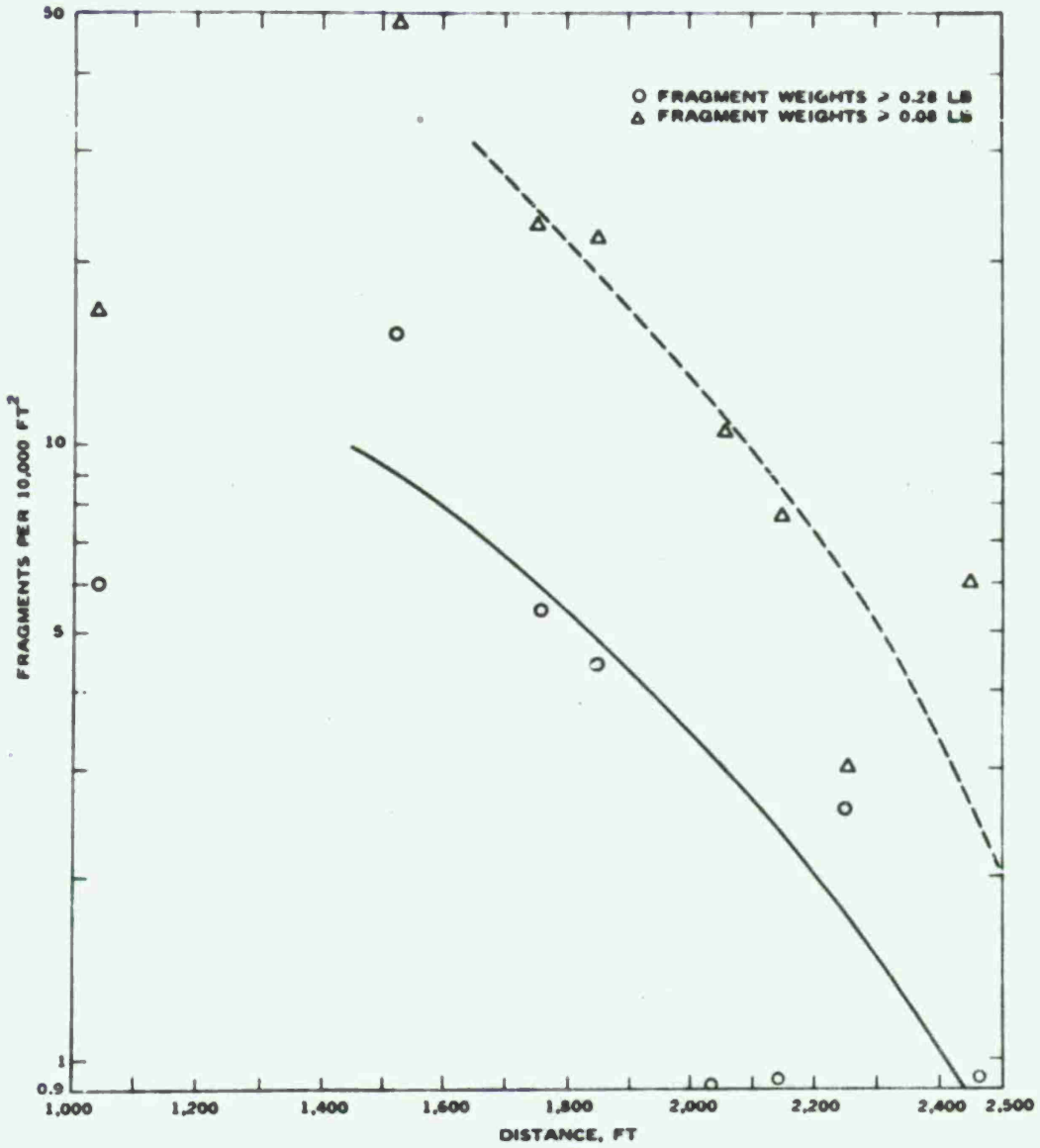


Figure 51. Number of Fragments per 10,000 ft² Versus Distance West of Donor.

Examination of Figures 49 through 51 shows that none of the fragment areas searched provided a density of more than one 0.28-pound fragment per 600 $ft^2$. Fragment densities of one 0.08-pound fragment per 600 $ft^2$ were encountered approximately as follows:

| *Direction from donor* | *Distance from donor, ft* |
|---|---|
| North and south | 1,600 |
| West | 1,900 |
| Northwest and southeast | 1,700 |

## DATA DERIVED FROM INSTRUMENTATION

### Event Times

With the exception of data derived from BRL self-recording gauges, all data were recorded on a time base: standard IRIG Format B for the motion pictures, and binary coded 1,000-hertz timing for magnetic tape data from piezoelectric blast gauges, linear motion transducers, and accelerometers.

Test event times derived from assessment of the piezoelectric gauge data and accelerometer data were based on a zero time pulse indication derived from an ionization probe buried in the donor stack. A backup attempt to derive zero time from a light sensing device mounted atop Igloo D did not produce a consistently good signal.

### Motion-Picture Photography

The main test event was recorded photographically by ground-based 16-mm and 35-mm cameras using color film. Film speeds were varied from 10 frames per second for some overall views to 1,000 frames per second for cameras placed in the magazines to 4,500 frames per second for exterior cameras focused on headwalls and doorways. The cameras operated as planned; however, many of the exterior photographs lacked crispness because of thermal air effects associated with the season of the year and the time of day. Additionally photoflash lighting used within the igloos was not properly timed.

### Motion Instrumentation

Linear motion transducers positioned to measure movement of the concrete headwall above or

TABLE 8. Summary of Linear Motion Transducer Data.

| Igloo location of headwall transducers | Max. velocity, ft/sec | Av. velocity from initial motion to peak excursion, ft/sec | Time from initiation of motion to max. velocity, msec | Av. acceleration from initial motion to max. velocity, g | Remarks |
|---|---|---|---|---|---|
| A | 13.8 | 9.25 | 10.80 | 40 | Door stops at head of door; heavy concrete haunches from headwall to roof. |
| B | 14.3 | 10.40 | 17.00 | 26 | Reinforced concrete projection above door opening to stiffen headwall. |
| C | 33.3 | 31.50 | 6.75 | 153 | Steel dowel to resist door movement at top; less effective than door stops of other igloos. |
| D | 39.6 | 34.10 | 7.90 | 156 | Heavy one-piece steel door overlapping door opening at top. |
| E | 44.1 | 32.90 | 6.10 | 224 | Door stops at top of door opening; distorted, but remaining in place. Energy transfer from door to top of headwall believed more complete than in other igloos. |

near the center of the doorways of the five acceptor igloos recorded data from which motion values listed in Table 8 were derived. The large variation in motion values among igloos is attributed to the differences in headwall construction and in doorstop devices for inhibiting the movement of the tops of the doors relative to the concrete headwalls. Brief descriptions are given in the Remarks column of this table, and photographs and tabulation of wall movements measured statically appear in other sections of the report.

Data derived from accelerometers are shown in Table 9. In general, the first motion after zero time is consistent with the arrival of the blast wave, with two notable exceptions, that is, the left door leaves of Igloos B and C. No explanation is attempted for what appears to be a delay in first motion of about 5.6 milliseconds at these positions. All accelerometer records were brief because of the damage incurred by the doors on which the accelerometers were mounted. The records exhibit no significant frequencies because the motion was primarily translation rather than vibration. The right-hand column of the table was derived by a rough computation of theoretical maximum acceleration of an unrestrained body having the same mass as the test door per unit of exposed area and experiencing blast pressure equal to that recorded as an average for the first millisecond of overpressure (approximating, but less than, the maximum overpressure).

TABLE 9. Summary of Accelerometer Data.

| Igloo | Location of sensor | First motion, msec | Peak acceleration, g | Typical acceleration values after peak, g [a] | Calculated maximum free-body acceleration, g |
|---|---|---|---|---|---|
| A | Left door leaf | 37.8 | ...[b] | ...[b] | 870 |
| | Right door leaf | 38.3 | ...[b] | ...[b] | |
| B | Left door leaf | 41.3 | ...[c] | ...[c] | 940 |
| | Right door leaf | 35.6 | 1,200 | 750 to 850 | |
| C | Left door leaf | 41.5 | ...[c] | ...[c] | 1,310 |
| | Right door leaf | 35.9 | ...[b] | ...[b] | |
| D | Left center, door | 35.8 | 750 | 475 to 550 | 780 |
| | Right center, door | 35.8 | ...[b] | 500 to 600 | |
| E | Left door leaf | 36.2 | 730 | 400 to 450 | 1,180 |
| | Right door leaf | 36.1 | 975 | 550 | |

[a] Range of values recorded 1 to 4 milliseconds after initial motion.
[b] Unreadable.
[c] Unreliable; time of first motion inconsistent with other data.

## Blast Gauge Data

**General.** The blast gauge instrumentation consisted of two basically different types of gauges: (1) BRL self-recording mechanical gauges placed at distances ranging from 730 to 3,400 feet from the donor center (Table 10) and (2) Kistler piezoelectric gauges, with relatively better frequency-response characteristics, placed in the headwalls of the magazines and in the ground 2 feet in front of the igloo headwalls. One electronic strain gauge placed in the ground at Igloo B did not function.

Data from Kistler piezoelectric gauges and BRL mechanical gauges are presented in Tables 10 and 11.

**BRL Gauges.** Data from BRL gauges are given in Table 10. The computer assessment of BRL records produced (1) tabulations of the overpressure and impulse versus time and (2) plots of the data. Figures 52 through 55 show the plotted data for 11 of the 13 BRL gauges. In addition, the computer plotted the first part of the overpressure curve on a semilogarithmic scale and fitted a least squares line to the curve, permitting an extrapolation to zero time for determining the most likely real initial overpressure. Figure 56 shows such a plot. This procedure was designed to reduce the effect of slow response by the BRL gauges at the leading edge of the shock wave.

Similarly, the computer plotted the trailing edge of the positive phase of the overpressure curve on a semilogarithmic scale and fitted a straight line to it, permitting extrapolation to the most likely positive-phase duration (Figure 57). The program also included the computation of impulse based on these extrapolations. The pressures experienced at the sites of the BRL gauges were considerably less than those predicted for these locations.

TABLE 10. Summary of BRL Gauge Data.

| Gauge location | | Peak overpressure, psi | | Impulse, psi-msec | | Duration of overpressure, computer extrap., msec |
|---|---|---|---|---|---|---|
| Gauge line | Distance from donor center, ft | Direct reading | Computer extrap. | Direct reading | Computer extrap. | |
| NW | 730 | 1.04 | 1.09 | 50.7 | 51.0 | 142 |
| NW | 730 | 1.01 | 1.14 | 47.9 | 48.9 | 132 |
| NW | 1,130 | 0.71 | 0.62 | 31.8 | 32.7 | 109 |
| NW | 1,130 | 0.64 | 0.63 | ... | ... | ... |
| NW | 1,210 | 0.55 | 0.57 | 29.7 | 30.7 | 158 |
| NW | 1,210 | 0.49 | 0.50 | 27.9 | 28.4 | 157 |
| NW | 1,700 | 0.37 | 0.38 | 22.3 | 22.6 | 187 |
| NW | 1,700 | 0.41 | 0.44 | 24.3 | 24.8 | 174 |
| NW | 3,400 | 0.17 | 0.18 | 12.7 | 13.1 | 212 |
| NW | 3,400 | 0.23 | 0.25 | 14.0 | 15.5 | 192 |
| SW | 730 | 1.41 | 1.38 | 54.4 | 56.1 | 118 |

TABLE 11. Summary of Piezoelectric Gauge Data.

| Gauge location [a] | Gauge distance from donor center, ft | Peak overpressure, psi | | Impulse, psi-msec | Time of arrival relative to zero time, msec |
|---|---|---|---|---|---|
| | | Incident | Reflected | | |
| A, r. w. | 153 | ... | 270 | 1740 | 39.6 |
| A, l. w. | 148 | ... | ...[b] | ...[b] | 37.6 |
| A, r. g. | 148 | 80 | ...[b] | ...[b] | 38.2[d]/41.2[e] |
| B, r. w. | 148 | ... | 260 | 1744 | 36.6 |
| B, l. w. | 148 | ... | ...[b] | ...[b] | 36.5 |
| B, r. g. | 145 | 62 | ...[b] | ...[b] | 34.5[d]/37.8[e] |
| C, r. w. | 148 | ... | 245 | 1480 | 35.8 |
| C, l. w. | 148 | ... | ...[b] | ...[b] | 36.3 |
| C, r. g. | 145 | 60 | ...[b] | | |
| D, r. w. | 148 | ... | 270 | 2195 | 35.3 |
| D, l. w. | 153 | ... | ...[b] | ...[b] | 37.2 |
| D, r. g. | 147 | 60 | ...[b] | ...[b] | 37.5[d]/... |
| E, r. w. | 148 | ... | 200 | 1200 | 36.5 |
| E, l. w. | 148 | ... | 210 | 1295 | 36.3 |
| E, r. g. | 145 | 70 | 180 | ...[b] | 35.8[d]/38.7[e] |
| E, l. g. | 145 | ...[c] | ...[c] | ...[c] | ...[c] |

[a] A, B, C, D, and E refer to igloo identities; r. and l. refer to right and left positions; g. and w. refer to ground and wall locations.

[b] This portion of record difficult to read and considered unreliable.

[c] No record.

[d] Time of incident blast.

[e] Time of reflected blast.

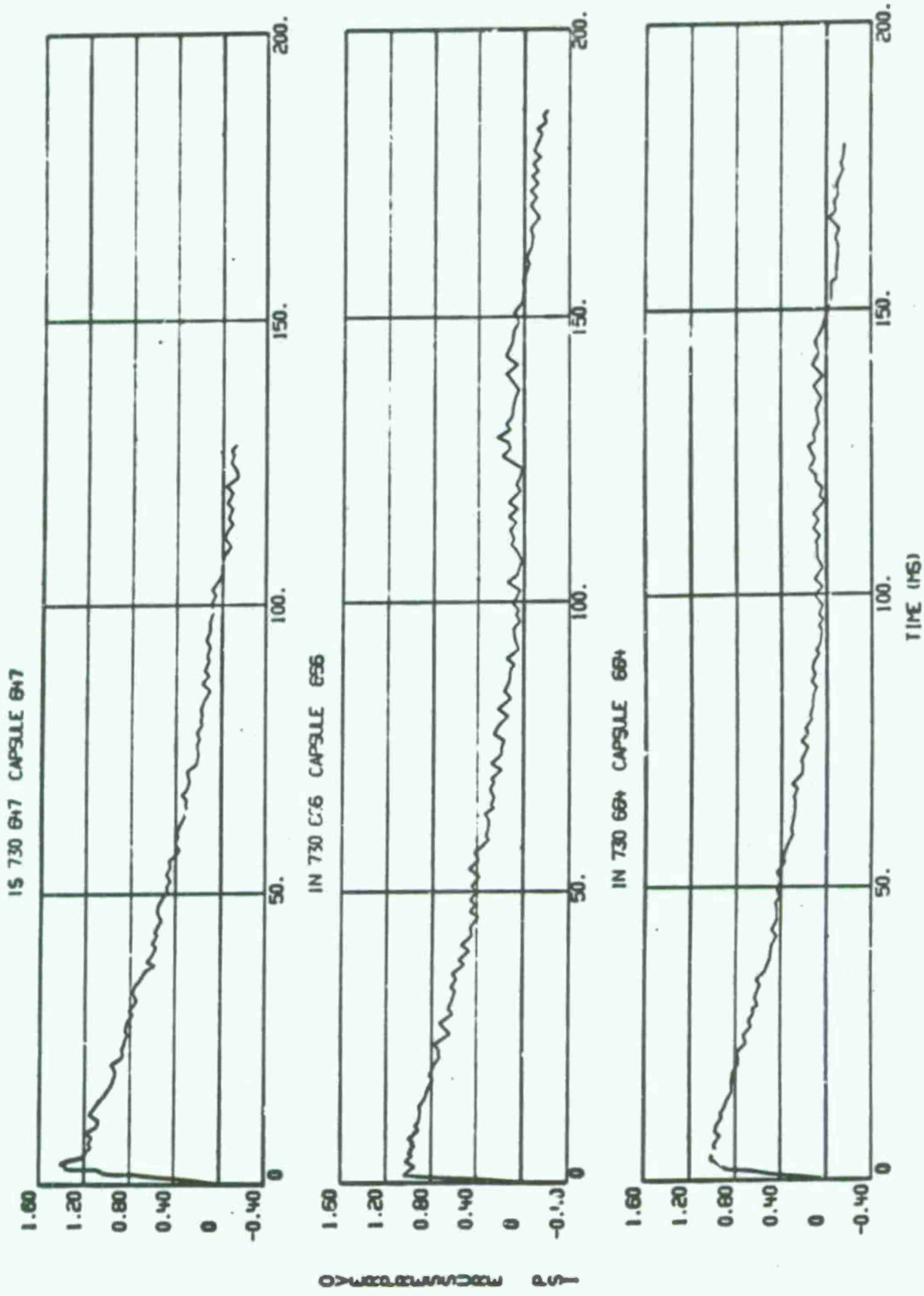


Figure 52. Data Plots for BRL Gauges 1S and 1N.

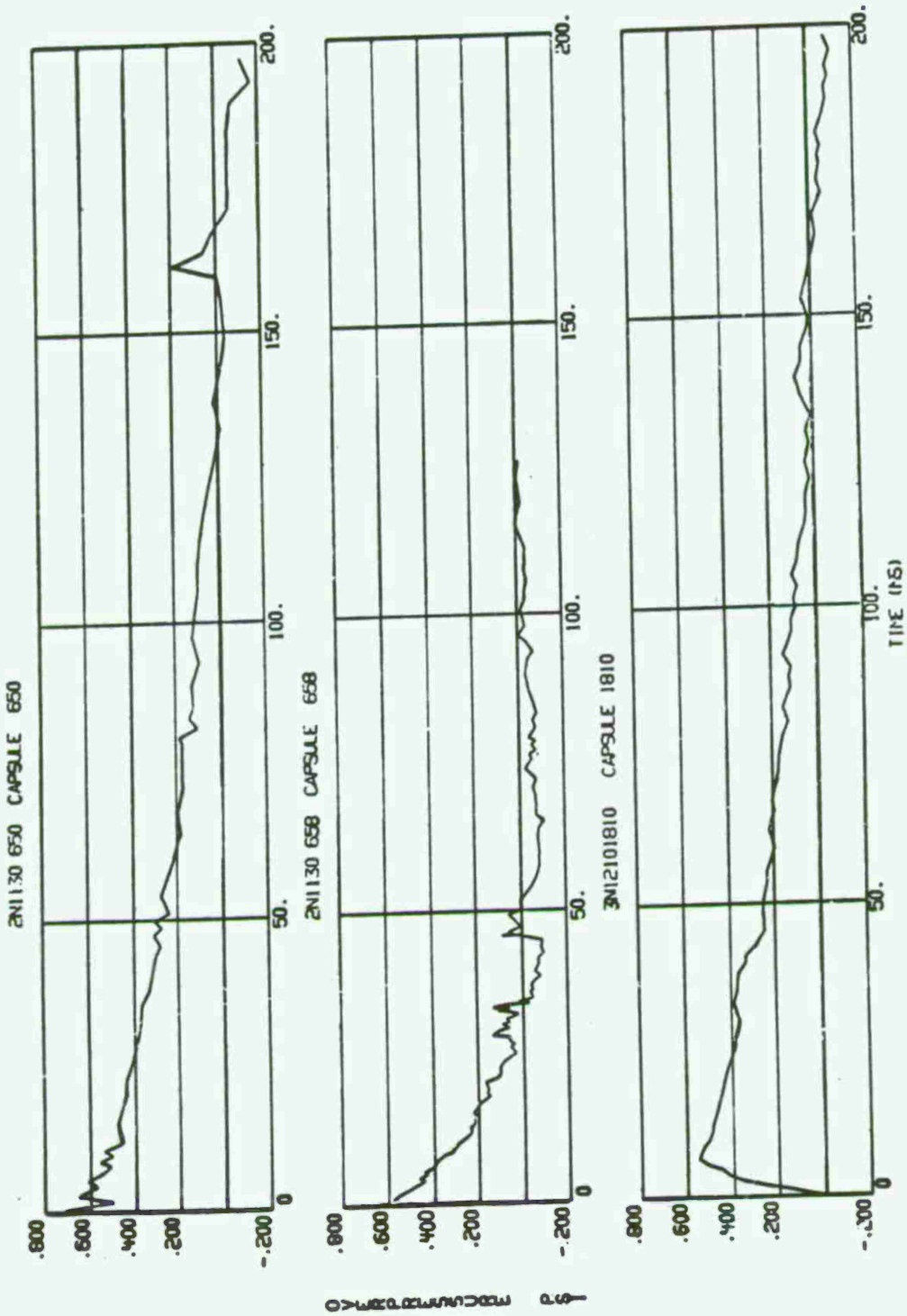


Figure 53. Data Plots for BRL Gauges 2N and 3N.

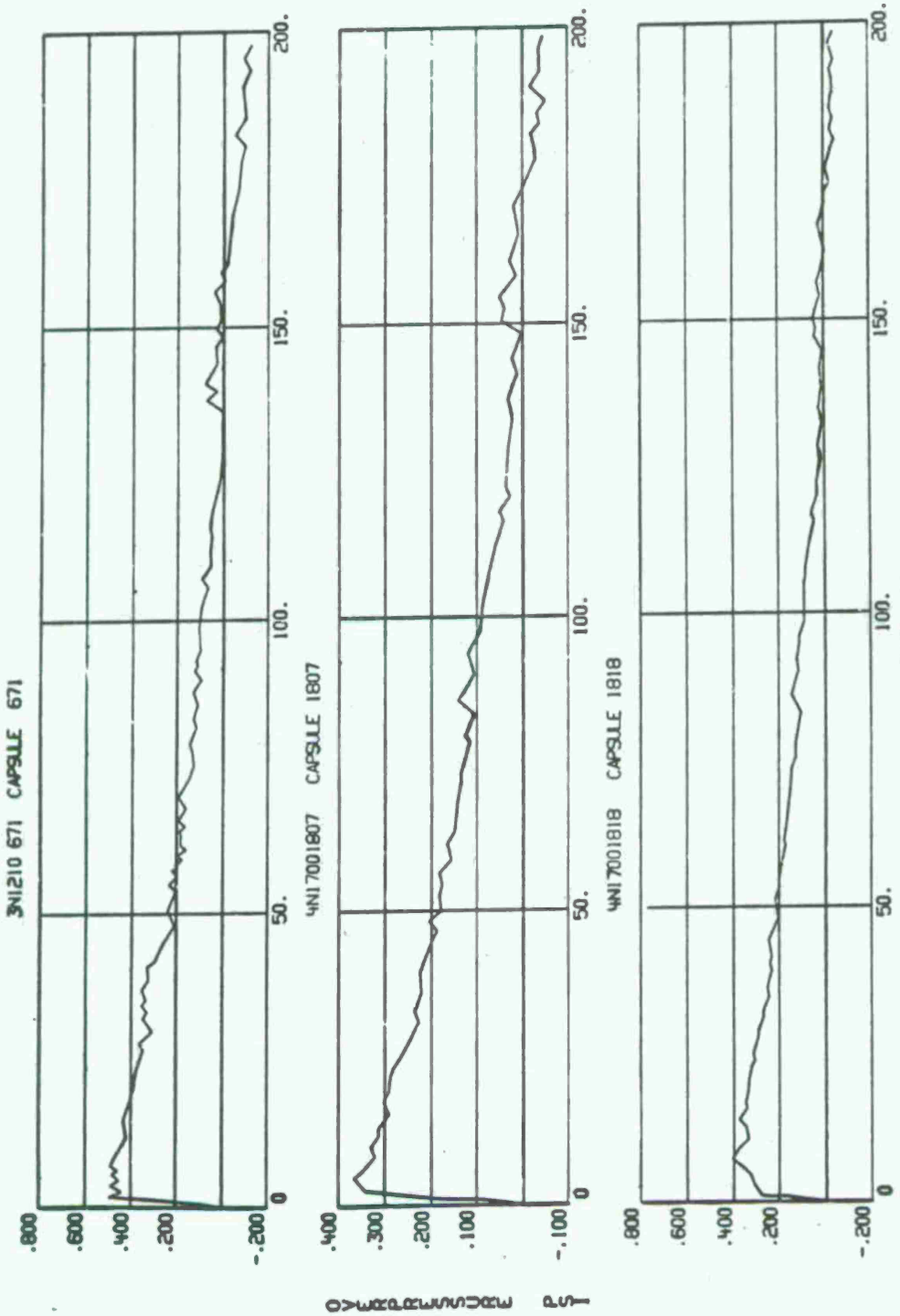


Figure 54. Data Plots for BRL Gauges 3N and 4N.

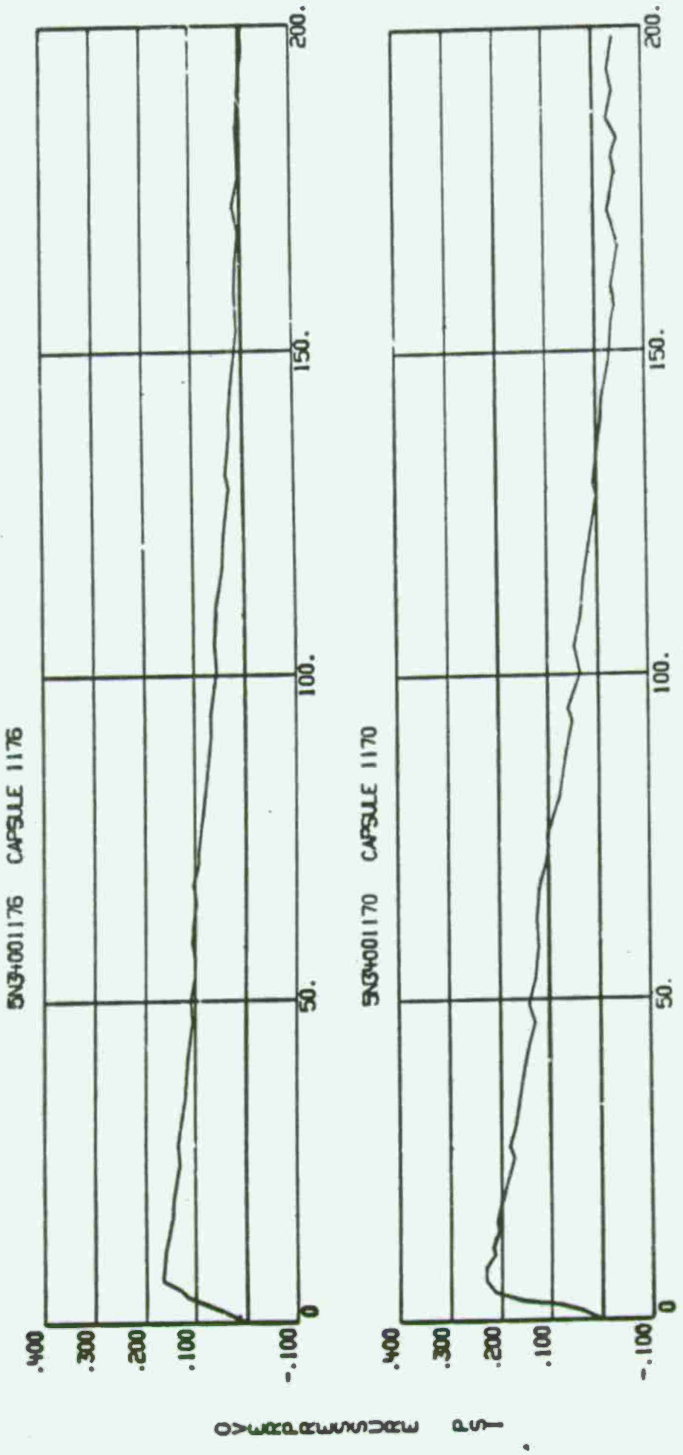


Figure 55. Data Plots for BRL Gauges 5N.

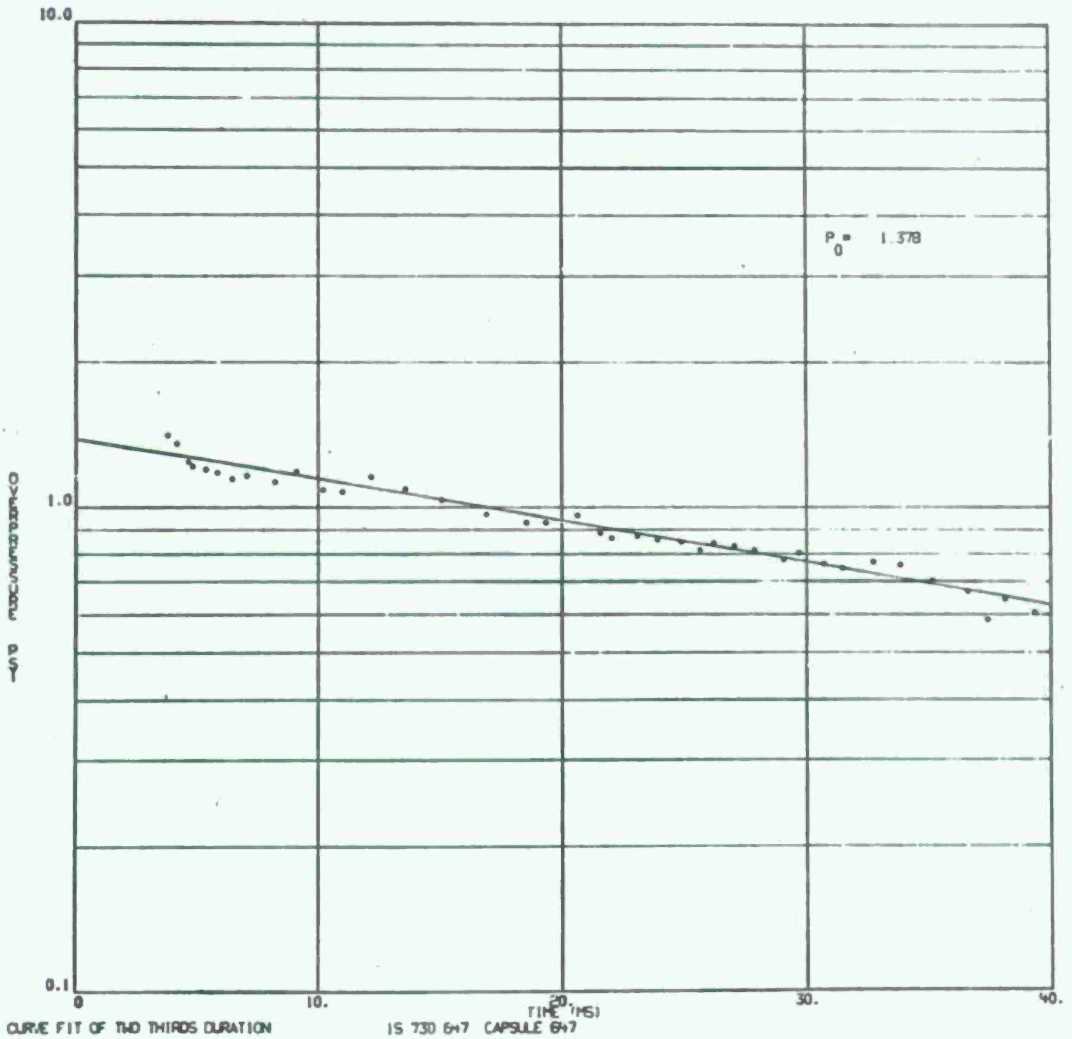


Figure 56. Computer Plot of First Part of Overpressure Curve From BRL Gauge 1S.

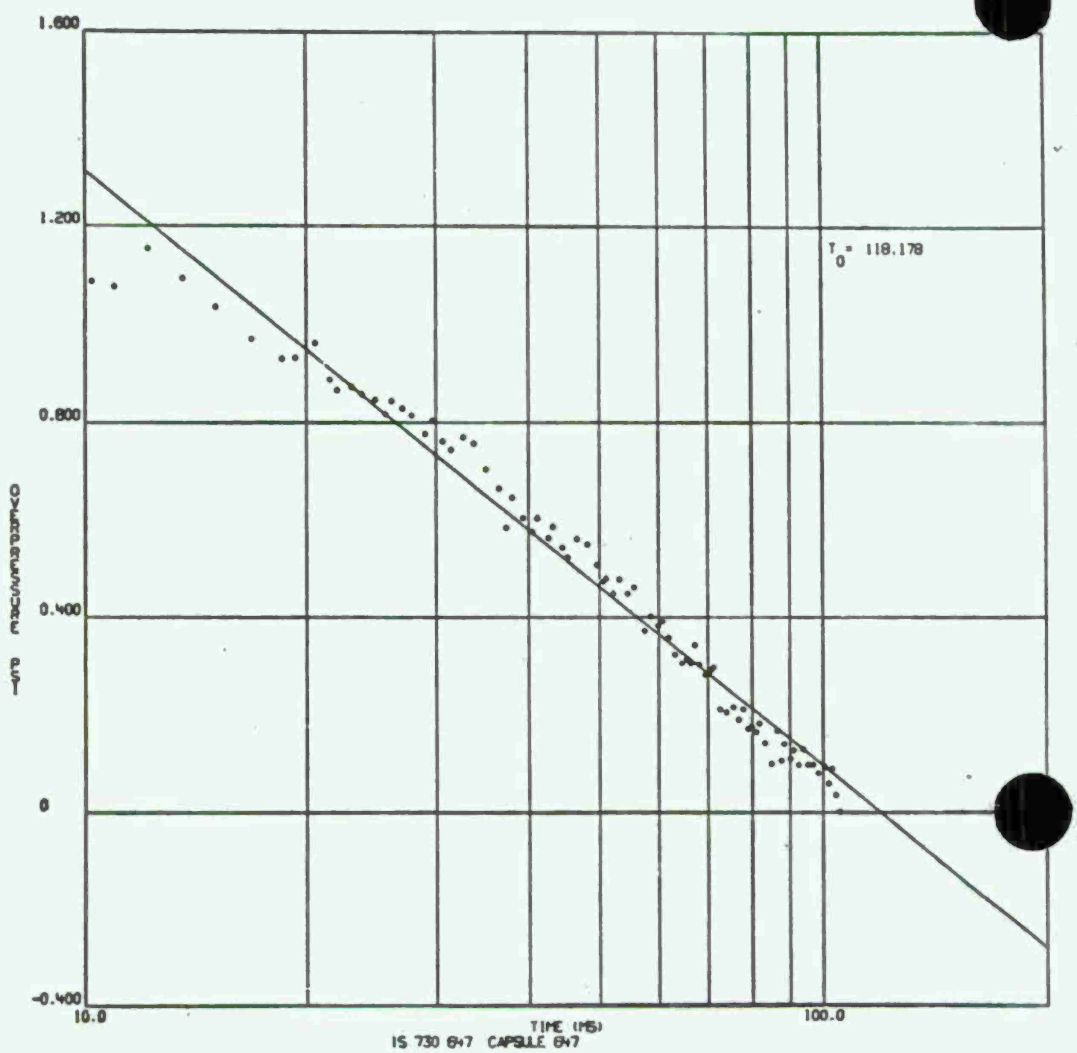


Figure 57. Computer Plot of Trailing Edge of Overpressure Curve From BRL Gauge 1S.

**Piezoelectric Gauges.** Data from Kistler piezoelectric gauges are presented in Table 11. The overall quality of these gauge records was adversely affected to some degree because the maximum overpressures exceeded those predicted and also exceeded the calibration limits. Additionally, the initial or zero positions of the records for the ground and left wall gauges at Igloos A, B, C, and D were dropped from the center frequency of the recorder toward the lower band edge with the expectation of a positive signal from the amplifier. Instead, the signal from the amplifier was negative. (The newly received amplifier/gauge combinations gave signals in reverse of those

experienced with similar but older equipment.) As a result, the linearity of the records and their relationship to the calibrations are somewhat suspect for the gauges listed above. Despite these problems, the gauge data considered in the aggregate with other data give solid evidence that the overpressures experienced were considerably higher than predicted or than the overpressure impinging on the igloo headwalls in the ESKIMO I test.

## DISCUSSION OF DATA DERIVED FROM INSTRUMENTATION

Figure 58 shows values of overpressure versus scaled distance ($\lambda$) for tests 1C, 2C, 3C, 4C, and 5C described in Reference 4. The explosive charges used in these tests are described below:

| *Test no.* | *Charge shape* | *Explosive weight, lb* |
|---|---|---|
| 1C | Approximated a cube | 5,000 |
| 2C | Approximated a cube | 20,000 |
| 3C | Approximated a cube | 10,000 |
| 4C | Approximated a cube | 10,000 |
| 5C | 4 ft × 4 ft in plan form × 25 ft high | 20,000 |

In the above five tests the explosive charge consisted of reclaimed TNT cast in cut-down ammunition boxes with each box containing 50 pounds of explosive.

Figure 58 also shows a plot of a standard overpressure versus scaled distance curve derived from Reference 5. This curve was based on hemispherical stacks of explosive. In comparing the plots of above described tests 1C through 5C with the standard curve, note that values of overpressure for the cubical or plane-faced charge geometries are consistently higher than those of the standard curve for scaled distances ($\lambda$) lower than 10 ft/lb$^{1/3}$ and are consistently lower for higher $\lambda$ values.

Figure 59 shows a comparison of overpressure and impulse curves derived from data in above-described tests with the standard BRL curves and with overpressure and impulse data from ESKIMO II. Note that the general tendencies shown in the prior plane-faced geometries are repeated in ESKIMO II. The following observations can also be made:

1. Close-in overpressures and impulses recorded by the piezoelectric gauges tend to be slightly higher at north and south positions off the triangular faces of the bomb stack than they are at east and west locations off the sloping faces of the stack. However, time-of-arrival values from the gauges and accelerometers tend to show more uniformity.

2. Relatively far field overpressures recorded by the BRL gauges on the WNW radial tend to be lower than data derived from the cubes and the high square columnar geometries in Reference 4 and considerably lower than the BRL standard curves. The single data point on the WSW radial line shows the best agreement with the curve representing the plane-faced geometry of Reference 4.

The points shown for ESKIMO II assume a TNT equivalent weight of 24,000 pounds. The blast wave produced by the bomb stack behaved much like 24,000 pounds of TNT in a cube configuration at a scaled distance approximating 5, but at scaled distances of 25 and greater on the NNW radial, it behaved more nearly like 12,000 to 15,000 pounds of TNT in a cube configuration.

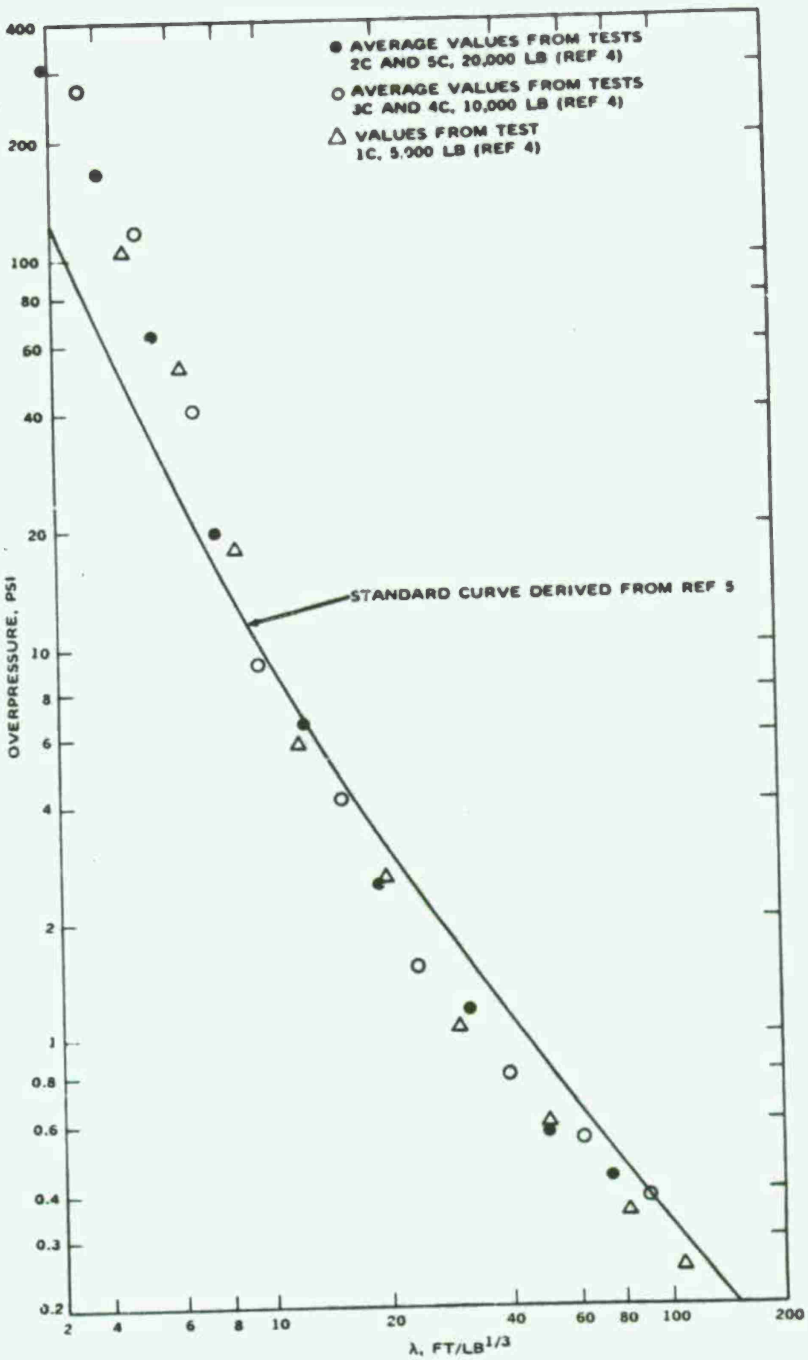


Figure 58. Plot of Overpressure Versus Scaled Distance (λ) From Plane-Sided Explosive Stacks Compared With a Standard Curve Derived From Hemispherical Stacks.

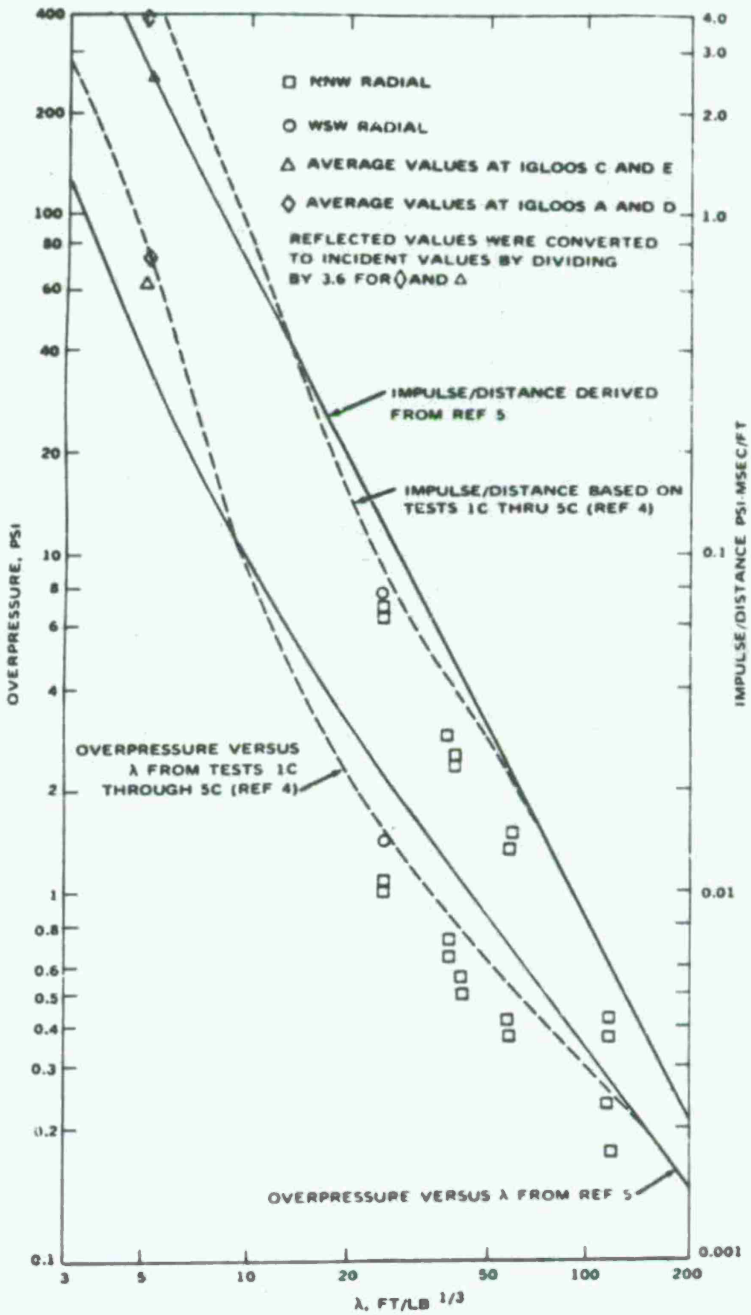


Figure 59. Comparison of ESKIMO II Blast Data With Other Selected Blast Data. Assumed effective W = 24,000 pounds.

## CONCLUSIONS

Because the near field blast loading exceeded that planned, the igloo structures were subjected to an overtest. Despite this overtest the large single leaf sliding door on Igloo D (south) withstood the blast loading without breakup or severe distortion. Likewise, the Stradley-type headwall used for Igloo B (northeast) incurred a clearly acceptable degree of damage.

ESKIMO III, the next in the series, will test the capability of the noncircular arch remaining in Igloo B to withstand blast loads imposed side-on by the detonation of a stack of donor bombs contained in an 80-foot-long magazine parallel to Igloo B with a clear separation distance of $1.25 \times W^{1/3}$.

The slightly damaged headwall of Igloo B will be replaced with a headwall of similar concept redesigned to accommodate a single leaf sliding door essentially similar to that used in Igloo D. If successful in the ESKIMO III test, the combination of the 1-gauge corrugated noncircular arch with the Stradley-type headwall concept and the one-piece sliding door will be considered a strong candidate for a standard magazine design.

The door modifications tested in Igloo E (west) are not considered successful and, therefore, not a reasonable expedient for upgrading existing magazines.

The test reaffirmed the need for achieving a balance in the strength of headwalls and doors. Results at Igloo D demonstrated the severe damage sustained by this type of wall when combined with a strong door that does not significantly distort or yield under load, and thus transfers its loading to the headwalls.

Damage experienced by Igloo A (north) was insufficient to cause detonation of acceptor charges but did cause initiation of acceptor fires and also considerable acceptor breakup. The headwall and door designs are not considered adequate for the blast loadings experienced in this test (well above the planned loading at this igloo). However, it should be noted that the door stop devices at the door head and sill did remain in place. The concept of providing door support by transfer of door loads to the rigid structural planes of the floor and ceiling is a rational approach structurally and, where operational processes permit, might deserve cost comparison with the horizontally spanning door and vertical pilaster combination.

Results and general conclusions from the study of the effects of the blast on the window test cubicles and vehicles are described in Appendix B. The conclusions are summarized as follows:

1. The test supported the U.S. inhabited building distance standards and the U.S. public highway separation distances. In no case did the automobile damage exceed the level considered tolerable by most U.S. authorities.

2. The absence of window damage at 3,400 feet, twice the NATO inhabited building distance, suggests that this distance is unduly conservative.

The above conclusions regarding window and vehicle damage are based on an assumed equivalent explosive loading of 24,000 pounds of TNT. Although overpressure and impulse values recorded by gauges in the far field were lower than expected, and although it is considered possible that the same amount of donor explosive packaged or stacked differently could produce higher pressures and impulses at the building and vehicle locations, it is believed that the results represent a reasonably typical storage situation and are more realistic than idealized donor configurations such as hemispheres of bulk explosive.

## REFERENCES

1. Naval Weapons Center. *Eskimo I Magazine Separation Test*, by Frederick H. Weals. China Lake, Calif., NWC, April 1973. 84 pp. (NWC TP 5430.)

2. General American Transportation Corporation. *Explosion Effects Computation Aids*, by L. E. Fugelso, L. M. Weiner, and T. H. Schiffman. Niles, Ill., GATC, June 1972. (Final Report, GARD Project No. 1540.)

3. Zaker, T. A. "Trajectory Calculations in Fragment Hazard Analysis," *Minutes, Thirteenth Annual Explosives Safety Seminar*, 14–16 September 1971, Washington, D.C., ASESB, 1971. Pp. 101-16.

4. Naval Weapons Center. *High Explosive Equivalency Tests of Large Solid Propellant Motors*, by URS Systems Corporation. China Lake, Calif., NWC, September 1968. 46 pp. (NWC TP 4643.)

5. Ballistic Research Laboratories. *Air Blast Parameters Versus Distance for Hemispherical TNT Surface Bursts*. Aberdeen Proving Ground, Md., BRL, September 1966. (BRL Report No. 1344.)

# Appendix A

# ESKIMO II LOADING PREDICTIONS

by

R. E. Reisler
and
W. Baity
Ballistic Research Laboratories
Aberdeen Proving Ground, Maryland

December 1973

This appendix was prepared at the request of DDESB as a contribution to the final technical report on the ESKIMO II test.

## BALLISTIC RESEARCH LABORATORIES

RReisler/WBaity/rjs
Aberdeen Proving Ground, Maryland
December 1973

# ESKIMO II LOADING PREDICTIONS

## ABSTRACT

The Ballistic Research Laboratories responded to an informal request by the Department of Defense Explosives Safety Board to determine the charge weight to be used in the Eskimo II test that would generate a 30 psi overpressure and yield an 1100 psi-millisecond impulse at a specific position on the headwall of an earth-covered steel arch igloo magazine located at a ground range of 147 feet.

A set of predictions was derived using the BRL computer program SLOFF. The inputs simulated hemispherical TNT charge yields of $W^{1/3}$ equaling 21.5, 22.9 and 24.7 at ground ranges such that the side-on pressure was 20, 25, 30 and 40 psi. Evaluations were made using overpressure decay rates derived by both Brode and Kingery.

The charge source was restricted to 750-lb M117 bombs. Based on hemispherical TNT surface burst studies, the effective yield of M117 bombs and the loading prediction of SLOFF, recommendations for a 72 M117 bomb source were made. The predicted side-on pressure was 38 psi with an 1100 psi-millisecond impulse at the specified headwall position. Since the cylindrical shape of bombs precluded hemispherical stacking, the alternative of triangular stacking was suggested.

# I. INTRODUCTION

The Ballistic Research Laboratories (BRL) responded to an informal request by the Department of Defense Explosives Safety Board (DDESB) to determine the charge weight to be used in the Eskimo II[1]* test. This experiment was designed to obtain blast loading and response data on full scale storage igloos of varied headwall and door construction. To make effective use of the capital assets remaining after the completion of Eskimo I test[2], it was decided to centrally locate the charge such that the three remaining storage igloo headwalls and the two to be added would be subjected to similar loading. Results from Eskimo I and previous model studies indicated that a charge which would generate a 30 psi overpressure and yield an 1160 psi-millisecond impulse at a specific position on the headwall was desirable. The DODESB final specifications were that the ground range would be 147 feet and that the impulse should be 1100 psi-milliseconds with side-on pressure being the variable parameter.

A set of predictions was derived using the BRL computer program SLOFF**. The inputs to the program included positive phase overpressures ranging from 20 to 40 psi maximum side-on pressure with the decay rate and duration corresponding to that expected from hemispherical TNT charges at specific ground ranges. The output, expected impulse at the designated position on the headwall, was extrapolated to provide the proper impulse at the selected ground range which in turn indicated the TNT equivalent charge to be used.

# II. APPLICATION OF SLOFF TO ESKIMO II

SLOFF is based on empirically derived equations and designed to predict the loading on any rectangular surface oriented normal to the direction of travel of a plane shock wave[3]. Modifications were made so that the program could evaluate the single point of interest on the magazine headwall polygon. The program can evaluate the effect of rectangular opening in the front surface but in this series the doors were considered as capable of withstanding the loading. It should be mentioned that the program makes no provision to handle reflections or compression waves generated by surface irregularities or objects in proximity to the area of interest.

Input parameters included the maximum side-on pressure and positive phase duration associated with a hemisphere of TNT resting on the ground. The hemispherical TNT data in Reference 4 provided appropriate base information for the test conditions. Three charge weights of 10,000 lb, 12,000 lb, and 15,000 lb were chosen with a maximum free field side-on overpressure of 20, 25, 30 and 40 psi. The positive phase durations and ground range for these conditions were then determined from the same reference.

Two evaluations of the impulse at the gage position for the twelve conditions were made using different equations to describe the decay of the overpressure function. The first calculation used equations describing the exponential decay suggested by Brode[5] and the second used the empirically

* Superscript numbers denoted references listed on page 65
** Computer program - Shock Loading On Front Face

TABLE I RESULTS FOR 10,000 lb, 12,000 lb, and 15,000 lb TNT

| CHARGE WEIGHT (lb) | GROUND RANGE (ft) | OVER PRESSURE (psi) | POSITIVE PHASE DURATION (msec) | PREDICTED IMPULSE Note A (psi-msec) | PREDICTED IMPULSE Note B (psi-msec) |
|---|---|---|---|---|---|
| 15,000 | 123.3 | 40 | 38.7 | 912 | 992 |
| | 141.8 | 30 | 40.4 | 754 | 879 |
| | 155.4 | 25 | 44.4 | 666 | 778 |
| | 172.6 | 20 | 49.3 | 572 | 660 |
| 12,000 | 114.4 | 40 | 35.9 | 858 | 935 |
| | 131.6 | 30 | 37.5 | 710 | 828 |
| | 144.2 | 25 | 41.2 | 627 | 733 |
| | 160.2 | 20 | 45.8 | 540 | 623 |
| 10,000 | 107.7 | 40 | 33.8 | 816 | 888 |
| | 123.8 | 30 | 35.3 | 676 | 789 |
| | 135.7 | 25 | 28.8 | 597 | 700 |
| | 150.8 | 20 | 43.1 | 514 | 595 |

Note A. Kingery
B. Brode

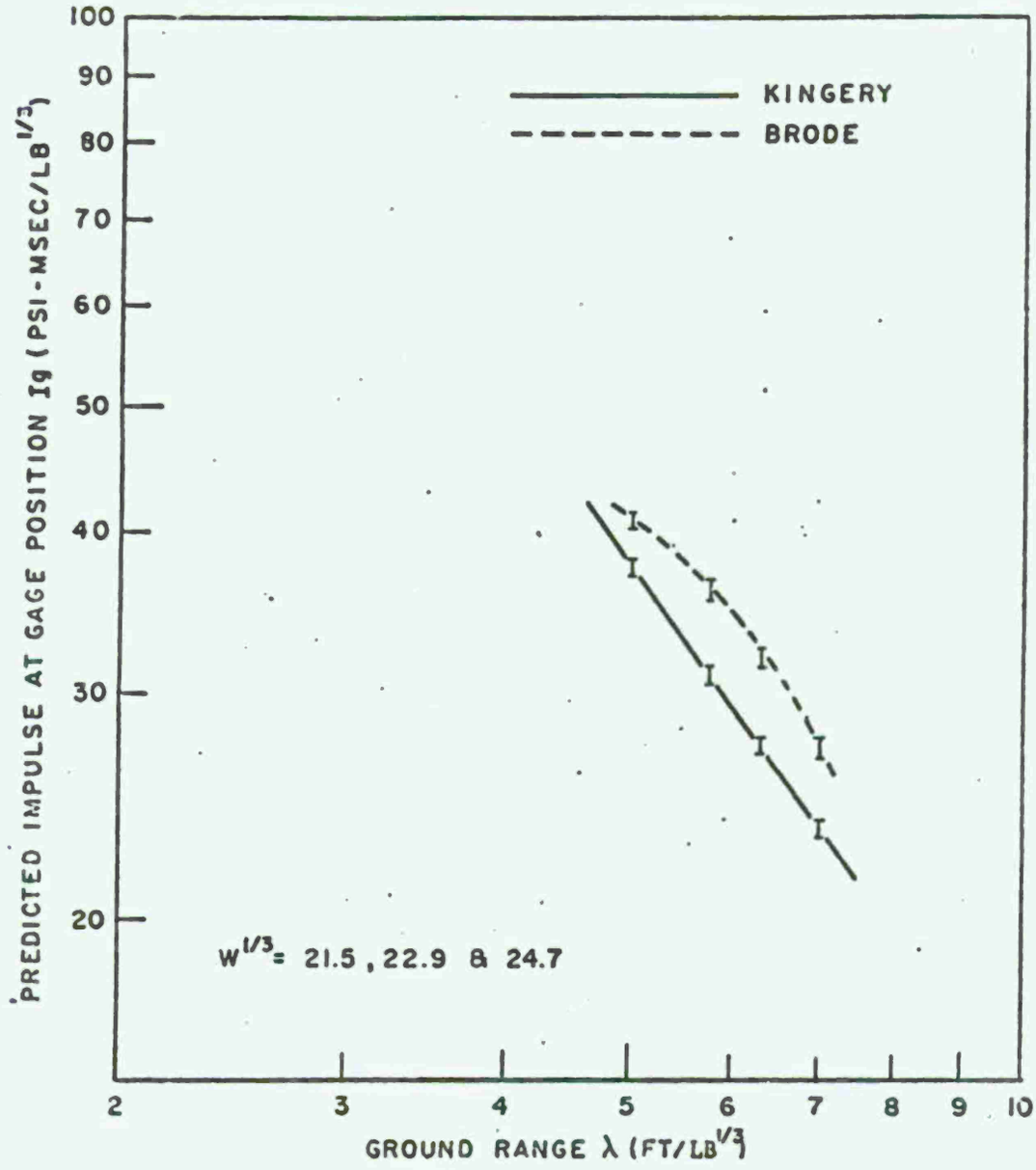


FIGURE 1 PREDICTED IMPULSE Vs GROUND RANGE

TABLE II RESULTS FOR 24,000 lb TNT

| CHARGE WEIGHT (lb) | GROUND RANGE (ft) | OVER PRESSURE (psi) | POSITIVE PHASE DURATION (msec) | PREDICTED IMPULSE Note A (psi-msec) | PREDICTED IMPULSE Note B (psi-msec) |
|---|---|---|---|---|---|
| 24,000 | 144.0 | 40 | 45.2 | 1068 | 1160 |
| | 165.6 | 30 | 47.2 | 882 | 1082 |
| | 181.4 | 25 | 51.3 | 779 | 910 |
| | 201.6 | 20 | 57.6 | 670 | 772 |

Note A. Kingery
B. Brode

TABLE III PREDICTED RESULTS

| CHARGE | GROUND RANGE (ft) | OVER PRESSURE (psi) | POSITIVE PHASE DURATION (msec) | PREDICTED IMPULSE (psi-msec) |
|---|---|---|---|---|
| 72 M117 Bombs | 147 | 38 | 45.5 | 1100 |

Note: Sea level conditions

derived equations suggested by Kingery[6]. The results, tabulated in Table I, show the impulse loading for these charge weights to be much less than the desired 1100 psi-millisecond. Subsequently, two additional charge weights of 20,000 lb. and 24,000 lb. were selected and the data scaled for these conditions. It was considered adequate for this exercise to use cube root scaling for the impulse loading as depicted in Figure 1 in lieu of several additional computer runs. The results of the 24,000 lb charge weight are presented in Table II. This data enabled the determination of the parameters associated with the specific ground range of 147 feet selected by DODESB as presented in Table III. All evaluations were made at standard sea level conditions as requested.

## III. COMMENTS

Recommendation of a relatively clean predictable source such as ammonium nitrate/fuel oil[7,8,9] was made, but because of other considerations the source was restricted to 750 lb M117 bombs surrounded by an earthen revetment. The effective yield of the M117 bomb[10], derived by determining the TNT equivalent weight of the explosive filler and using the modified Fano formula to estimate the energy available to the blast wave, suggested a nominal 72 bombs as equivalent to the recommended TNT charge. Since bomb shape precluded hemispherical stacking, the alternative of triangular stacking was suggested. No air blast data from the detonation of a stack of bombs of this geometry was available; however, small charge experiments conducted by DRI[11] and BRL[12] with bare cylindrical charges fired in free air and on the ground offered some information. In these experiments the effects of charge geometry on the blast wave was observed. In the case of a right circular cylinder, a bridge wave forms off the corners from the interaction of the primary end wave and the primary side wave. The direction of propagation is at 45° to the axis of the cylinder. Higher side-on pressures associated with these interactions were measured in an area subtended by a 30° arc in the direction of propagation. Applying this observation to the shape of the bomb stack suggested that these higher pressure regions would not affect the shock loading of igloo headwalls facing the sides of the bomb stack.

Another applicable geometry effect observed in small charge experiments was the increased near field peak pressure associated with an increase in presented area of the charge in that direction. Overall dimensions of the stack would approximate a base of 129 inches with a height of 112 inches and a side width of 102 inches. This charge geometry presents an area greater on the sides than on the ends, but the difference was considered tolerable.

Even though the donor charge offered a number of uncertainties - such as correspondence in effective yield, edge effects from the stack shape, correspondence in overpressure wave shape, coalescence of multiple shocks and their expansion over the revetment into a clean wave in the near field - it was anticipated that a good pressure-time history would be recorded and that this could be used as an input to a modified SLOFF program that would evaluate the average loading on the magazine doors. Correlation of the test measurements and predictions will be made after the test data has been evaluated.

## REFERENCES


1. Perkins, R. G., "Eskimo I", Fourteenth Annual Explosives Safety Seminar Minutes, Department of Defense Explosive Safety Board, November 1972.

2. Warren, T. W., et.al., "Interior Blast Pressures of Acceptor Magazines: Eskimo I", Fourteenth Annual Explosives Safety Seminar Minutes, Department of Defense Explosive Safety Board, November 1972.

3. Baity, W. M., "Loading Predictions for Eskimo II", Fifteenth Annual Explosives Safety Seminar Minutes, Department of Defense Explosives Safety Board, September 1973.

4. Kingery, C. N., "Air Blast Parameters vs Distance for Hemispherical TNT Surface Bursts", Ballistic Research Laboratories, Report No. 1344, September 1966.

5. Brode, H. L., "A Review of Nuclear Explosion Phenomena Pertinent to Protective Construction", Rand Document No. R-425-PR, Rand Corp., Los Angeles, California, May 1964.

6. Kingery, C. N., et.al., "Airblast Overpressure Versus Time Histories Nuclear and TNT Surface Bursts", Ballistic Research Laboratories, Report No. 1638, March 1973.

7. Sadwin, L. D., and Swisdak, Jr., M. M., "AN/FO Charge Preparation for Large Scale Tests", U.S. Naval Ordnance Laboratory, White Oak, Md., NOLTR 70-205, 8 October 1970.

8. Giglio-Tos, L. and Reisler, R. E., "Air Blast Studies of Large Ammonium Nitrate/Fuel Oil Explosions", Ballistic Research Laboratories Memorandum Report No. 2057, August 1970.

9. Sadwin, L. D. and Swisdak, Jr., M. M., "Performance of Multiton AN/FO Detonation", U.S. Naval Ordnance Laboratory, White Oak, NOLTR 73-105, 2 July 1973.

10. Fugelso, L. E., et.al., "A Computation Aid for Estimating Blast Damage from Accidental Detonation of Stored Munitions," Fourteenth Annual Explosive Safety Seminar, November 1972.

11. Wisotski, J. and Snyer, W. H., "Characteristics of Blast Waves Obtained from Cylindrical High Explosive Charges", DRI#2286, November 1965, University of Denver, Denver Research Institute, Denver, Colorado, 80210.

12. Reisler, R. E., et.al., "Air Blast Parameters from Pentolite Cylinders Detonated on the Ground", BRL Memorandum Report to be published.

## Appendix B

# AIRBLAST EFFECTS ON WINDOWS IN BUILDINGS AND AUTOMOBILES ON THE ESKIMO II EVENT

by

E. R. Fletcher
D. R. Richmond
R. K. Jones

Lovelace Foundation for Medical Education and Research
Albuquerque, New Mexico 87108

September 1973

This appendix contains six photographs of window test structures and automobiles that were added by NWC to supplement data provided by the Lovelace Foundation.

# AIRBLAST EFFECTS ON WINDOWS IN BUILDINGS AND AUTOMOBILES ON THE ESKIMO II EVENT

E. R. Fletcher, D. R. Richmond, and R. K. Jones
Lovelace Foundation for Medical Education and Research
Albuquerque, New Mexico 87108

## INTRODUCTION

### Objectives

The objectives of this project were:

1. to determine the velocities, masses, and spatial densities of the fragments from three types of standard plate-glass windows* mounted in closed, cubical structures at three ranges on the Eskimo II test;
2. to study the response of a clothed anthropomorphic dummy (a) standing behind one of the plate-glass windows and (b) sitting in an automobile; and
3. to estimate the hazards to occupants of buildings and automobiles exposed to similar levels of airblast.

### Background

There are many civilian and military organizations concerned with the safety of personnel in the advent of a nearby accidental or intentional detonation of explosive materials. One major problem area has been the evaluation of the flying-glass hazard to occupants of buildings, houses, and automobiles. Experimental and theoretical studies have produced a fair amount of information regarding the conditions under which ordinary windows will break, but considerably less is known about the characteristics of the resultant fragments. Reference 1 summarizes the available pertinent data which were obtained mostly by trapping glass fragments in sheets of Styrofoam (expanded polystyrene) placed behind windows in houses located in the vicinity of nuclear and HE detonations at overpressure levels between 1.0 and 5.0 psi. Most of these data were for windows with a glass thickness of from 0.082 to 0.13 inches, whereas the plate glass commonly used in buildings has a thickness of from 0.18 to 0.28 inches. The only data in Reference 1 for plate glass were obtained from five identical windows in one house exposed at an overpressure level of 2.7 psi. Thus, the Eskimo II test provided an opportunity to fill the gap by exposing plate-glass windows of several designs to lower overpressure levels than those that had been previously tested.

* Sheet-glass windows were also included in the tests.

## PROCEDURE

### Modules

Ten 9-foot cubical boxes called modules were fabricated and positioned along the northwest radial (see Figure 1) by China Lake personnel. Three modules abutted one another at the 3400-foot range, three at 1700 feet, and four at 1210 feet. The only openings into each module were a hole where a window was mounted and an access door which was closed during the blast. All of the windows faced ground zero. Figure 2 shows a preshot view of the modules at the 1700-foot range.

### Windows

The three types of windows tested are shown at the bottom of Table I. Types W1 and W2, designated as projected and horizontal-sliding, respectively, are commercial-type windows used extensively in government buildings and comply with, but do not exceed, the Architectural Aluminum Manufacturers Association (AAMA) specifications. The Type W3, window-walls, were mounted in a neoprene structural gasket system used in Federal office buildings but no AAMA specifications are available. Three Type W1, four Type W2, and three Type W3 windows were mounted one each in the ten modules. One window of each type was tested at each of the three ranges. The additional Type W2 window was located at the 1210-foot range. Some of the panes were spray painted different colors to aid in identifying the sources of the trapped fragments (see Table I).

### Styrofoam

A Styrofoam witness plate was mounted on the inside back wall of each of six of the modules at the 1700- and 1210-foot ranges in an attempt to trap glass fragments if the window was broken by the blast wave. The witness plates were fabricated at the Lovelace Foundation using low-density Styrofoam (Type II, described in Reference 2) glued to 1/2-inch plywood. Each witness plate included two pieces of Styrofoam each 90 inches high, 32.5 inches wide, and 6 inches thick. Prior to fabrication, calibration techniques described in Reference 2 were used to develop a formula for determining the velocity of a fragment from its mass and the volume of the impression it made in the Styrofoam. In each module the distance from the window to the surface of the Styrofoam was approximately 84 inches.

### Cloth Sheets

A cloth sheet (95 inches wide, 95 inches high) was hung behind the window in each of the three modules at the 3400-foot range in order to estimate possible penetration of clothing if the windows broke. The four sides of the sheets were fastened to wooden frames positioned 47 inches behind the windows.

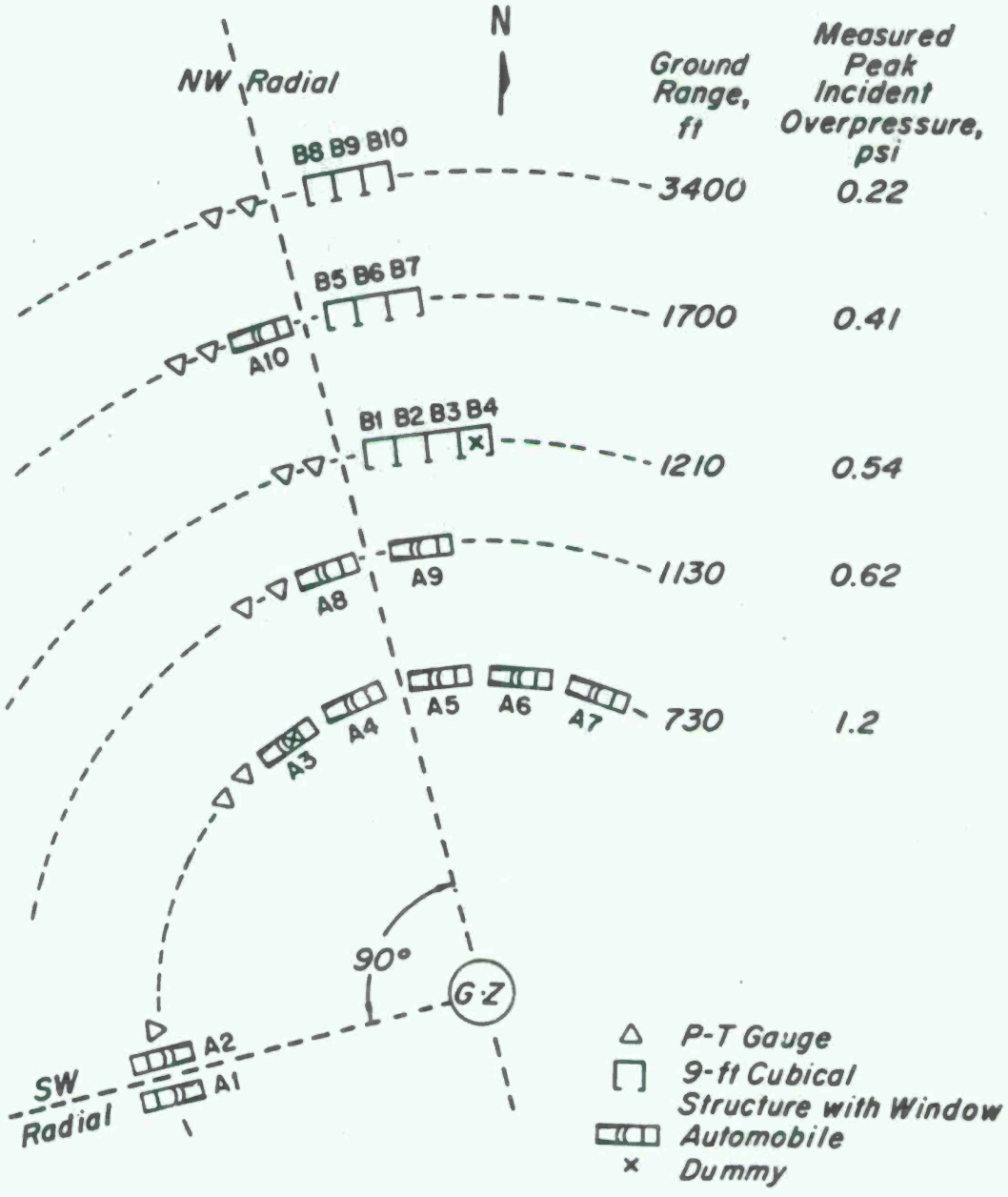


Figure 1. Field Layout for Eskimo II Test.

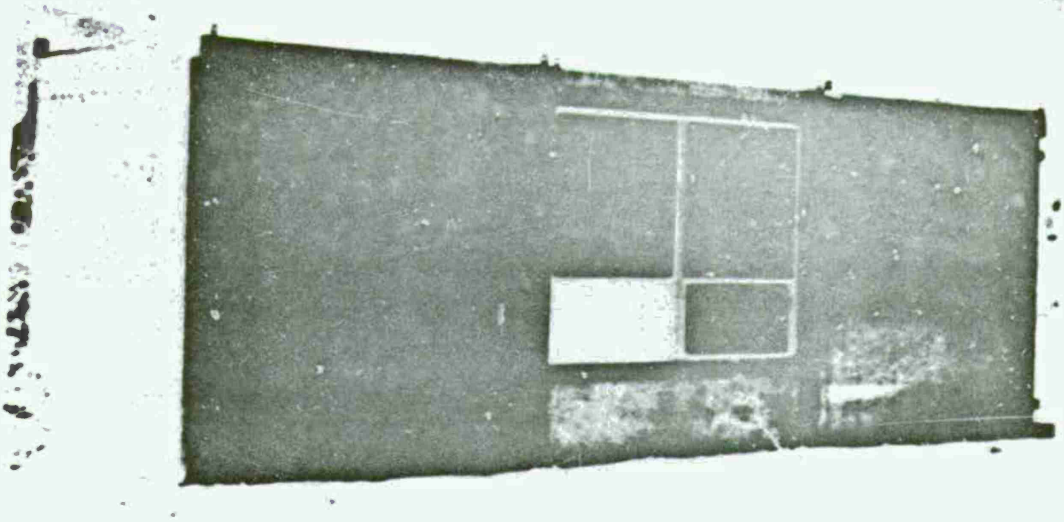

Figure 2. Preshot View of (from left to right) Modules B5, B6, and B7.

## TABLE I

## DESCRIPTION OF THE WINDOWS IN THE MODULES

| Window Type | Parameters for Individual Panes | | | | | |
|---|---|---|---|---|---|---|
| | Number | Color* | Width, in. | Height, in. | Type of Glass | Frame Type |
| W1 | P1 | Copper | 45 | 45 | Plate | Fixed |
| | P2 | Green | 45 | 45 | Plate | Fixed |
| | P3 | Silver | 42 | 20 | Sheet | Top Opening |
| | P4 | Black | 42 | 20 | Sheet | Top Opening |
| W2 | P1 | Copper | 34 | 48 | Sheet | Horizontal Sliding |
| | P2 | Green | 34 | 48 | Plate | Fixed |
| W3 | P1 | Copper | 44 | 90 | Plate | Fixed |
| | P2 | Green | 48 | 90 | Plate | Fixed |

* A thin coat of paint was sprayed on both sides of each pane at 1210 and 1700 ft ground range but not at the 3400 ft ground range.

FRONT VIEWS OF THREE MODULES INDICATING WINDOW TYPE AND PANE NUMBERS

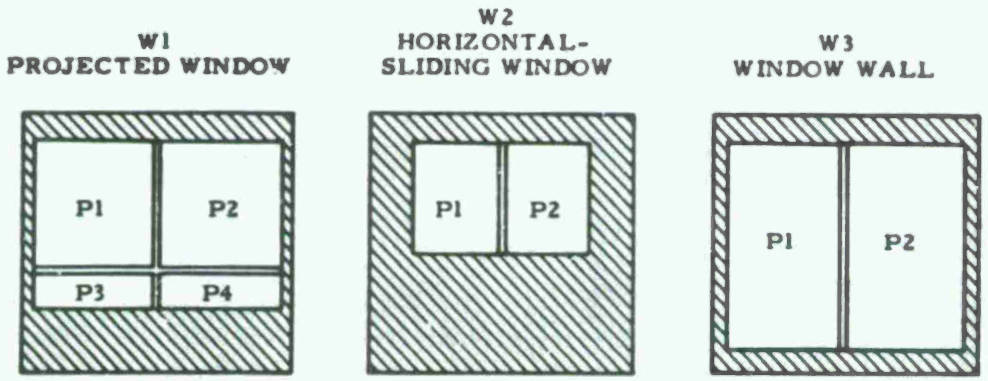

### Automobiles

Ten conventional automobiles were utilized on this test (see Figure 1); eight were situated left-side-on on the northwest radial (one at 1700 feet, two at 1130 feet, and five at 730 feet), and two were exposed face-on on the southwest radial (730 feet). No Styrofoam was placed in any of the automobiles.

### Dummies

Two anthropomorphic dummies attired in summer civilian clothing were supplied by the Lovelace Foundation for this test. One of the dummies was standing 35 inches behind pane P2 in the B4 module at 1210 feet. This module did not contain any Styrofoam witness plates. The dummy faced the window with his chest resting lightly against a narrow metal rod intended to stabilize his position prior to shock arrival while not interfering with subsequent possible blast displacement. The other dummy was secured by means of a lap seat belt in the driver's seat of a left-side-on station wagon located at 730 feet on the northwest radial (see Figure 1).

### Cameras

Two high-speed (400 frames per second) motion-picture cameras were used by China Lake personnel to record the responses of the two dummies. A reference grid was painted on the portion of the module wall in the field of view of the camera in order to facilitate velocity determinations for the glass fragments and the dummy.

### Overpressure Gauges

Eleven self-recording BRL mechanical gauges were positioned, two each, at the 3400-, 1700-, 1210-, 1130-, and 730-foot ranges on the northwest radial and one at the 730-foot range on the southwest radial. These were supplied by China Lake.

## RESULTS AND DISCUSSION

### General

All of the modules remained structurally intact and none of the cloth sheets or Styrofoam witness plates were damaged or displaced by the blast experience. A total of 426 fragments were trapped from 14 of the 17 panes which broke. Window damage was noted in eight of the ten automobiles on the layout. Dummy and glass responses were satisfactorily documented with both motion-picture cameras. Good pressure-time records were obtained from all gauges and average measured peak incident overpressures are given in Figure 1 for the five ranges of interest.

## Windows in Modules

The 26 panes of glass exposed in the modules are listed in Table II along with such information as glass thickness, whether or not the pane broke, and the number of fragments trapped. All ten panes at 1210 feet, seven of the eight panes at 1700 feet, and none of the eight panes at 3400 feet broke. As expected, only a portion of the glass from the broken panes was actually trapped. This is indicated by the number of fragments on the floor below the Styrofoam shown in Figure 3, a postshot view through the frame of pane P1 in module B2. Table II also contains the average measured peak incident overpressure, $P_i$, the calculated (using $P_i$) peak overpressure in the reflected wave at the front of the modules, $P_r$, and the average measured duration of the positive phase of the incident overpressure, $t_p$.

The masses and velocities were determined by procedures described in Reference 2 for all but five fragments which struck so close to other fragments that the measured volumes of the impressions in the Styrofoam were suspect. As in the past, it was noted that for each pane an approximately linear relationship existed between the logarithms of the velocities and the logarithms of the masses of the fragments. A least-squares linear-regression analysis was performed for each pane and the results appear in Table II where $V_{50}$ and $M_{50}$ are the geometric mean fragment velocity and mass, respectively; $b$ and $E_b$ are the slope and the standard error in the slope of the regression line, respectively; and $E_{gv}$ is the geometric standard error of estimate of fragment velocity. In addition, $A_{50}$ is the geometric mean frontal area of the fragments (calculated from the density and thickness of the glass and $M_{50}$), and $E_{gm}$ and $E_{ga}$ are the geometric standard deviation of the fragment masses and frontal areas, respectively. All 426 fragments were used in computing the densities of trapped fragments which, for each pane, tended to be constant over an area of Styrofoam equal to the size of the pane. This area was, in general, centered somewhat below the center of the pane as a result of the fragments' having fallen (due to gravity) in traversing the distance from the frame to the Styrofoam. Likewise, the density of trapped fragments for an entire window (i.e., counting the fragments from all of the panes) tended to be approximately constant over an area of Styrofoam equal in size to the window but displaced downward. The computed average densities (designated as $\rho_d$ and $\rho_w$ for the individual panes and entire windows, respectively) over these areas of approximately constant density are listed in Table II.

It was noted that the fragment data for panes of approximately the same thickness located at the same ground range tended to be very similar. Therefor the data were combined into four groups representing panes approximately 1/4- or 1/8-inch-thick located at the 1210- or 1700-foot ground range. These groups are shown in Figures 4 through 7. The results of a regression analysis for each of the four groups are given in Table II where it can be noted that for six panes of approximately 1/4-inch-thick glass at 1210 feet the mean velocity of trapped fragments was 52.1 ft/sec compared to 52 ft/sec for the pane which struck the dummy as estimated from the motion-picture record.

Figures 4 through 7 also contain the regression lines as well as lines drawn one standard error of estimate on either side of the regression lines. In addition, the figures contain curves indicating the probability of a fragment's penetrating 1 cm of soft tissue as given in Reference 3. It can be seen that, of the 421 trapped fragments for which masses and velocities are available, only ten had at least a 1.0-percent probability of penetrating 1 cm of soft tissue. These fragments are listed in Table III. Nine of the ten occurred at the 1210-foot range where fragments were trapped behind eight panes giving an average of about one fragment per pane with a significant (≥1.0 percent) probability of penetrating 1 cm of soft tissue. The highest probability computed at this range was 44 percent. In

TABLE II

FRAGMENT DATA FOR THE WINDOWS IN THE MODULES

| Ground Range, ft | $P_i$, psi | $P_r$, psi | $t_p$, msec | Module Number | Window Type | Pane Number | Glass Thickness, in. | Number of Trapped Fragments | $V_{50}$, ft/sec | $M_{50}$, gm | $A_{50}$, in.$^2$ | $E_{gm}$ or $E_{ga}$ | b | $\sigma_b$ | $\Sigma_{gv}$ | $\rho_d$, frags. per ft$^2$ | $\rho_w$, frags. per ft$^2$ |
|---|---|---|---|---|---|---|---|---|---|---|---|---|---|---|---|---|---|
| 1210 | 0.56 | 1.10 | 158 | B1 | W2 | P1 | 0.219 | 42 | 66.6 | 4.14 | 0.467 | 3.35 | -0.215 | 0.0451 | 1.39 | 3.10 | 2.05 |
| | | | | | | P2 | 0.227 | 10 | 35.9 | 9.07 | 0.987 | 7.38 | -0.237 | 0.0564 | 1.40 | 0.866 | |
| | | | | B2 | W3 | P1 | 0.226 | 22 | 35.6 | 25.6 | 2.80 | 4.10 | -0.188 | 0.0766 | 1.62 | 1.27 | 2.58 |
| | | | | | | P2 | 0.225 | 58 | 59.9 | 6.52 | 0.716 | 4.87 | -0.231 | 0.0431 | 1.57 | 3.61 | |
| | | | | B3 | W1 | P1 | 0.231 | 19 | 52.9 | 12.2 | 1.30 | 4.73 | -0.229 | 0.0490 | 1.38 | 1.99 | 6.54 |
| | | | | | | P2 | 0.224 | 25 | 51.4 | 8.09 | 0.892 | 3.38 | -0.275 | 0.0709 | 1.51 | 2.55 | |
| | | | | | | P3 | 0.121 | 59 | 66.6 | 2.51 | 0.512 | 3.57 | -0.211 | 0.0316 | 1.36 | 6.09 | |
| | | | | | | P4 | 0.120 | 84 | 72.0 | 1.19 | 0.245 | 3.66 | -0.113 | 0.0304 | 1.42 | 7.20 | |
| | | | | B4 | W2 | P1 | 0.219 | ** | - | - | - | - | - | - | - | - | - |
| | | | | | | P2 | 0.226 | ** | 52† | - | - | - | - | - | - | - | |
| | | | | Data from B1, B2, and B3 combined | | | 0.120 | 143 | 69.2 | 1.64 | 0.337 | 3.77 | -0.155 | 0.0220 | 1.42 | 6.92 | |
| | | | | | | | 0.224 | 176 | 52.1 | 8.09 | 0.892 | 4.48 | -0.244 | 0.0217 | 1.54 | 2.33 | |
| 1700 | 0.41 | 0.83 | 180 | B5 | W3 | P1 | 0.227 | 1 | 11.8 | 15.0 | 1.63 | - | - | - | - | 0.111 | 0.831 |
| | | | | | | P* | 0.226 | 15 | 40.0 | 9.37 | 1.03 | 3.62 | -0.345 | 0.125 | 1.83 | 1.55 | |
| | | | | B6 | W1 | P1 | 0.232 | 0 | - | - | - | - | - | - | - | 0 | 4.49 |
| | | | | | | P2 | 0.225 | 11 | 37.8 | 4.78 | 0.525 | 8.35 | -0.139 | 0.0452 | 1.35 | 0.997 | |
| | | | | | | P3 | 0.120 | 46 | 58.4 | 1.82 | 0.374 | 3.67 | -0.238 | 0.0473 | 1.51 | 5.10 | |
| | | | | | | P4 | 0.120 | 26 | 72.9 | 0.655 | 0.135 | 3.34 | -0.284 | 0.0402 | 1.44 | 2.88 | |
| | | | | B7 | W2 | P1* | 0.219 | 0 | - | - | - | - | - | - | - | 0 | 0.166 |
| | | | | | | P2 | 0.227 | 3 | 50.4 | 9.82 | 1.07 | - | - | - | - | 0.332 | |
| | | | | Data from B5, B6, and B7 combined | | | 0.120 | 72 | 63.3 | 1.36 | 0.259 | 3.86 | -0.248 | 0.0343 | 1.48 | 3.99 | |
| | | | | | | | 0.226 | 38 | 38.4 | 7.47 | 0.816 | 5.05 | -0.237 | 0.0664 | 1.78 | 8.598 | |
| 3400 | 0.22 | 0.44 | 202 | B8 | W3 | P1* | 0.232 | ** | - | - | - | - | - | - | - | 0 | 0 |
| | | | | | | P2* | 0.227 | ** | - | - | - | - | - | - | - | 0 | |
| | | | | B9 | W1 | P1* | 0.232 | ** | - | - | - | - | - | - | - | 0 | 0 |
| | | | | | | P2* | 0.227 | ** | - | - | - | - | - | - | - | 0 | |
| | | | | | | P3* | 0.119 | ** | - | - | - | - | - | - | - | 0 | |
| | | | | | | P4* | 0.123 | ** | - | - | - | - | - | - | - | 0 | |
| | | | | B10 | W2 | P1* | 0.219 | ** | - | - | - | - | - | - | - | 0 | 0 |
| | | | | | | P2* | 0.227 | ** | - | - | - | - | - | - | - | 0 | |
| Total Number of Trapped Fragments | | | | | | | | 421‡ | | | | | | | | | |

* This pane did not break.
** There was no Styrofoam in the module containing this pane.
† Velocity estimated from the motion-picture record (397 frames per second).
‡ Overall, an additional 5 fragments were trapped for which M and V were not calculated (see text) bringing total number of fragments trapped to 426.

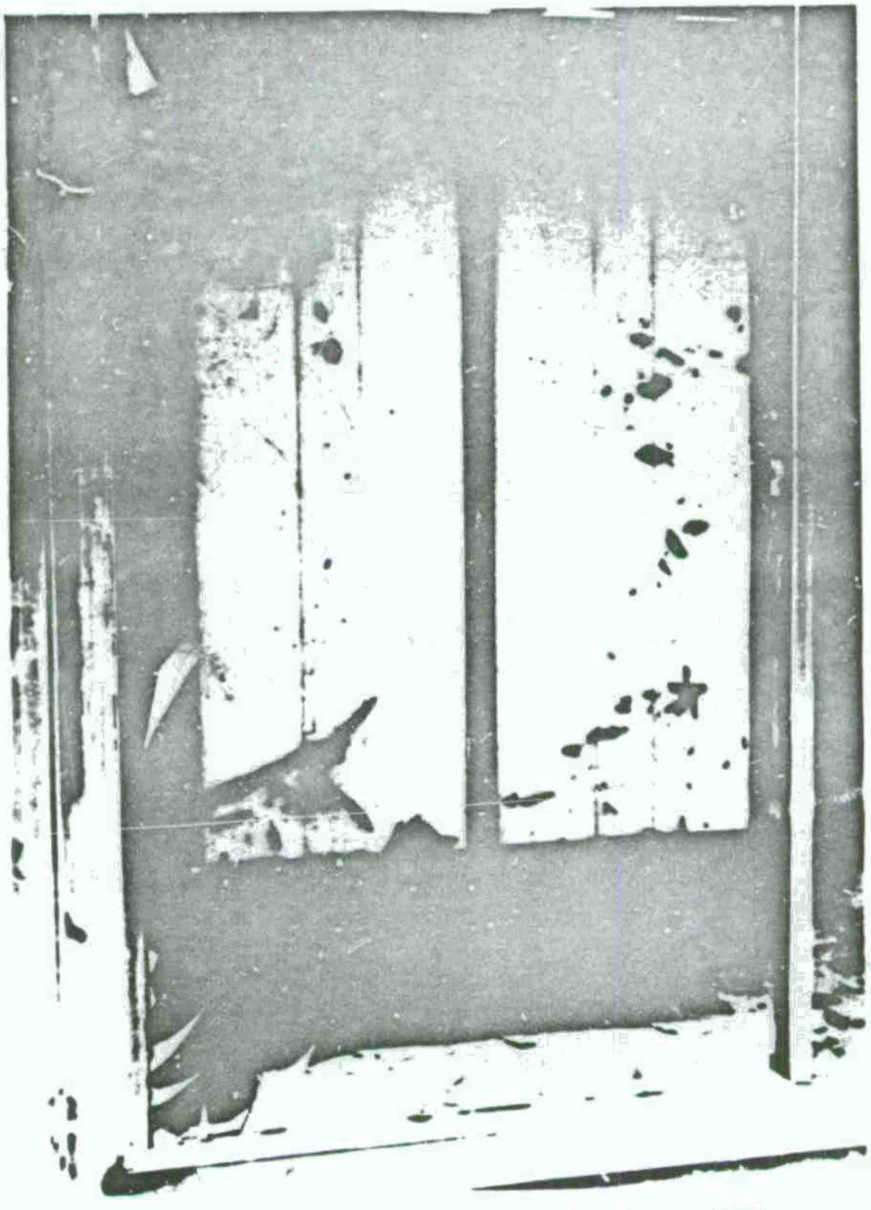

Figure 3. Postshot View Through the Flame of P1 Showing the Styrofoam Witness Plate in B2.

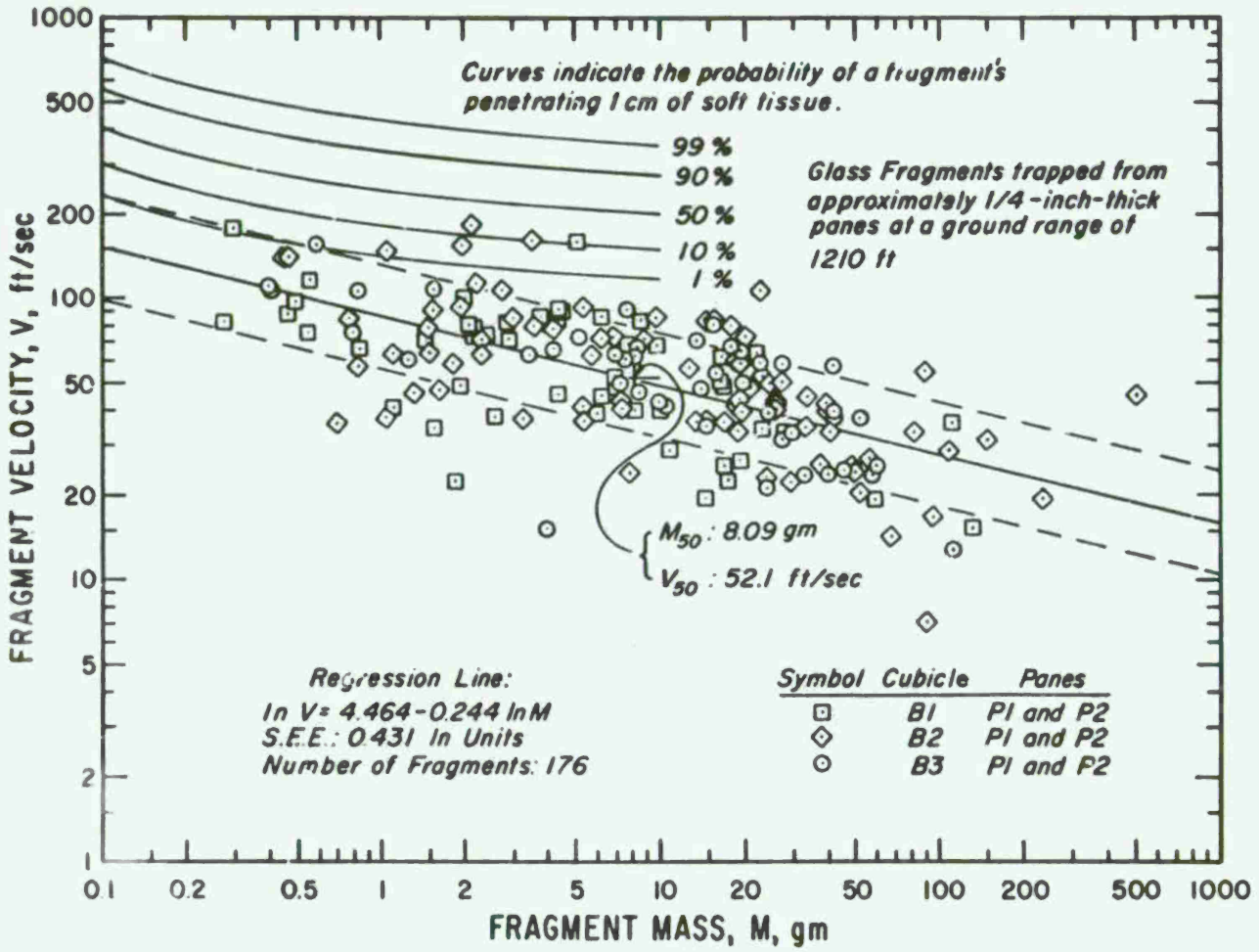


Figure 4. Glass Fragments Trapped from Approximately 1/4-Inch-Thick Panes at a Ground Range of 1210 Feet.

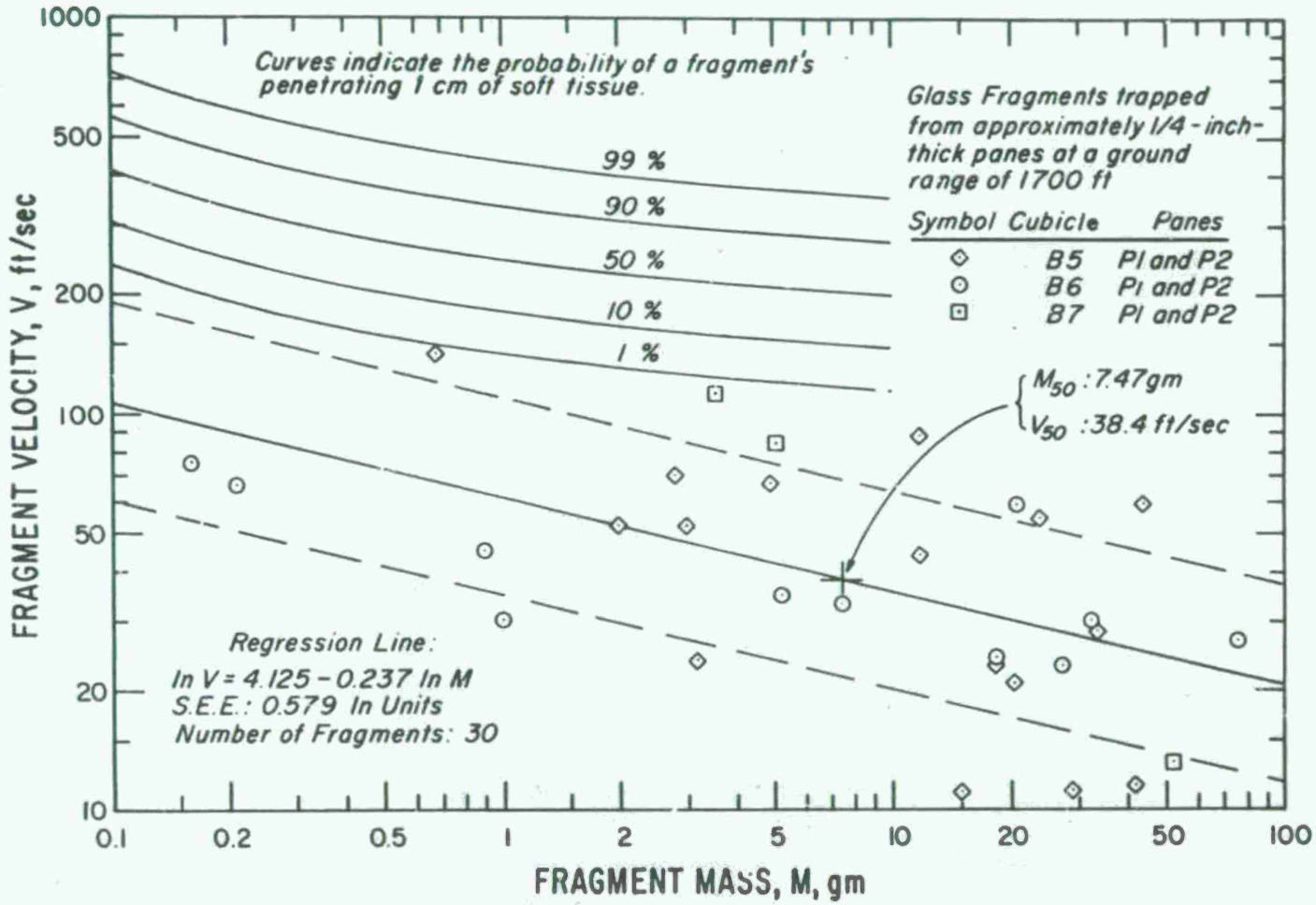


Figure 5. Glass Fragments Trapped from Approximately 1/4-Inch-Thick Panes at a Ground Range of 1700 Feet.

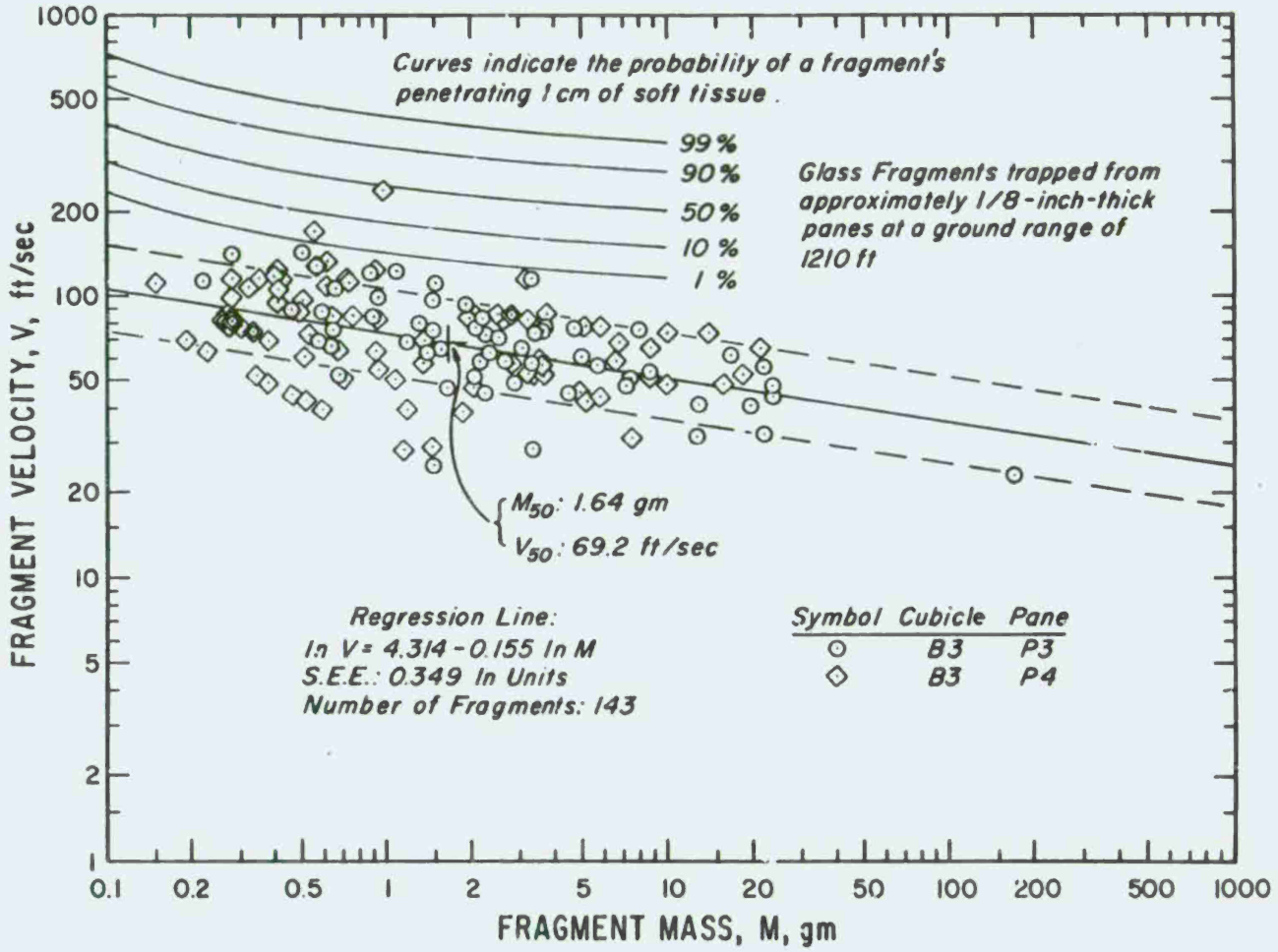


Figure 6. Glass Fragments Trapped from Approximately 1/8-Inch-Thick Panes at a Ground Range of 1210 Feet.

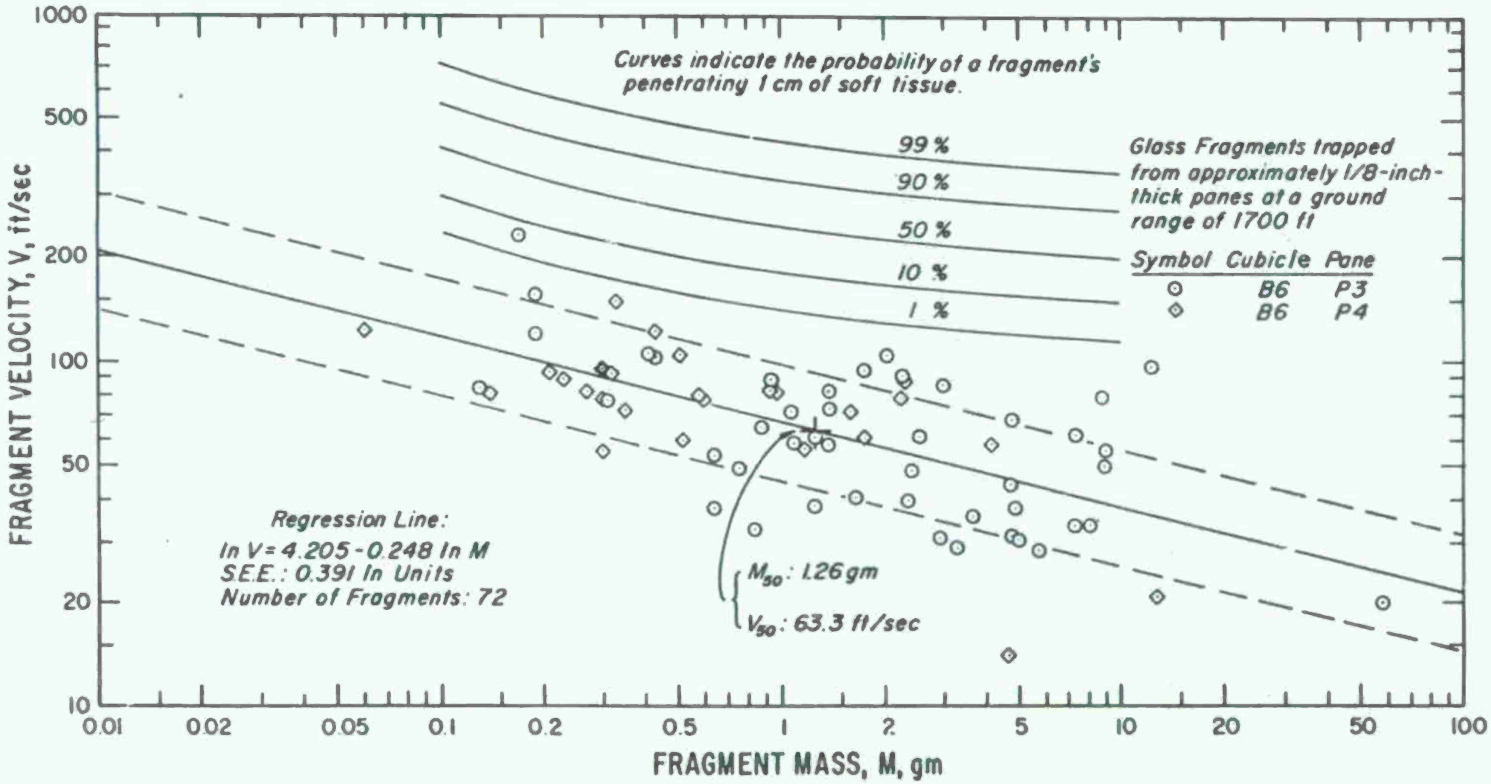


Figure 7. Glass Fragments Trapped from Approximately 1/8-Inch-Thick Panes at a Ground Range of 1700 Feet.

## TABLE III

### WINDOW GLASS FRAGMENTS WITH A SIGNIFICANT* PROBABILITY OF PENETRATING 1 CM OF SOFT TISSUE

| Module Number | Pane Number | Fragment Mass, gm | Fragment Velocity, ft/sec | Probability of Penetrating 1 cm of Soft Tissue, percent |
|---|---|---|---|---|
| B1 | P1 | 0.29 | 178 | 1.4 |
| | | 5.03 | 160 | 12.0 |
| B2 | P2 | 1.03 | 149 | 1.6 |
| | | 1.95 | 154 | 4.0 |
| | | 3.51 | 162 | 11.0 |
| | | 2.11 | 187 | 21.0 |
| B3 | P2 | 0.58 | 154 | 1.1 |
| | P4 | 0.55 | 169 | 2.3 |
| | | 0.97 | 239 | 44.0 |
| B6 | P3 | 0.17 | 233 | 4.0 |

* ≥1.0 percent.

contrast, only one fragment with a significant probability (4.0 percent) of penetrating was caught behind the eight panes at the 1700-foot range giving an average of about one-tenth fragment per pane.

In order to make comparisons between this and prior experiments, the current data were plotted in Figures 8 through 10 which were modified from Reference 1. In these figures, it can be seen that the fragment velocities, frontal areas, and densities for the current data tend to line up reasonably well with the corresponding values for the prior data when plotted against effective peak overpressure, taken to be $P_r$ for the current data since all the windows faced the advancing blast wave. However, on all three figures the current data tend to fall above the regression curve based on the prior data only. Thus, the current data suggest that in each case the shape of the regression curve might need to be modified for the lower overpressures. In the case of the mean fragment velocity, this is probably because the fragments with low velocities will not be caught in the Styrofoam.

## Dummy in Module

The window pane (P2) 35 inches in front of the dummy was broken by the blast wave. From the motion-picture record it was determined that many fragments struck the upper half of the dummy with an average velocity of about 52 ft/sec. However, the only effects noted on the dummy were three 1/8-inch-diameter holes in the shirt. One was located near the left shoulder and two were along the left arm about the level of the elbow. There was no damage or lacerations to the dummy itself beneath the small holes in the shirt and the fragments did not adhere to the material.

As a result of being struck by the blast wave and glass, the dummy was accelerated such that his head and center of mass were moving backward at 1.2 and 0.75 ft/sec, respectively. He was found in a supine position and, although the actual impact could not be seen in the film record, it was estimated that his head and center of mass impacted the floor at vertical velocities of 20 and 13 ft/sec, respectively. It was further estimated that the dummy required about 1.3 sec to impact the floor which is about twice the predicted average time required for the glass fragments to fall to the floor. It would thus be expected that the dummy would fall on top of the glass fragments on the floor, and such was found to be the case. Several large cuts were found on the back of the hat and shirt of the dummy as a result of his having fallen onto the glass.

## Windows in Automobiles

The locations of the automobiles on the layout are indicated in Figure 1, and the observed window damage is documented in Table IV. At 730 feet (1.2 psi) the most common damage was to windshields and door windows, particularly on the side of the automobile facing the oncoming blast wave. On the average, about two windows per automobile were damaged, of which approximately one half completely broke out and one half sustained multiple fractures but remained in place. Both automobiles at 1130 feet (0.62 psi) sustained only multiple fractures of the windshields. None of the windows in the automobile at 1700 feet (0.41 psi) were damaged. There was no evidence that any of the automobile windows were broken by bomb fragments or crater ejecta rather than by the airblast itself.

Fragments from the window which broke out in automobile A3 traveled across the field of

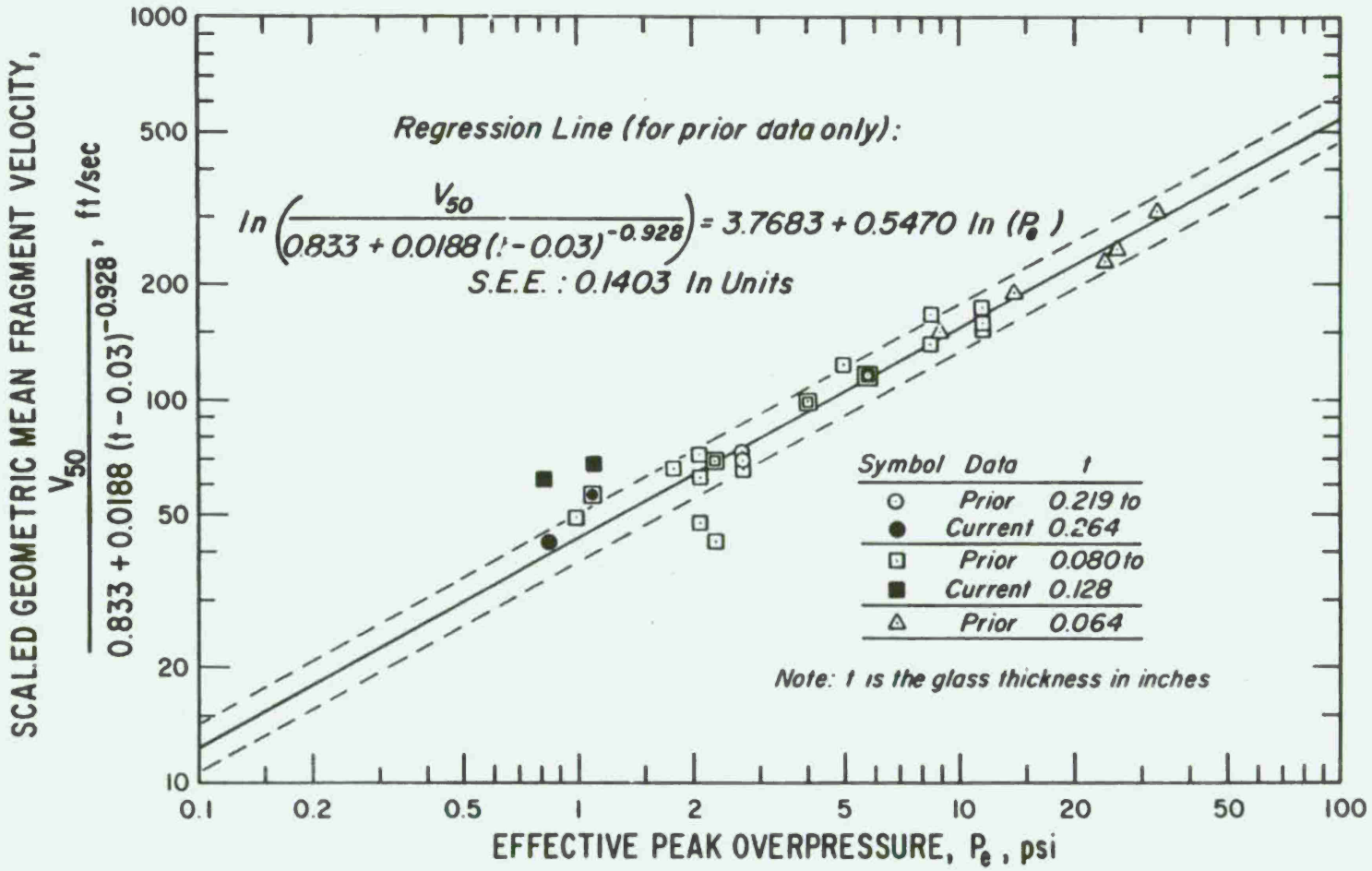


Figure 8. Scaled Geometric-Mean Fragment Velocity vs. Effective Peak Overpressure.

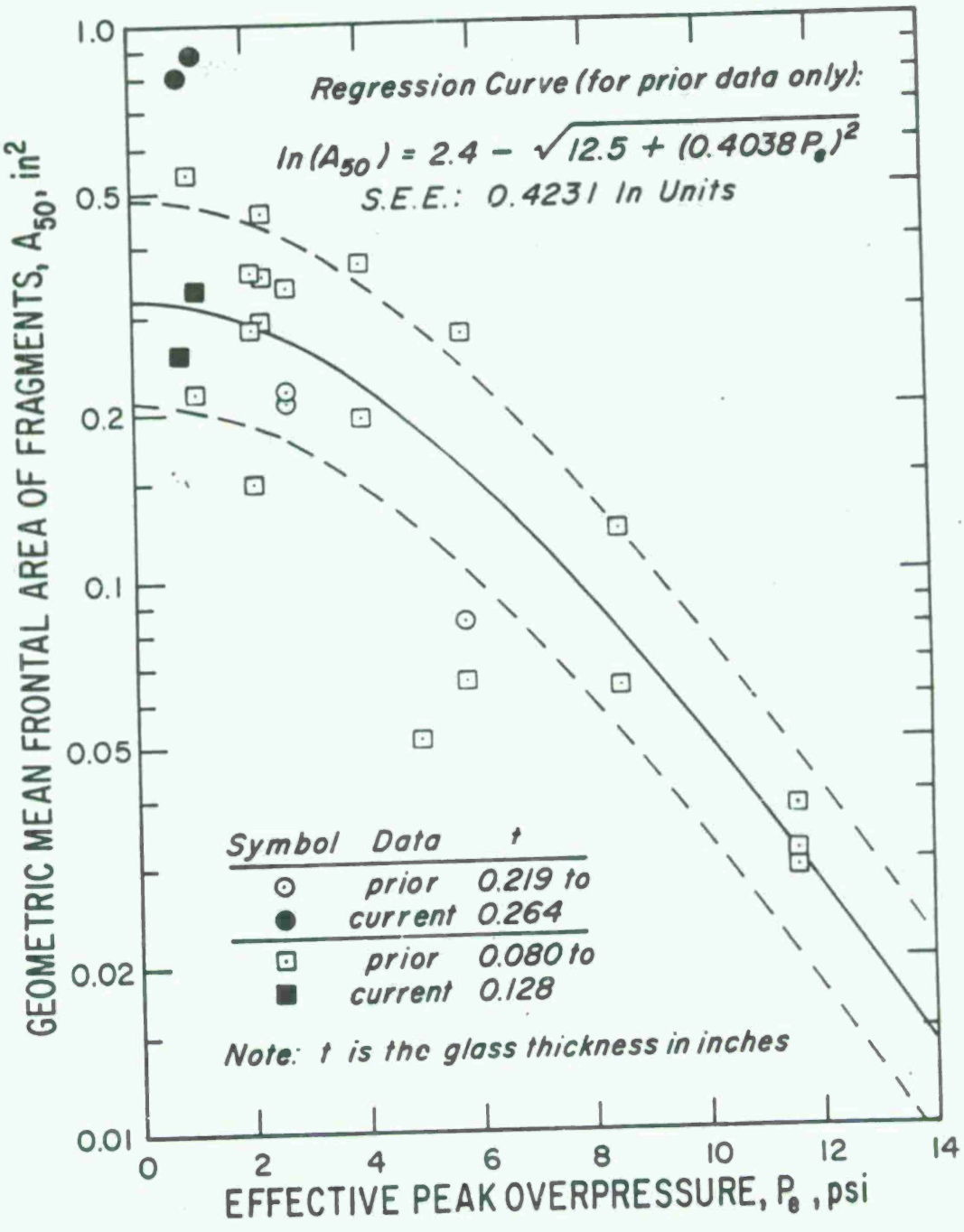


Figure 9. Geometric-Mean Frontal Area of Fragments vs. Effective Peak Overpressure.

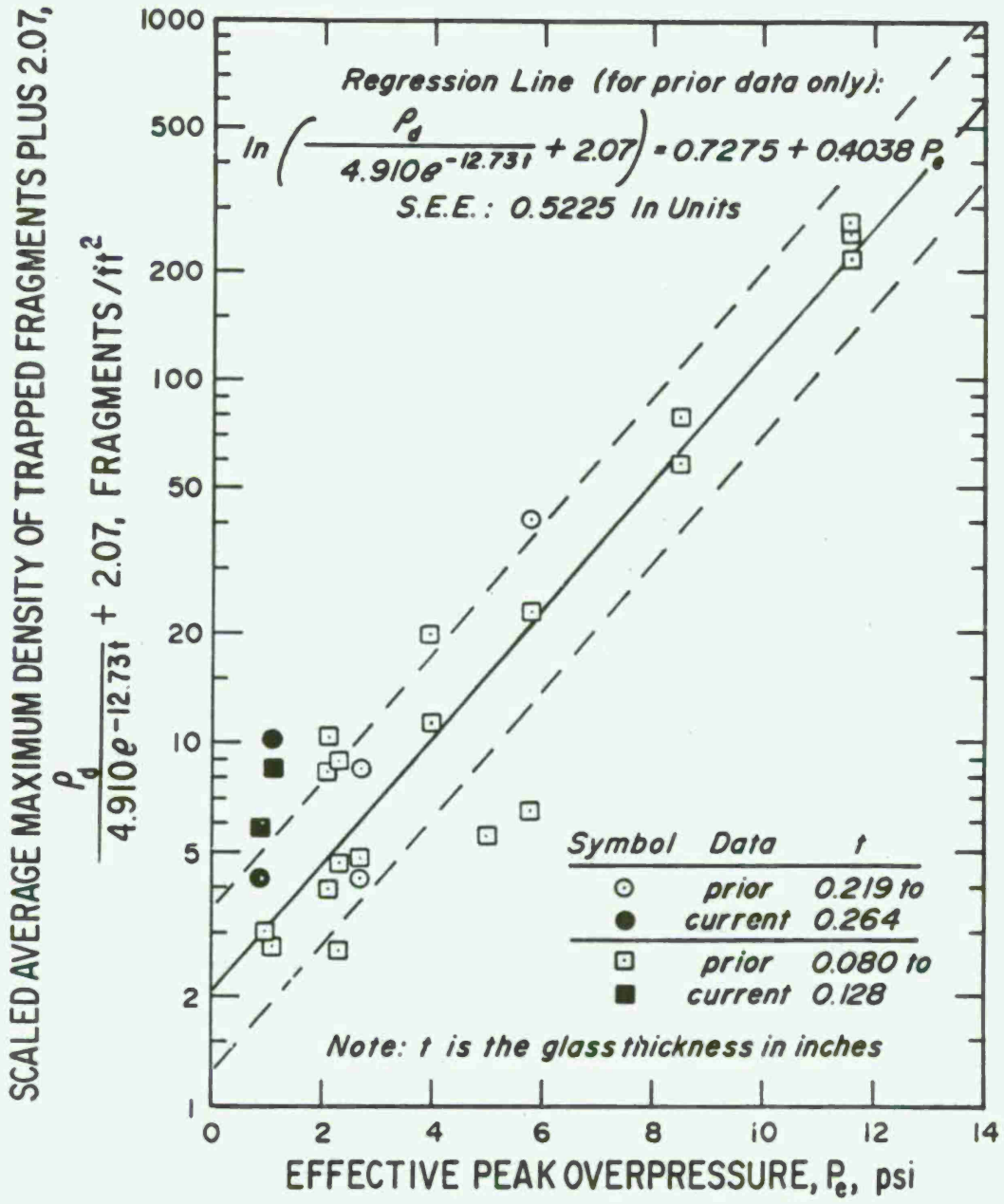


Figure 10. Scaled Average Maximum Density of Trapped Fragments Plus 2.07 vs. Effective Peak Overpressure.

TABLE IV

AUTOMOBILE WINDOW DAMAGE

| Ground Range, ft | $P_i$, psi | Automobile | | | Windows Damaged | Extent of Window Damage |
|---|---|---|---|---|---|---|
| | | Orientation | Number | Description | | |
| 730 | 1.2 | Face-On | A1 | Renault | None | None |
| | | | A2 | Pontiac | Windshield<br>Left Rear-Door<br>Right Front-Door<br>Right Rear-Door | Completely broken out<br>Multiple fractures<br>Completely broken out<br>Multiple fractures |
| | | Left Side-On | A3 | Dodge* Station Wagon | Windshield<br>Left Rear-Door (Side)** | Multiple fractures<br>Completely broken out |
| | | | A4 | VW | Left Door | Completely broken out |
| | | | A5 | Peugeot | Left Front-Door<br>Right Front-Door | Completely broken out<br>Completely broken out |
| | | | A6 | Chevrolet | Windshield<br>Left Rear-Door | Multiple fractures<br>Completely broken out |
| | | | A7 | Dodge Fuel Truck | Left Door<br>Left Vent | Multiple fractures<br>Multiple fractures |
| 1130 | 0.62 | Left Side-On | A8 | VW Bus | Windshield | Multiple fractures |
| | | | A9 | Lincoln | Windshield | Multiple fractures |
| 1700 | 0.41 | Left Side-On | A10 | Buick | None | None |

* An anthropomorphic dummy was secured in the driver's seat of this station wagon by means of a lap seat belt.

** Analysis of the film record from the camera (402 frames per second) viewing this window indicated that the fragments had a mean velocity of about 11 ft/sec.

Note: There was no evidence that any of the automobile windows were broken by bomb fragments or crater ejecta rather than by the airblast itself.

view of the motion-picture camera. From analyzing this record, it was determined that their average velocity was about 11 ft/sec. It is estimated that fragments with this low of a velocity would have a very small probability of penetrating 1 cm. of soft tissue.

## Dummy in Automobile

No damage was observed to the dummy secured by means of a lap seat belt in the driver's seat of the left-side-on station wagon (A3) at 730 feet (1.2 psi). The only window which broke out in this automobile was the one in the left rear side door, but none of the fragments struck the dummy. From the motion-picture record it was determined that the dummy suffered no significant displacement during the blast experience.

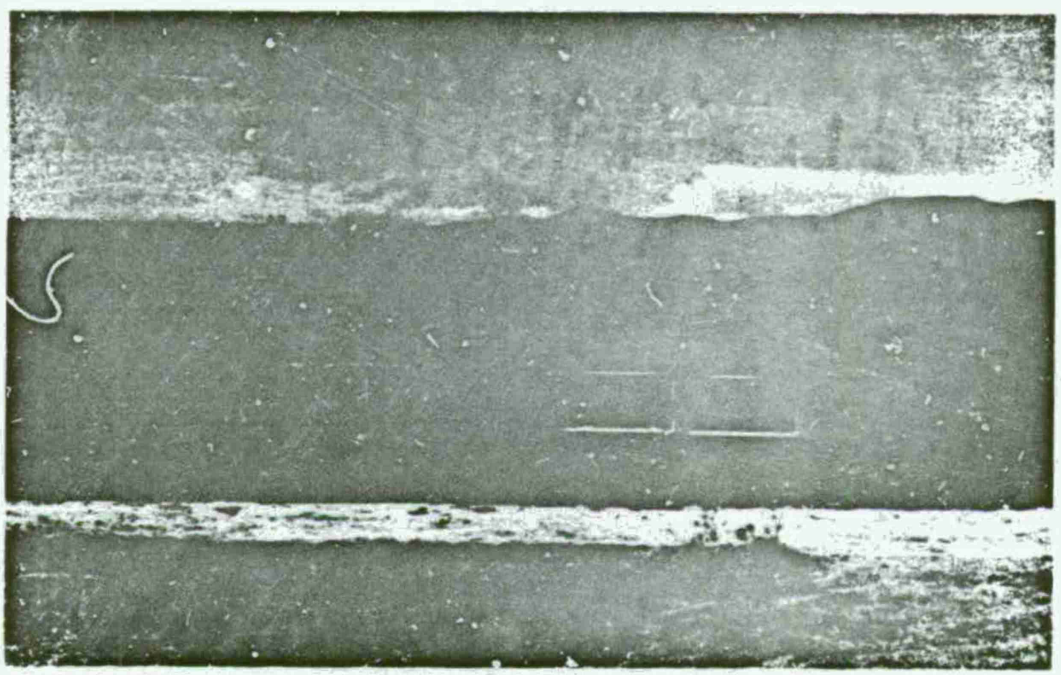

Window Cubes at 1,210 Feet. All windows were shattered by the blast.

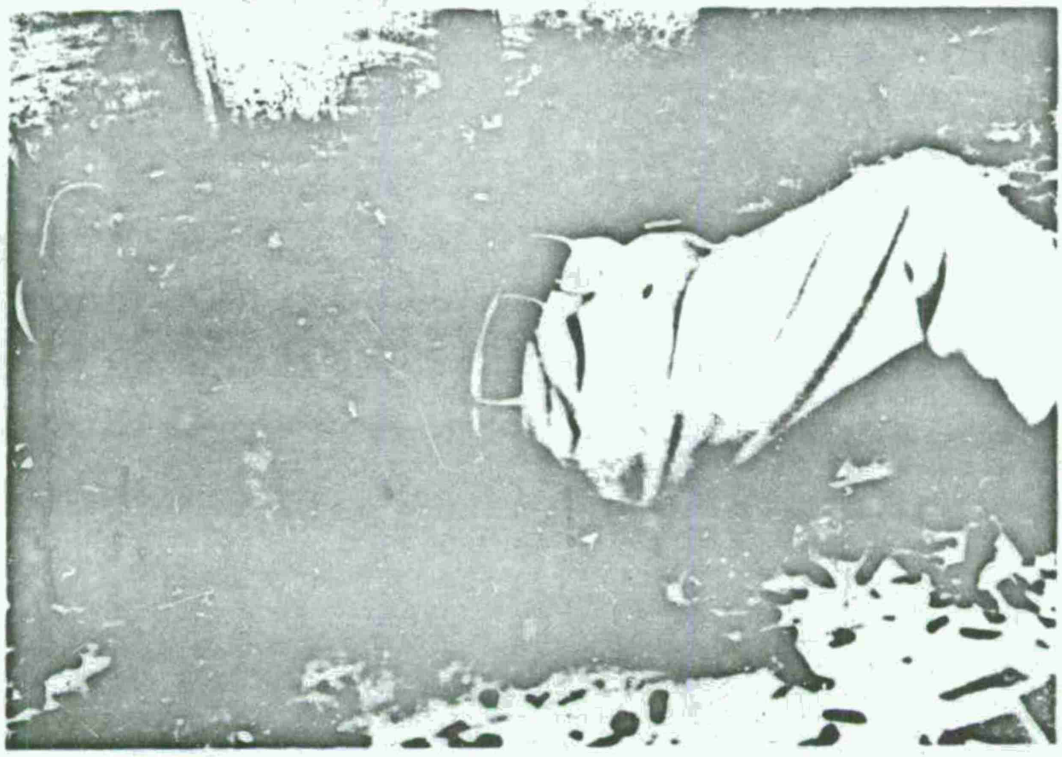

Life-Size Dummy in Window Cube at 1,210 Feet.

Window Cubes at 1,700 Feet. All window panes were broken out except one.

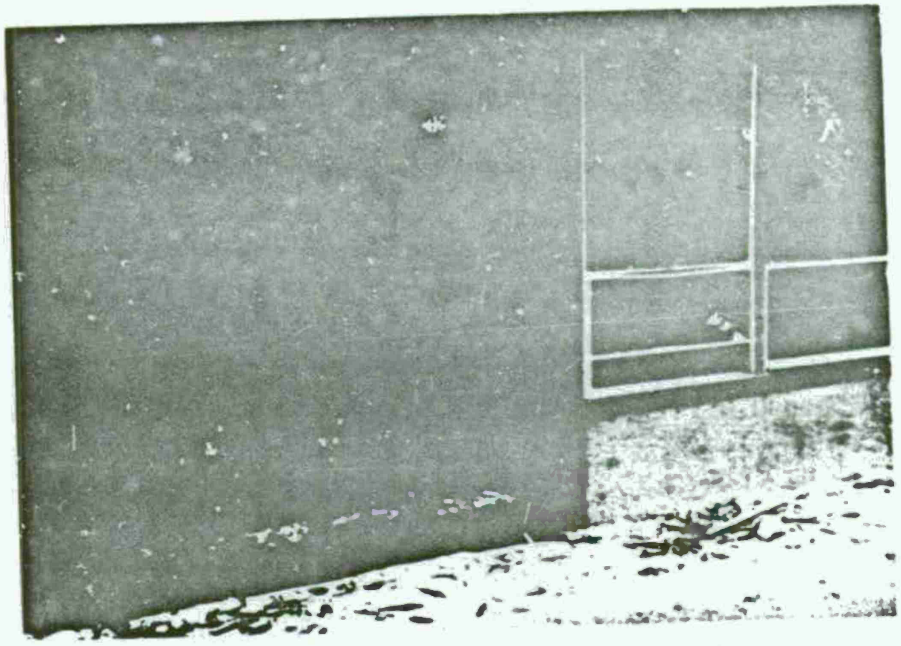

Window Cubes at 1,700 Feet Showing Glass Shards in Glass Traps.

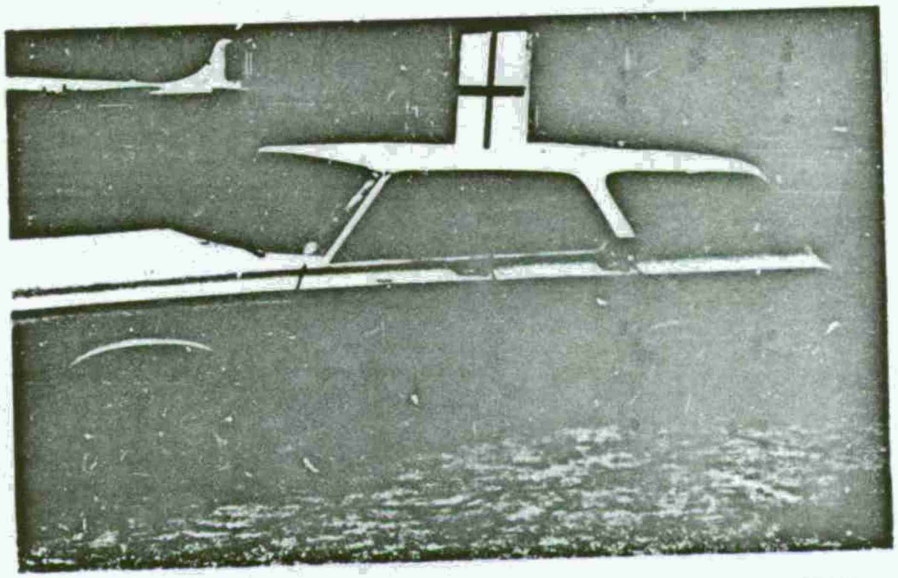

Damaged Station Wagon at 730 Feet. Note broken side windows and shattered windshield.

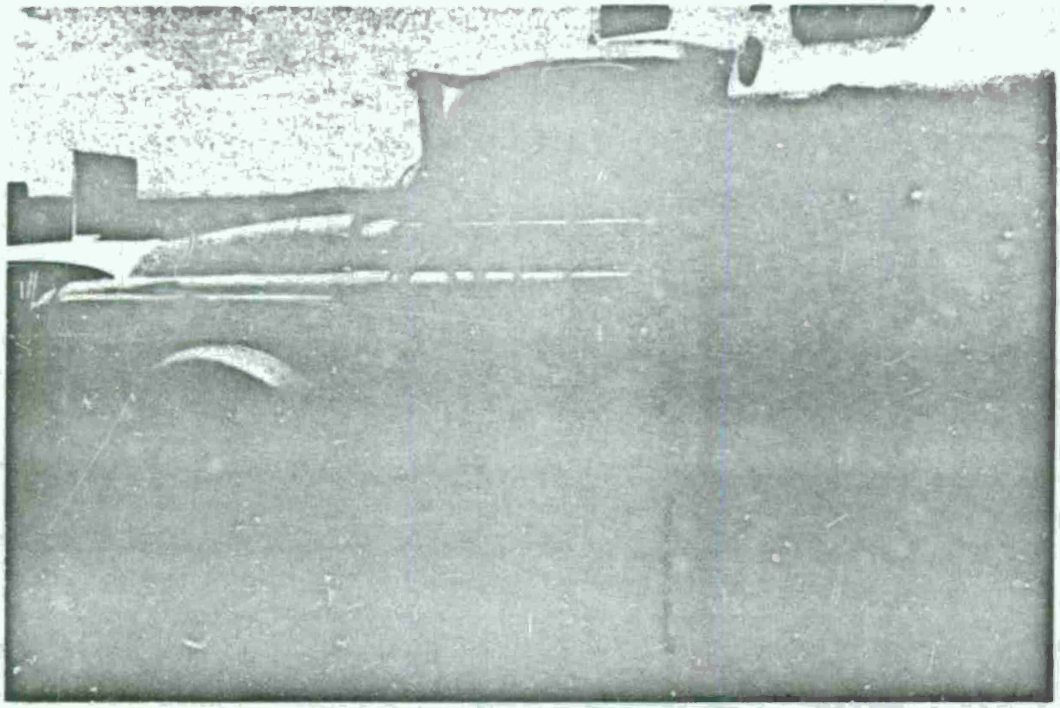

Fuel Tanker at 730 Feet Showing Glass Damage and Denting of Door and Fender.

## REFERENCES

1. Fletcher, E. R., Richmond, D. R., and Jones, R. K., "Velocities, Masses, and Spatial Distributions of Glass Fragments from Windows Broken by Airblast," Defense Nuclear Agency Report in preparation.

2. Fletcher, E. R., Richmond, D. R., Bowen, I. G., and White, C. S., "An Estimation of the Personnel Hazards from a Multi-Ton Blast in a Coniferous Forest," Final Report, DASA 2020, Defense Nuclear Agency, Department of Defense, Washington, D. C., November 1967.

3. Glasstone, S. (Editor), "The Effects of Nuclear Weapons," U. S. Government Printing Office, Washington, D. C., April 1962.